Investigation of the Molluscum Contagiosum Virus Protein MC089 as a Novel Inhibitor of Interferon Regulatory Factor 3 Activation

Trinity College Dublin
Coláiste na Tríonóide, Baile Átha Cliath
The University of Dublin

This thesis is submitted to Trinity College Dublin for the degree of Doctor of Philosophy in Immunology

2024

By Mariya Al Hamrashdi

Supervisor: Prof. Gareth Brady

School of Medicine

Trinity College Dublin

Declaration

I declare that this thesis has not been submitted as an exercise for a degree at this or any other university and it is entirely my own work. I agree to deposit this thesis in the University's open access institutional repository or allow the Library to do so on my behalf, subject to Irish Copyright Legislation and Trinity College Library conditions of use and acknowledgement. I consent to the examiner retaining a copy of the thesis beyond the examining period, should they so wish (EU GDPR May 2018).

Statement of Plagiarism

I declare that the work of this thesis is my own and that any other sources employed are acknowledged appropriately by academic citing and referencing.

Mariya Al Hamrashdi

Acknowledgments

Firstly, I would like to show my gratitude to Prof. Gareth Brady, my supervisor and my mentor, for his continued support and guidance in all possible aspects throughout this work. I truly appreciate the trust you put in me to work with you on this extraordinary project. An experience that I will cherish forever that not only helped me grow as a scientist but also as a person.

I would also like to thank Prof. Andrew Bowie for his contribution to the project's materials and Prof. Andreas Pichlmair for his contribution to the preliminary data. I would sincerely like to thank all the members of the TRIG group Carla, Tom, Ola, Clara, Aya, Sudharshana, and Ryan for all their help and company. I appreciate the wonderful working environment you all created over the years. To all members of TTMI, thank you for making this institution a fantastic workplace!

I would like to greatly thank my family for all of their support and love. My parents, my twin brother, and all of my siblings, I appreciate all of you.

Finally, I thankfully acknowledge the funding of this work by Science Foundation Ireland (SFI), grant number 19/FFP/6848 - 210295-16377.

Table of Contents

List of Figures

List of Tables

List of Abbreviations

ADAR1	Adenosine deaminase acting on RNA 1
AP-MS	Affinity purification and mass spectrometry
BSA	Bovine serum albumin
CBP	CREB-binding protein
CC2	Coiled-coil 2
$CdCl_2$	Cadmium Chloride
cGAMP	Cyclic guanosine monophosphate (GMP)-adenosine monophosphate (AMP)
cGAS	Cyclic GMP–AMP synthase
DAMPs	Damage-associated molecular patterns
DBD	DNA- binding domain
DMEM	Dulbecco's Modified Eagle Medium
dsDNA	Double-stranded DNA
EBV	Epstein-Barr Virus
ER	Endoplasmic reticulum
FAF1	FAS-Associated Factor
FBS	Fetal bovine serum
GSK3	Glycogen synthase kinase 3
HEK293	Human embryonic kidney 293
HIV-1	Human immunodeficiency virus 1
Hsp70	Heat shock protein 70
HSV	Herpes simplex virus
IAD	IRF-associated domain
IAV	Influenza A virus

IBDV	Infectious bursal disease virus
IFNs	Interferons
IKK	IκB kinase
IKKα	IκB alpha
IKKβ	IκB beta
IKKε	IκB kinase epsilon
IKKi	Inducible IκB kinase
IP	Immunoprecipitation
IRF	Interferon regulatory factor
ISG	IFN interferon-stimulated gene
ISRE	Interferon-stimulated response element
JEV	Japanese encephalitis virus
KD	Kinase domain
LAM	Luciferase assay mixture
MAVS	Mitochondrial antiviral-signalling protein
MHC	Major histocompatibility complex
MDA5	Melanoma differentiation-associated gene 5
MCV	Molluscum contagiosum virus
MEFs	Mouse embryonic fibroblasts
MERS-CoV	Middle East respiratory syndrome coronavirus
MH2	MAD homology 2
MS	Multiple sclerosis
MVA	Modified vaccinia Ankara
MxA	Myxovirus resistance A
MyD88	Myeloid differentiation primary response 88

NAK	NF-κB-activating kinase
NAP1	NF-kappa-B-activating kinase-associated protein 1
NAS1	Non-structural protein 1
NBD	NEMO-binding domain
NEMO	NF-kappa-B essential modulator
NF-κB	Nuclear factor kappa-light-chain-enhancer of activated B cells
Nsp3	Non-structural protein 3
OAS	2′-5′-oligoadenylate synthetase
OPTN	Optineurin
ORFs	Open reading frames (ORFs)
PAMPs	Pathogen associated molecular pattern
PBS	Phosphate- buffered saline
Pol III	RNA polymerase III
PLpro	Papain-like protease
PRD	Positive regulatory domain
PRRs	Pattern recognition receptors
PRV	Pseudorabies virus
RA	Rheumatoid arthritis
RIG-I	Retinoic acid-inducible gene I
RLRs	RIG-I-like receptors
RSV	Respiratory syncytial virus
SARS-CoV-2	Severe acute respiratory syndrome coronavirus 2
SDD	Scaffold dimerization domain
SeV	Sendai virus
SLE	Systemic lupus erythematosus

SPI-1	Serine proteinase inhibitor 2
STING	Stimulator of interferon genes
TAB2/3	TGF-beta activated kinase 1 binding protein 2/3
TAK1	TGF-β-activated kinase 1
TANK	TRAF family member-associated NF-kappa-B activator
TAX1BP1	Tax1-binding protein 1
TBK1	Tank-binding kinase 1
TBKBP1	TBK Binding Protein 1
TGFβ	Transforming growth factor-β
TI-IFNs	Type I Interferons
TIR	Toll-interleukin-1
TLRs	Toll-like receptors
TLR3	Toll-like receptor 3
TNF	Tumour necrosis factor
TRAF	TNF receptor-associated factor
TRAF3	TNF receptor-associated factor 3
TRAF3IP3	TRAF3 interacting protein 3
TRIF	TIR-domain-containing adapter-inducing IFNβ
TRIM	Tripartite motif-containing protein
ULD	Ubiquitin-like domain
VACV	Vaccinia virus
VACV C6	Vaccinia virus C6
VDAC2	Voltage-dependent anion channel 2

Abstract

Molluscum contagiosum virus (MCV) is a human-specific poxvirus that causes highly common, mild, papular skin lesions. The lesions are notable for exerting minimal to no inflammation but can persist for a long duration without an effective antiviral response from the host. As part of the Poxviridae, MCV encodes multiple potent immunomodulators that target innate immune signaling pathways from early virus sensing to interferon (IFN) and inflammatory responses leading to clearance. Two major families of transcription factors are responsible for driving the immune responses to viruses: the nuclear factor kappa B (NF-κB) and the Interferon Regulatory Factor (IRF) families. Whilst NF-κB broadly drives both pro-inflammatory and IFN gene expression, IRFs have more direct control over antiviral IFN induction, of which, IRF3 has the strongest role in driving the initial wave of type I IFN (TI-IFN) expression. Here we report that the MCV protein MC089 specifically inhibits IRF activation from both DNA and RNA sensing pathways making it the first characterized MCV inhibitor to selectively target IRF activation to date. MC089 targets specific IRF3-activation complexes containing IKKε and its scaffold proteins TBKBP1 and NAP1. Additionally, MC089 particularly targets the RIG-I sensing pathway by associating with MAVS on mitochondria. MC089 displays specificity in its inhibition of IRF3 activation, preventing serine 396 phosphorylation and impeding TI-IFN response without affecting phosphorylation of serine 386. This remark, along with MC089 binding specificity to its target proteins, may give novel insights into the regulation of antiviral IRF3 activation.

Lay Abstract

Molluscum contagiosum virus (MCV) infects humans causing harmless, small, pink, skin papules with minimal or no overt signs of an immune response from the host against the invader. Like all well-characterized poxviruses, it is becoming clear that MCV encodes arrays of inhibitors that suppress the host's innate responses, potentially in a human-specific manner. The first line of immune responses to viruses is driven by soluble factors known as Interferons (IFNs) which stimulate cells surrounding virally infected cells to express genes that prepare them for incoming viruses and enhance virus detection machinery to become non-permissive to virus replication. IFN gene expression is controlled by a family of gene regulators known as Interferon Regulatory Factors (IRFs) that include IRF3, the primary regulator of IFN induction during the initial stages of virus sensing. Here, we discovered that MCV protein MC089 is a novel specific inhibitor of IRF signaling pathways that interacts with host proteins critical for IRF3 activation. These proteins are the IRF3 kinase IKKε and the kinase regulators TBKBP1 and NAP. MC089 also localizes to mitochondria and associates with the mitochondrial antiviral-signaling protein (MAVS), the regulator of the cytosolic RNA signaling pathway. MC089 targeting of this system blocks IRF3 activation by inhibiting an essential modification step in its activation, phosphorylation, at a specific amino acid residue site (serine 396). Consequently, MC089 suppresses the secretion of crucial types of IFNs named type I IFNs (TI-IFNs). These findings not only reveal a new way for MCV to inhibit human immunity but can also expand our understanding of IRF3-activating pathways.

Outputs

Publications, Conferences and Presntations

Publications

Al Hamrashdi M, Brady G. Regulation of IRF3 activation in human antiviral signaling pathways. Biochem Pharmacol. 2022; 200: 115026. doi: 10.1016/j.bcp.2022.115026.

Al Hamrashdi M, Perez CS, Pichlmair A, Bowie A, Brady G. Molluscum Contagiosum Virus Protein MC089 is a Novel Inhibitor of Interferon Regulatory Factor 3 Activation. **Submitted to Journal of General Virology**. 2024.

Conferences

Host-Pathogen Communication (HPC), Trinity College Dublin, Ireland, 10th -11th of November 2021.

Irish Society for Immunology, Maynooth University, Ireland, 1st – 2nd September 2022.

Presentations

Molluscum Contagiosum Virus Protein MC089 is a Novel Inhibitor of Interferon Regulatory Factor 3 Activation. Irish Society for Immunology, Maynooth University, Poster Presentation, 1st – 2nd September 2022.

Molluscum Contagiosum Virus Protein MC089 is a Novel Inhibitor of Interferon Regulatory Factor 3 Activation. Translational Medicine Institute Immunology Meeting, Online, 20th September 2022.

Molluscum Contagiosum Virus Protein MC089 is a Novel Inhibitor of Interferon Regulatory Factor 3 Activation. Translational Medicine Institute Immunology Meeting, Online, 16th July 2021.

Chapter 1: Introduction

This chapter includes extracts originally published in Biomedical Pharmacology. Al Hamrashdi M (Author), Brady G (Reviewer). Regulation of IRF3 activation in human antiviral signaling pathways. Biochem Pharmacol. 2022; 200: 115026. doi: 10.1016/j.bcp.2022.115026.

1.1 Human Antiviral Immunity

The human defense system against pathogens depends on coordinated, sequential immune responses termed innate and adaptive immunity. The first set of defense responses is reacted rapidly by the innate immunity, which if required, will also lead to the activation of the more specific clonal adaptive immunity (1). Viruses enter the human body through the mucosal membranes or the skin, both are initial innate barriers and are covered with epithelial cells expressing specialized sensors to pathogens known as pattern recognition receptors (PRRs) (2-5). Upon the activation of PRRs, they trigger off signal transduction pathways that ultimately lead to virus clearance (6). Along with epithelial cells, the innate immunity relies on the recruitment of effector white blood cells (leukocytes), such as macrophages, neutrophils, dendritic cells and natural killer cells, secreting in a balanced feedback loop, small factors known as cytokines, chemotactic cytokines (chemokines), and blood plasma proteins (1, 7-10).

On the other hand, the adaptive immunity is a highly specific clonal system with an immunological memory that allows rapid responses to a secondary exposure to the same pathogen or antigenically-related ones (11). The specificity of adaptive responses resides

in clonally expanded T-cells (cell-mediated immunity) and B-cells (antibody-mediated immunity) that express receptors recognizing unique molecular components (antigens) of pathogens (12-14).

1.1.1 Interferons in Innate Antiviral Immunity

Upon virus entry, the innate immune receptors, PRRs, recognize the pathogen-associated molecular patterns (PAMPs) shared among viruses, principally viral nucleic acids, resulting in rapid innate responses that are triggered within hours of infection (1, 7, 15, 16).

The production of interferons (IFNs) is a critical component of human innate immunity against intracellular infectious agents like viruses. These antiviral cytokines drive pathways that induce the expression of effector interferon-stimulated genes (ISGs) that are translated into specialized proteins that severely hamper virus propagation in infected tissue or prevent it entirely (17-19). There are more than 600 known ISG proteins, including PRRs, interferon regulatory factors (IRFs) and signaling proteins, that positively and negatively regulate a balanced IFN-induced state (20-22). Antiviral ISG enzymes include the interferon-induced, double-stranded RNA-activated protein kinase (PKR), which inhibits virus replication through phosphorylation of eukaryotic initiation factor 2 needed for viral mRNA translation, and the 2′-5′-oligoadenylate synthetase/ribonuclease L (OAS/RNase L) system proteins that degrade viral genomes. Additionally, interferon-inducible GTPases, such as the myxovirus (influenza virus) resistance A (MxA), can interfere with virus assembly by preventing the transportation of viral nucleocapsid protein to the Golgi (23-27). One of the most studied ISG proteins is the ubiquitin-like interferon-stimulating gene 15 (ISG15) protein that through ISGylation, an enzymatic cascade reaction, can covalently bind viral and cellular proteins to inhibit virus replication and prevent virus release from

the infected cell (27-29). To counteract the effect of ISG15, viruses encode inhibitors that target the host ISG15 protein, such as the poxvirus vaccinia virus E3 protein and the severe acute respiratory syndrome coronavirus 2 (SARS-CoV-2) papain-like protease (PLpro) (28, 30).

IFNs also work in concert with other cytokines, such as tumour necrosis factor (TNF), to stimulate apoptosis of infected cells (31-33). The antiviral state induced by IFNs plays wider roles in triggering adaptive immunity, which includes, but is not limited to, the activation of cytotoxic T cells which specifically target infected cells for destruction (34).

Interestingly, the discovery of IFNs was somewhat accidental during the early era of virology research in the 1950s. In 1957, Alick Isaacs and Jean Lindenmann were studying the phenomenon of viral interference where the host becomes resistant to a certain viral infection due to a previous similar virus exposure. They infected chick embryos with inactivated influenza virus and found them to be resistant against a second exposure to active influenza due to the secretion of a protein that interfered with the replication of the virus, hence, it was called “interferon” (35-38). Simultaneously, Japanese researchers independently discovered this phenomenon when they infected rabbits with live vaccinia virus after previously injecting them with inactive vaccinia. In this study, they named the protein that inhibited the infection “virus inhibitory factor” (36, 39). Since their discovery, IFNs have been recognized as critical cytokines of antiviral immunity.

IFNs are classified into three groups: type-I, -II, and -III IFNs (TI-IFNs, TII-IFN and TIII-IFNs), of which TI-IFNs are the largest group and bind to the TI-IFN receptor, known as IFNα/β receptor (IFNAR). In humans, TI-IFNs include IFNβ, IFNε, IFN kappa (IFNκ), IFN omega (IFNω), and 13 subtypes of IFNα. TII-IFN is represented by IFN gamma (IFNγ) which binds specifically to IFNγ receptor (IFNGR), while TIII-IFNs are subtypes

of IFN lambda (IFNλ) that act as ligands to IFNλ receptor (IFNLR) (40-42). TI-IFNs are the most studied IFNs and one of the first cytokines to be produced upon viral recognition. Whilst they are induced in many different types of immune cells, with IFNα and IFNβ being the most expressed TI-IFNs in infected cells, IFNγ and TIII-IFNs are produced predominantly by natural killer (NK) cells and epithelial barrier cells, respectively (40, 43-45). Secreted IFNγ from NK cells during innate immunity can lead to the activation of cell-mediated immunity by either acting as a signal that promotes the differentiation of cytotoxic T-cells or as an inducer for the expression of major histocompatibility complex (MHC) class II molecules required for the activation of T-helper cells (46-48). Alternatively, TIII-IFNs are believed to have a similar role to TI-IFNs as innate antiviral cytokines that induce the expression of multiple sets of ISGs, mainly, in the initial stage of virus infection. However, unlike TI-IFNs, TIII-IFNs are specific to epithelial surfaces on mucosal tissues (49-52). Therefore, although all interferons exert antiviral activity, TI-IFNs drive the most potent antiviral effects leading to the antiviral state that can directly suppress viral replication (53).

Upon PRR sensing of virus infection, two families of transcription factors are primarily responsible for the upregulation of pro-inflammatory cytokines and TI-IFN gene expression: nuclear factor kappa-light-chain-enhancer of activated B cells (NF-κB) and IRFs. The NF-κB family induces both pro-inflammatory cytokines and IFN genes with more direct control over the former (54-57). On the other hand, the IRF family is more directly involved in driving the expression of TI-IFNs genes (58-61). Most notably, the IFNβ gene promoter contains two sites, known as positive regulatory domains (PRDs) I and III, to bind to IRFs and only one binding site, PRDII, for NF-κB transcription factors. It also contains a site (PRDIV) for activating protein-1 (AP-1) transcriptions factors, related

to cellular and immune responses, activated by c-Jun N-terminal kinases (JNKs), members of mitogen-activated protein kinases (MAPKs) (62, 63). To date, the IFNα gene promoter is known to only include elements to bind IRFs that are called positive regulatory domain-like elements (PRD-LEs), also known as virus-responsive elements (VREs) (64, 65) (**Fig.1.1.1**). Recent findings in last few years have shown that NF-κB and IRFs signaling pathways are cross-regulated (54, 66, 67). However, there is still not much known about the level of interaction between their activation pathways once signaling has branched off to commit events traditionally thought specific to each transcription factor set.

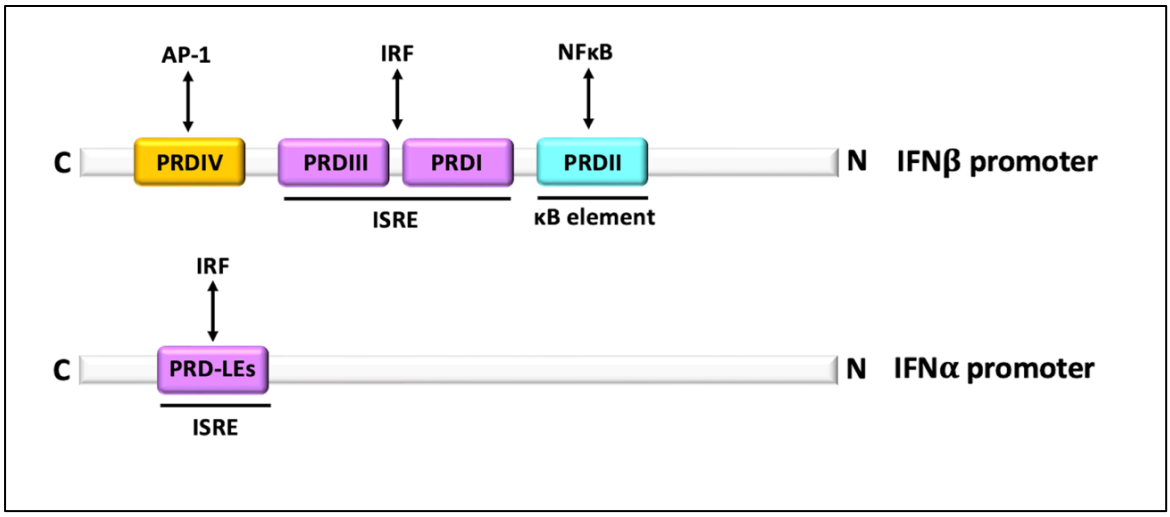

Figure 1.1.1 Schematic of the positive regulatory elements of IFNβ and IFNα promoters. IFNβ contains two sites, PRDIII and PRDI, to bind to IRFs, such as IRF3 and IRF7. NF-κB and AP-1 transcription factors recognize PRDII and PRDIV, respectively. There is one site, regulatory domain-like elements (PRD-LEs), on the IFNα promoter to only interact with IRFs. (N) N-terminus, (C) C-terminus.

The activation of both sets of transcription factors depends on triggering signaling cascades via phosphorylation and ubiquitination of a series of adaptor proteins and kinases. Phosphorylation is a crucial post-translational modification (PTM) carried out by protein kinases to activate adaptor proteins and transcription factors in cellular signaling

transduction (68). The kinases, which are also activated by phosphorylation, are enzymes that catalyze the transfer of phosphate groups from ATPs to the target proteins on their amino acid residues: around 86% of phosphorylated residues are serine, followed by threonine residues ∼12% and tyrosine residues ∼2% (68-70). Phosphorylation works in coordination with ubiquitination which is another essential PTM in signal transduction leading to the recruitment of proteins into signaling localization to enable protein-protein interactions or proteasomal degradation (71). During ubiquitination, a small protein of 76 amino acid residues, known as ubiquitin, is covalently attached by ubiquitin enzyme ligase (E3) to lysine residues of the target protein through one of the ubiquitin lysine residues, K6, K11, K27, K29, K44, K48 and K63, or the methionine (M1) residue on its N-terminus (71, 72).

1.1.2 Pattern Recognition Receptors (PRRs)

PRRs are specialized proteins differentially expressed in most cells, with the highest expression in effector innate cells, and have different cellular localization and ligand specificity. However, most antiviral PRRs can trigger signaling cascades through adaptor protein recruitment ultimately resulting in the activation of transcription factors to induce gene expression. This, in turn, results in inflammatory responses and cytokine production that eliminate the virus and initiate adaptive immunity (1, 6, 7, 73). **Table 1** summarizes the major human PRRs of antiviral immunity.

Table 1. Major human pattern recognition receptors (PRRs) of innate antiviral immunity.

PRR	Viral ligand	Adaptor protein	Main signaling pathway(s)	Reference(s)
TLR3	dsRNA	TRIF	NF-κB and IRFs	(74)
TLR7/TLR8	ssRNA	Myd88	NF-κB and IRFs	(75)
TLR9	DNA	Myd88	NF-κB and IRFs	(76)
RIG-I	5' triphosphate RNA	MAVS	NF-κB and IRFs	(77)
MDA5	Long RNA strands	MAVS	NF-κB and IRFs	(77)
cGAS	dsDNA	STING	NF-κB and IRFs	(78)
DDX41	DNA	STING	NF-κB and IRFs	(79)
IFI16	DNA	STING	NF-κB and IRFs	(80)
AIM2	dsDNA	ASC	Caspase 1	(81)
DAI	DNA/RNA	RIP-1/3 and STING	NF-κB, necroptosis and IRFs	(82-84)

Abbreviations: TLR, Toll-like receptor; RIG-1, Retinoic acid-inducible gene I; MDA-5, Melanoma differentiation-associated gene-5; cGAS, Cyclic GMP-AMP synthase, DDX41, DEAD (Asp-Glu-Ala-Asp) box polypeptide 41; IFI16, Gamma-interferon-inducible protein 16; AIM2, Absent in melanoma 2; DAI, DNA-dependent activator of IFN-regulatory factors; TRIF, TIR domain-containing adaptor-inducing interferon-β; Myd88, Myeloid differentiation primary response 88; MAVS, Mitochondrial antiviral-signaling protein; STING, stimulator of interferon genes; ASC, Apoptosis-associated speck-like protein; RIP, Receptor-interacting protein kinase 1; NF-κB, nuclear factor kappa-light-chain-enhancer of activated B cells; IRFs, Interferon regulatory factors; Caspase 1, Scaffold cysteine-dependent aspartate specific protease 1.

Toll-like receptors (TLRs) have become one of the most well-studied PRRs since their discovery in *Drosophila* in the 1980s (85). In humans, there are currently ten members of TLRs (TLR1-10), of which four are viral sensors located in the endosome, namely, TLR3, TLR7, TLR8 and TLR9 (86-88). Each viral TLR recognizes a specific ligand: TLR3 detects

dsRNA, both TLR7 and TLR8 sense ssRNA, and TLR9 binds to DNA containing cytosine–phosphate–guanine (CpG) dideoxynucleotide motif (74-76, 86, 89, 90). Viral TLRs are mainly composed of an N-terminal domain (NTD) that binds to the ligand through its leucine-rich repeats (LRRs), and a cytoplasmic C-terminal domain (CTD) that interacts with the adaptor proteins for signal transduction (91). The NTD and the CTD are connected by a helix transmembrane domain (TMD) **(Fig.1.1.2)** (91, 92). The LRR motif of the NTD, also known as the ectodomain, forms a hydrophobic core resulting in the horseshoe shape of TLRs. Additionally, TLRs, such as TLR3, form homodimers upon binding to the viral genome through the extracellular N-terminal domain (91, 93-95). On the other hand, the CTD is homologous to the signaling domain of the interleukin-1 (IL-1) receptor, termed toll-interleukin-1 receptor (TIR) domain, which initiates downstream signaling via interaction with cytoplasmic adaptor proteins that include TIR domain-containing adaptor-inducing interferon-β (TRIF) with TLR3, and myeloid differentiation primary response 88 (Myd88) with TLR7, TLR8 and TLR9 (86, 91, 96-98). Both TRIF and Myd88 can trigger the activation of NF-*κ*B and IRFs (99).

In 2004, retinoic acid-inducible gene I (RIG-I)-like receptors (RLRs) have been identified as a family of RNA sensors located in the cytosol (100). There are currently three known members of RLRs, RIG-1, melanoma differentiation-associated gene-5 (MDA-5) and laboratory of Genetics and Physiology 2 (LGP2) (77, 101-103). All three RLRs share a C-terminal domain (CTD) that recognizes RNA and two helicase domains of the superfamily 2 (SF2) that catalyze ATP to bind RNA **(Fig.1.1.2)** (101, 104-107). Both RIG-I and MDA5 contain, at the N-terminus, two caspase recruitment domains (CARDs) which form oligomers to recruit the adaptor protein mitochondrial antiviral-signaling protein (MAVS) and activate downstream NF-*κ*B and IRFs (101, 104-108). The CTD and helicases of RIG-

I and MDA-5 sensors differ in their alignment to RNA which specifies their RNA ligands; the CTD and helicases of RIG-I receptors orient to form a cleft to mainly interact with short 5′-triphosphorylated RNA, while MDA-5 receptors assemble long helical filaments on long RNA strands (100, 102, 104, 109-111). LGP2 lacks the signaling domains which means it does not interact with downstream signaling proteins, but it has been found to act as a coactivator of MDA-5 via binding dsRNA (112). The exact role of LGP2 in RIG-I sensing still requires further elaboration although it has been shown to inhibit RIG-I-driven NF-κB and IRF activation which indicates that it rather acts as a negative regulator of the pathways (113, 114).

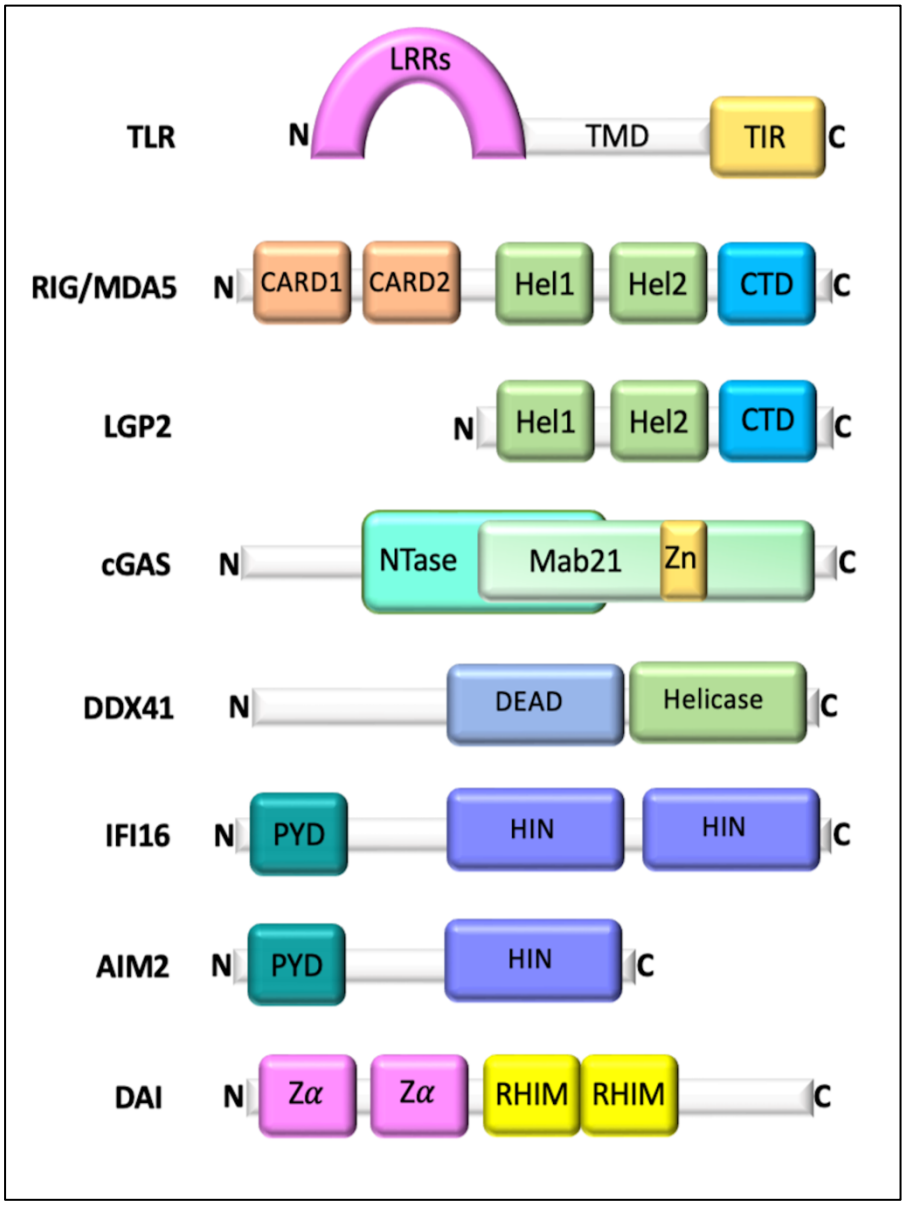

Figure 1.1.2 Domain organization of the major human pattern recognition receptors (PRRs). Each sensor contains DNA/RNA-binding domain(s) to detect viral genome and signaling domain(s) to interact with adaptor molecules and activate antiviral transcription factors, except for LGP2 lacking a downstream signaling motif. (LRRs) leucine-rich repeats, (TMD) transmembrane domain, (TIR) toll-interleukin-1 receptor domain, (CARD) caspase recruitment domain, (Hel) helicase, (CTD) C-terminal domain, (NTase) nucleotidyltransferase core, (Mab21) male-abnormal 21 domain, (Zn) zinc ribbon motif, (DEAD) (Asp-Glu-Ala-Asp) box domain, (PYD) pyrin domain, (HIN) hematopoietic expression, interferon-inducible nature, and nuclear localization domain, (Zα) Z alpha

binding domain, receptor-interacting protein kinase (RIP)-homotypic interaction motif (RHIM), (N) N-terminus, (C) C-terminus.

Cyclic GMP-AMP synthase (cGAS) is another cytosolic viral sensor that specializes in binding dsDNA that trigger NF-κB and IRF signaling pathways through its corresponding adaptor protein stimulator of interferon genes (STING) (115, 116). cGAS is an enzyme of 522 amino acid residues, of which around 160 residues at the N-terminus are considered a disordered region (78, 117, 118). Alternatively, the C-terminal domain exerts the catalytic activity of cGAS and it is highly homologous to the nucleotidyltransferase (NTase) fold proteins of the male-abnormal 21 (Mab21) family **(Fig.1.1.2)** (78, 117, 119). The Mab21 domain also contains a zinc ribbon motif which allows for DNA interaction in a length-dependent manner (78, 120, 121). Upon binding to dsDNA, cGAS dimerizes to activate the catalyzation of the signaling molecule 2′3′-Cyclic GMP-AMP (cGAMP) using the substrates ATP and GTP (122, 123). In turn, cGAMP binds to STING leading to its migration from the endoplasmic reticulum (ER) to the Golgi where it activates the antiviral transcription factors (124).

Another cytosolic STING-dependent DNA sensor is DEAD (Asp-Glu-Ala-Asp) box polypeptide 41 (DDX41), an RNA helicase from the DEAD-box superfamily 2 (SF2) (79, 125, 126). The N-terminus of DDX41 is composed of a disordered motif followed by a DEAD-box domain and a helicase domain **(Fig.1.1.2)** (126, 127). As part of the SF2 family, DDX41 uses its DEAD/helicase domains to bind ATP and interact with DNA leading to the activation of STING via direct interaction and the subsequent activation of NF-κB and IRF pathways (79, 125).

In 2010, a new DNA sensor, gamma-interferon-inducible protein 16 (IFI16), was affinity purified from IFNβ-induced human monocytes using the non-adapted human DNA vaccinia virus (VACV) (80). IFI16 belongs to the pyrin and hematopoietic interferon-inducible nuclear (HIN) domain-containing (PYHIN) protein family that triggers antiviral sensing upon DNA detection (128). IFI16 holds the pyrin (PYD) domain at the N-terminus which through oligomerization, interacts with STING to initiate antiviral signaling pathways **(Fig.1.1.2)** (129). DNA recognition by IFI16 occurs through the folding of two hematopoietic expression, interferon-inducible nature, and nuclear localization (HIN) domains at the C-terminus (130). IFI16 is not the only protein related to the PYHIN family that binds cytosolic DNA as it was preceded by absent in melanoma 2 (AIM2) that interacts with dsDNA to activate inflammatory pathways (80, 131). Therefore, DNA sensors from the PYHIN family were given the term AIM2-like receptors (ALRs) (80). Whilst AIM2 also contains a PYD domain, it has only one C-terminal HIN domain (128), and It depends on its PYD domain to recruit its adaptor protein apoptosis-associated speck-like protein (ASC) through PYD-PYD interaction (132, 133). ASC uses its caspase activation and recruitment domain (CARD) to scaffold cysteine-dependent aspartate specific protease 1 (caspase 1) forming a proinflammatory multiprotein complex known as inflammasome (132-134). This results in the production of interleukin 1 (IL-1) and interleukin 18 (IL-18) which are critical cytokines for the subsequent activation of antiviral immune cells, such as leukocytes, and T-cell adaptive immunity (135, 136).

DNA-dependent activator of IFN-regulatory factors (DAI) is an innate sensor identified as a Z-DNA-binding protein 1 (ZBP1) for containing two binding domains at the N-terminus, known as Z alpha (Zα) **(Fig.1.1.2)** (82, 137). It recognizes Z-confirmational DNA/RNA structures which are left-handed zig-zag forms of double-stranded nucleic acids produced

in mammalian cells during gene transcription and protein recruitment (137, 138). Viruses can also produce Z-DNA/RNAs in infected cells, such as Z-RNAs generated by Influenza A virus (IAV) and severe acute respiratory syndrome coronavirus 2 (SARS-CoV-2), that act as ligands to DAI sensor (84, 139). Activated DAI interacts with signaling molecules through two receptor-interacting protein kinase (RIP)-homotypic interaction motifs (RHIMs) at its C-terminus. Sequentially, it induces NF-*κ*B and inflammatory cell death (necroptosis) signaling pathways via RIP-RIP interaction with receptor-interacting protein kinase 1 (RIPK1) and RIPK3, and IRF pathways through STING (82, 83, 140-142). Additionally, although RNA silencing of DAI in mouse fibroblast cells blocked IFN secretion, DAI-deficient mouse embryonic fibroblasts were able to induce normal levels of IFN (143, 144). This rather classifies DAI as a cell-specific DNA sensor, however, viruses producing DAI agonists, such as the E3L-encoded protein of vaccinia virus, suggests an essential role of DAI in antiviral immunity which should be further elaborated (144-146).

1.1.3 NF-*κ*B Activation in Antiviral Immunity

Upon the recognition of viruses through PRRs, antiviral transcription factors are activated through evolutionary conserved pathways of signal transduction (147, 148). In the 1980s, a protein was discovered to bind to the sequence motif 5'-GGGACTTTCC-3', known as κB DNA element, of the immunoglobulin κ light-chain enhancer in the nuclei of B-tumour cells and, therefore, named nuclear factor kappa-light-chain-enhancer of activated B cells (NF-*κ*B) (149-151). Today, NF-*κ*B has become one of the most studied transcription factors and one of the crucial regulators of inflammatory responses, cell survival and cell death (148, 152).

The term NF-*κ*B is not specific to a single transcription factor complex but to multiple proteins from the same family which form homo- and heterodimeric complexes to bind to

the κB consensus sequences at expression sites of target genes. Subunits form dimers with other members of the NF-*κ*B family through a shared Rel homology domain (RHD). The RHD, located at the N-terminus, does not only mediate dimerization, but also NF-*κ*B nuclear translocation and nuclear DNA-binding (153, 154). There are known five members of the NF-*κ*B family: p50 and p52 subunits encoded by the NF-*κ*B1 and NF-*κ*B2 genes, respectively, p65 subunit, also known as RelA, encoded by the RELA gene, c-Rel encoded by the REL gene and RelB encoded by the RELB gene. Only p65, c-Rel and RelB contain a transcriptional activation (TD) domain at the C-terminus for the induction of gene expression. Both p50 and p52 are processed as IκB (inhibitors of NF-*κ*B) precursor proteins p105 (NF-*κ*B1) and p100 (NF-*κ*B2), respectively (148, 153). RelB also contains an N-terminal leucine zipper (LZ) motif which, through dimerization, regulates gene expression by binding to coactivators and corepressors (155, 156) (**Fig.1.1.3A**).

In unstimulated cells, NF-*κ*B proteins mainly reside in the cytoplasm in an inactive form bound to IκB proteins with the nuclear localization signal (NLS) motif blocked (157). Upon PRR sensing of pathogens, phosphorylation-based ubiquitination signals, either canonical or non-canonical, result in the degradation of IκB inhibitors and the subsequent activation of NF-*κ*B dimers (158). The major IκB proteins include IκBα, IκBβ, IκBε, p105 and p100, and they all share a helix-turn-helix motif of around 33 amino acid residues (ankyrin repeat) that allows for interaction with other proteins (148, 157, 159, 160) (**Fig.1.1.3B**).

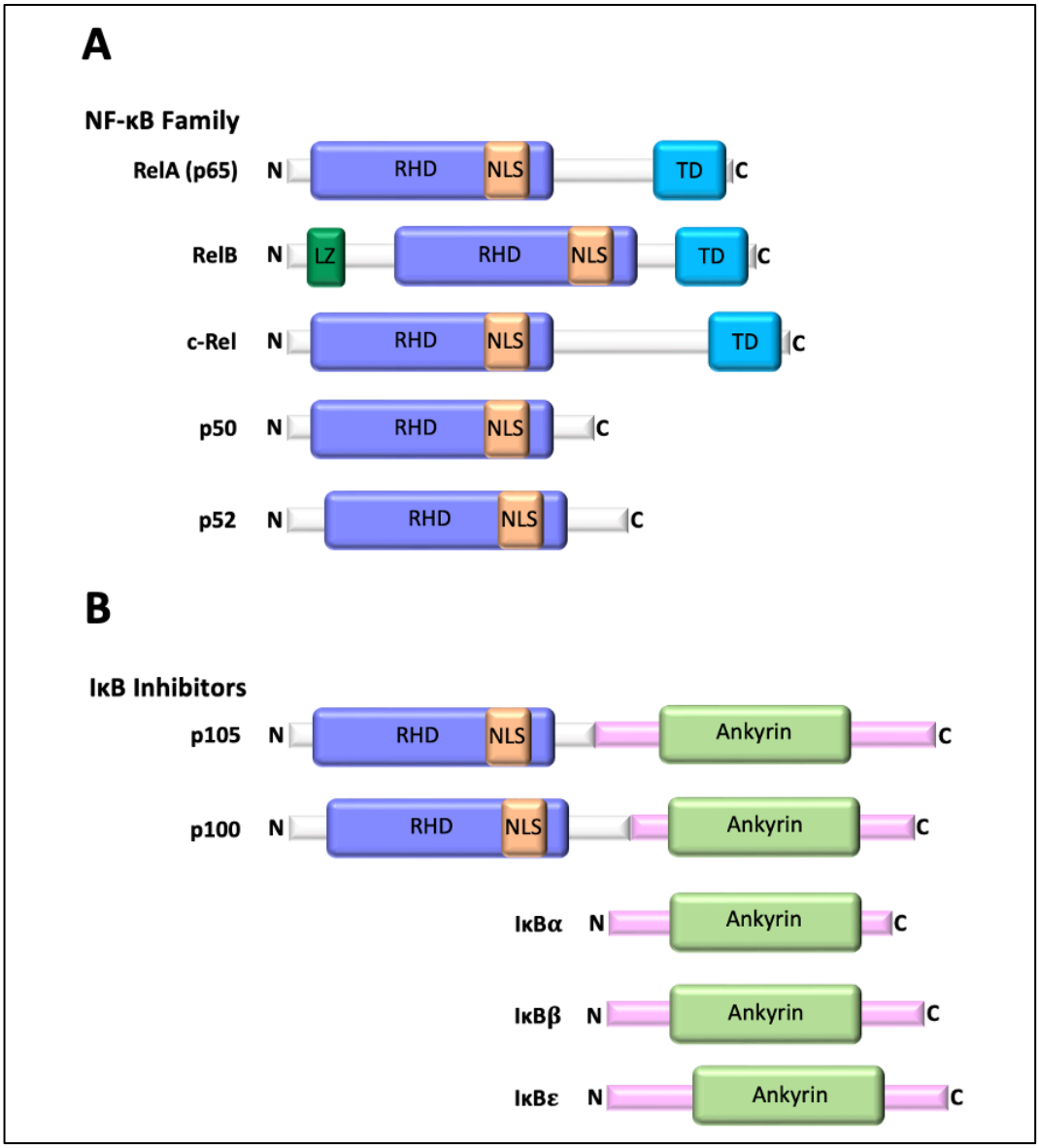

Figure 1.1.3 Domain organization of the major human NF-κB family and IκB inhibitors. (A) Proteins of the NF-κB family share a Rel homology domain (RHD) with multiple functions including dimerization, NF-κB nuclear translocation and nuclear DNA binding. RelB has a dimerization leucine zipper (LZ) motif to regulate gene expression. All proteins have a transactivation domain (TD) to promote gene expression, except for p50 and p52. (B) In resting cells, NF-κB transcription factors exist as dimers bound to IκB inhibitors by their helix-turn-helix motif (ankyrin repeat) to prevent their activation. p105 and p100 are precursors of p50 and p52, respectively. (N) N-terminus, (C) C-terminus.

The canonical NF-κB pathway is a rapid response to an external stimulus that depends on the IKK activation complex of NF-κB containing IκB kinases (IKKs) IKKalpha (IKKα) and IKKbeta (IKKβ), and the regulatory protein of IκB kinases nuclear factor κB (NF-κB) essential modulator (NEMO), also known as IKKgamma (IKKγ) (55, 161). IKKα and IKKβ are highly homologous sharing around 50 % identity and rely on phosphorylation of their serine residues, serine 176 and 180 of IKKα and serine 177 and 181 of IKKβ, to be activated (162-164). The phosphorylation sites of both kinases are located in the kinase domain at the N-terminus and followed by a leucine zipper (LZ) motif, a helix-loop-helix (HLH) domain and a NEMO-binding domain (NBD) (**Fig.1.1.8A**) (162, 163). IKKβ can also be ubiquitinated at the lysine residue 353 (L353) located at the ubiquitin-like domain (ULD) which is absent in IKKα and contributes to its IKKα-independence activation (163-165). NEMO is subjected to ubiquitination on multiple residue motifs, such as NEMO optineurin ABIN2 (NOA) and A20 binding and inhibitor of NF-κB (ABIN) and NEMO (UBAN), in corporation with a zinc finger motif (166-169) (**Fig.1.1.8A**). Although the IKK complex exclusions mainly purified as an IKKα/ IKKβ heterodimer bound to NEMO dimers, other forms of IKK complex can also exist including homodimers of the IKK kinases (163, 170).

Upon viral infection, PRRs, such as TLRs, RLRs and DNA sensors, engage their adaptor proteins (**Table 1**) to activate NF-κB dimers (171). TRIF, MyD88 and MAVS recruit tumour necrosis factor (TNF) receptor–associated factor (TRAF) proteins, as signaling molecules to activate IκB kinases (171). The TRAF family includes seven members, TRAF1-7, where all of them, apart from TRAF1, share a RING (Really Interesting New Gene) finger motif at the N-terminus allowing for the E3 ubiquitin ligase functionality to covalently attach ubiquitin (Ub) chains on IκB kinases (172, 173). All TRAFs, except for

TRAF7, also contain a homologous C-terminal domain for interaction with other signaling molecules and upstream kinases, such as the mitogen-activated protein transforming growth factor-β-activated kinase 1 (TAK1) (174-176). Therefore, TRAFs, like TRAF6, can recruit the IKK complex and TAK1 via ubiquitin polymers causing phosphorylation of IκB kinases by TAK1 or by autophosphorylation (171, 177). TRAFs also mediate NEMO K63-linked polyubiquitination and oligomerization, in turn, NEMO acts as a scaffold protein that recruits the IKK complex to TAK1 and NF-*κ*B transcription factors (164, 167, 178). The activated IκB kinases, mainly IKKβ, can then phosphorylate IκB inhibitors exposing them to ubiquitination by E3 ligase which tags them for proteasomal degradation (179, 180). Consequently, NF-*κ*B dimers, of which p50-p65 (RelA) are the most abundant heterodimers, are freed to translocate into the nucleus where they bind to κB DNA elements to regulate the expression of proinflammatory and immune genes, such as interleukin 1 (IL-1) and IFNβ (181-183). Along with PPRs, the canonical pathway can be switched on by proinflammatory cytokines, such as TNF and IL-1, upon their receptors ligation triggering a signaling pathway via TAK1 (176, 184) (**Fig.1.1.4A**).

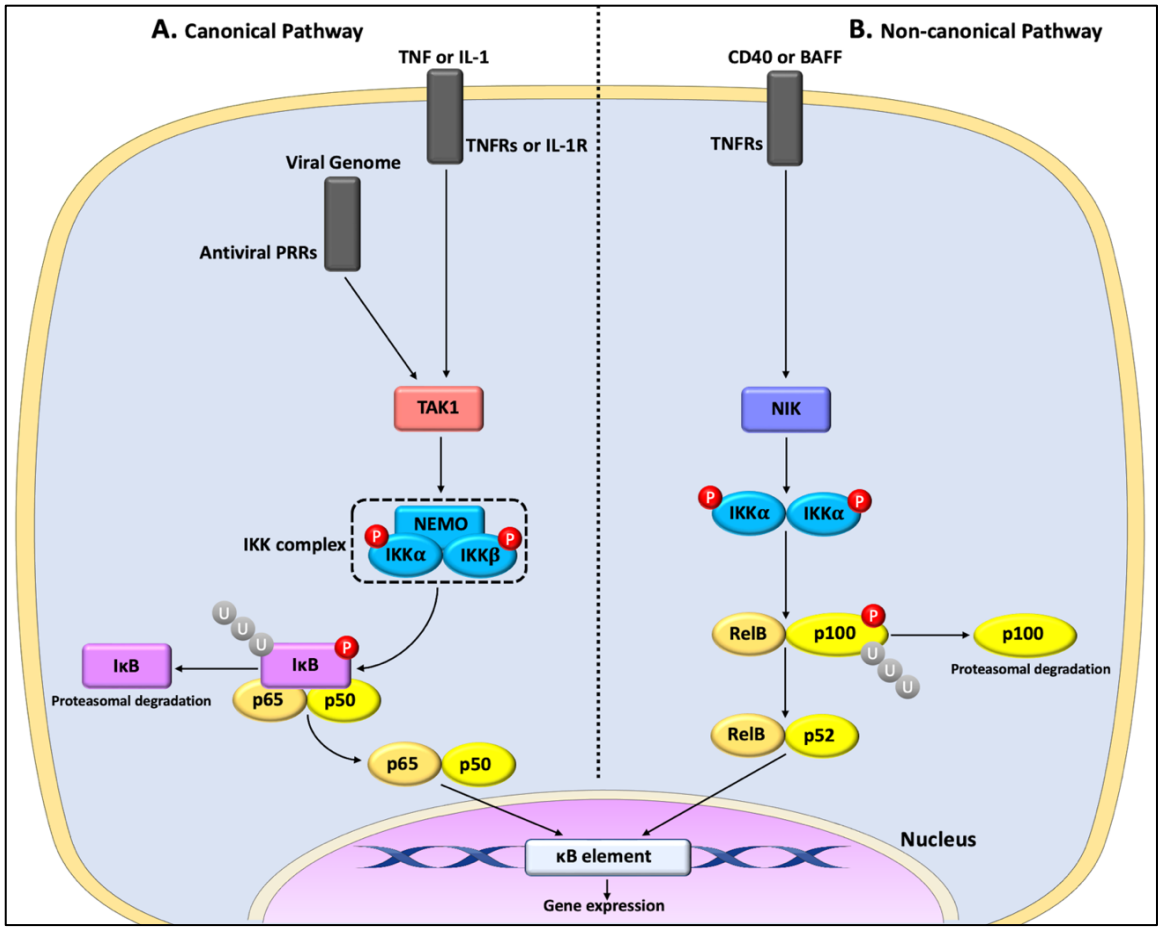

Figure 1.1.4 Canonical and non-canonical pathways of NF-κB activation. (A) In the canonical pathway, NF-κB can be activated by either PRRs, antiviral PRRs are mainly cytosolic or endosomal, or pro-inflammatory cytokines, such as TNF and IL-1. Ligand binding of PRRs, TNF receptors (TNFRs) or IL-1 receptor (IL-1R), activates the kinase TAK1 leading to the recruitment of the IKK complex: IKKα, IKKβ and the scaffold protein NEMO, and the subsequent phosphorylation of IκB kinases. Activated IKKα/IKKβ phosphorylates the IκB inhibitor exposing it to ubiquitination and proteasomal degradation. In turn, NF-κB dimers, such as p50-p65 (RelA), are free to translocate to the nucleus where they bind to a specific DNA sequence, known as κB DNA element, of the target gene promoter/enhancer. (B) In the non-canonical pathway, NF-κB is activated by TNFRs binding to their ligands, for example, CD40 or BFF, leading to the phosphorylation of IKKα in a NEMO-independent manner. Next, IKKα phosphorylates p100 resulting in its ubiquitination and

partial degradation into p52. Consequently, the p52-RelB heterodimer translocates to the nucleus to induce the expression of the target gene. Servier Medical Art (https://smart.servier.com/) was used to construct the illustration.

Alternatively, the non-canonical NF-*κ*B pathway is triggered by the TNF receptor (TNFRs) superfamily where the induced signal is conveyed by NF-κB-inducing kinase (NIK) (185). The alternative NF-*κ*B pathway mediates the switching to adaptive immunity since it integrates signals essential for adaptive cell maturation and differentiation. This includes CD40, a glycoprotein surface molecule of antigen-presenting cells (APCs) that introduce antigens to T and B cells, and B-cell activating factor (BAFF), a cytokine of TNF superfamily that activates B cells (164, 186-188). Upon ligation. The activation of TNFRs leads to the recruitment of NIKs which phosphorylate IκB kinases, namely IKKα, resulting in the phosphorylation and degradation of IκB inhibitors, and the subsequent activation of NF-*κ*B dimers, of which p52-RelB heterodimers are the most dominant forms (164, 189) (**Fig.1.1.4B**).

Regarding the route of NF-*κ*B activation, both canonical and non-canonical responses need to be tightly controlled to prevent the development of immune diseases and disorders related to chronic inflammation and cell survival, such as cancer, rheumatoid arthritis (RA), inflammatory bowel disease (IBD) and type I diabetes (56, 190-192) **(Table 2)**.

Table 2. Examples of NF-κB-related chronic inflammatory diseases and disorders.

Disorder	Pathogenesis	NF-κB-Involvement	Reference(s)
Cancer	Progressive transformation of cells to abnormal growth and spread (metastasis)	Chronic inflammation-tumour cell proliferation and survival	(175, 178)
RA	Persistent immune cell infiltration into synovial membranes of joints causing their destruction	Autoimmune chronic inflammation-abnormal proliferation of immune cells and Fibroblast-like synoviocytes (FLS) and osteoclast apoptosis	(179, 180)
IBD	Impaired immune responses to gut microbes damaging the digestive tract	Chronic inflammation-overproduction of proinflammatory cytokines and hyperactivation of mucosal immune cells	(41, 181, 182)
TI-diabetes	Autoreactive T cells attack of insulin-producing pancreatic cells	Autoimmune chronic inflammation-altered activation of T cells and apoptosis of pancreatic cells	(176, 183)

Abbreviations: RA, Rheumatoid arthritis; IBD, Inflammatory bowel disease; TI-diabetes, Type I diabetes.

1.1.4 The IRFs in Antiviral Immunity

The discovery of IRFs was dated back to 1988 when IRF1 was identified to specifically bind to IFNβ gene promoter (193, 194). To date, the human IRF family includes nine members (IRF1-9) (195-197). **Table 3** summarizes the major IRFs involved in antiviral TI-IFN induction. They share the DNA-binding domain (DBD) at the N-terminus that contains a conserved tryptophan-rich motif for binding IFN-stimulated response elements (ISREs)/IFN regulatory elements with the consensus sequence 5'-AANNGAAA-3' (198). Binding patten of ISREs depends on the signal, the cell-type and the transcription factor

and its associated cofactors and coactivators (199, 200). The IRF-associated domain (IAD) at the C-terminus is likely linked to the uniqueness of the transcriptional role of each IRF member (195-197). The C-terminus defines the activity of IRFs as it also includes sites for phosphorylation, dimerization and interaction with cofactors (201).

The autoinhibitory sites contained within the C-terminus of IRF3 **(Fig.1.1.6**), IRF5 and IRF7 are believed to block their transcriptional activity which is relieved upon phosphorylation allowing for dimerization and interaction with cofactors (201, 202). All three IRFs are essential for antiviral IFN regulation with IRF3 and IRF7 being the principal mediators of TI-IFNs, while IRF5 role in TI-IFN-induction is virus and cell-type specific (203-208). Although IRF7 is predominantly expressed in lymphoid cell types and IRF5 in dendritic cells and B cells, both proteins can be induced in other cell types by TI-IFN stimulation as part of the antiviral state (203, 209). Alternatively, IRF3 expression is found in all cell types making it the primary IRF used in antiviral responses that can also induce the activation of other IRFs, such as IRF7, through the activation of ISGs that mediates the early wave of TI-IFNs (210-214). Along with IFN-induction, IRFs can induce the expression of multiple other cytokines, for example, IRF5 induces the expression of proinflammatory cytokines, such as interleukin 6 (IL-6), by interacting with their regulatory elements downstream of TLR-MyD88 signaling pathway (215, 216).

Both IRF4 and IRF8 are involved in mediating the differentiation of immune cells through interaction with members of the transcription factor family erythroblast transformation specific (ETS), such as the PU.1 protein required for the activation of granulocytes, monocytes and B cells (217-219). Additionally, IRF6 is another IRF regulator of immune cell differentiation, including the major cell component of the skin, keratinocytes, by

inducing the expression of chemokines essential for epithelial cell differentiation, namely C-C motif ligand 5 (CCL5) (220, 221).

Table 3. Examples of fundamental IRFs in antiviral TI-IFN-induction.

IRF	Cell Type Expression	Induction as ISGs	Major Antiviral Action	Reference(s)
IRF3	Most cell types (Ubiquitously expressed)	No	Master inducer of early-stage TI-IFNs/Direct induction of ISGs	(210-214)
IRF5	Dendritic cells, myeloid cells, and B cells	Yes	Specific TI-IFN induction	(203, 205, 207)
IRF7	Lymphoid cells	Yes	Master inducer of late-stage TI-IFNs	(222, 223)
IRF9	Low levels in multiple cell types	Yes	Regulator of JAK/STAT-based IFN-induction	(224, 225)

Abbreviations: IRF, Interferon regulatory factor; TI-IFN, type I interferon; ISGs, IFN-stimulated genes; JAK, Janus kinase; STAT, signal transducers and activators of transcription.

IRF1 and IRF2 share the same IAD and work together in a competitive mode during virus sensing by which IRF1 acts as a transcriptional activator of IFN inducible genes and IRF2 as a repressor (226). IRF1, just like IRF5, is virus and cell-type specific and it is considered to be non-essential for the direct activation of IFNs upon sensing cytosolic viruses (62, 194). IRF2 inhibits IRF1-dependent IFN-induction but can also work as a positive regulator of proinflammatory cytokines (226-228).

IRF9 acts as a positive regulator of TI-IFNs through the Janus kinas-signal transducer and activator of transcription (JAK-STAT) pathway (**Fig.1.1.5**). Secreted TI-IFNs, for example

via PRR-driven IRF3 pathways, bind to their corresponding receptors IFNAR1 and IFNAR2 resulting in the phosphorylation of their receptor-bound JAK kinases tyrosine kinase 2 (TYK2) and Janus kinase 1 (JAK1), respectively (229). In turn, the activated JAK kinases recruit and phosphorylate STAT transcription factors, STAT1 and STAT2, which then recruit IRF9 forming an activated transcription tri-complex, known as IFN-stimulated gene factor 3 (ISGF3). This complex can then transfer to the nucleus and bind to ISRE of IFN-stimulated genes (ISGs) that include IRF7 which contributes the most in mediating the second wave of TI-IFNs (224, 230, 231). Therefore, IRF9, unlike other IRFs, does not act solely as a transcription factor, but it rather uses its IAD to interact with the coiled-coil (CC) domain of STAT2 to form the ISG3F complex, only then it becomes transcriptionally active. IFN-dependent ISG induction through STAT1/2 association with IRF9 contributes to the upregulation of different subsets of ISGs, such as IRF7, PRRs, OAS/RNase L system proteins (**Section 1.1.1**) and IFN-induced transmembrane proteins (IFITMs) which are protein factors that inhibit the entry of enveloped viruses through alteration of viral membrane fusion (199, 232).

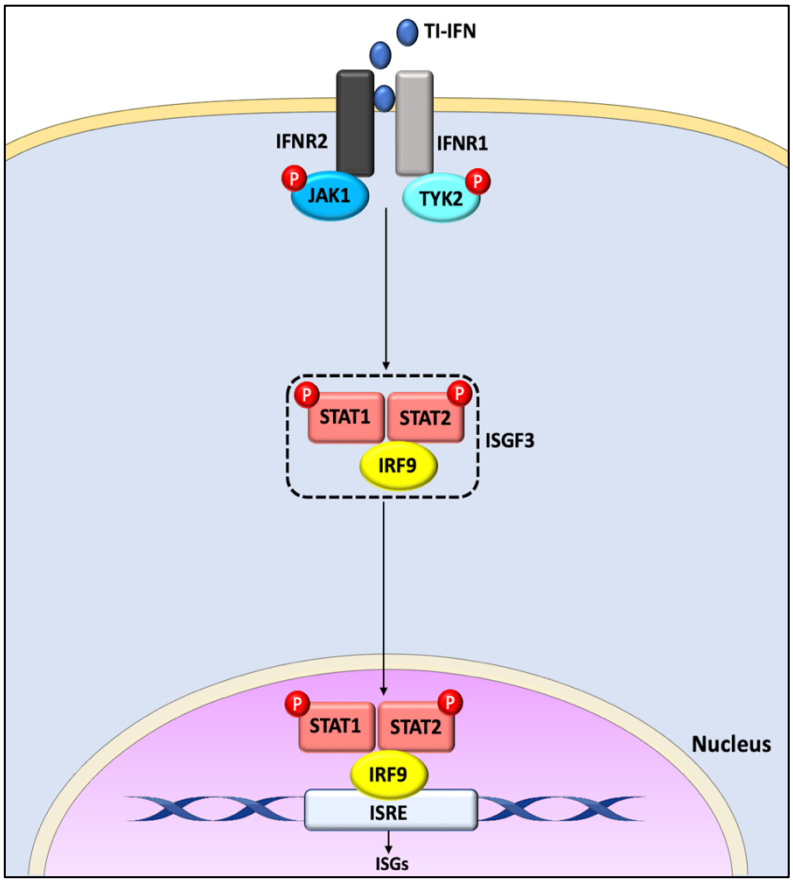

Figure 1.1.5 TI-IFN-induced JAK-STAT pathway. Ligand binding of TI-IFNs to their receptors, IFNR1 and IFNR2, activates their bound tyrosine kinases TYK2 and JAK1, respectively. This results in the formation of the transcription factor complex ISGF3 consisting of STAT1, STAT2 and IRF9. ISGF3 migrates to the nucleus and binds to the ISRE in the promoter region of ISGs to initiate gene expression. Servier Medical Art (https://smart.servier.com/) was used to construct the illustration.

1.1.5 IRF3 in Antiviral Immunity

IRF3 plays the strongest role in TI-IFN gene regulation at the early phase of antiviral innate immunity in most cells (233). The fact that viruses routinely evolve specific inhibitors of IRF3 activation highlights its importance in early antiviral human defenses (234-236) (**Table 4**). Additionally, defects in the molecular components of the IRF3 signaling pathways increase susceptibility to viral infections (237-240). Clarifying the molecular

anatomy and rate-limiting control points of the IRF3-activating system is not only essential to expand our knowledge of human antiviral immunity and immunization, but it is also a tool for a better understanding of type I interferonopathies given the key role of IRF3 signaling in these diseases (203, 211, 241, 242) (**Section 1.1.5.5**).

Two kinases have been associated with the direct activation of IRF3: IκB kinase epsilon (IKKε), also known as IKKi (Inducible IKK), and TANK-binding kinase-1 (TBK1), also called NAK (NF-κB-activating kinase). Upon virus infection, IRF3 kinases are believed to form complexes with scaffold proteins that direct them toward specific subcellular signaling for activation through phosphorylation and dimerization. NF-kappa-B-activating kinase-associated protein 1 (NAP1), TANK-binding kinase 1-binding protein 1 (TBKBP1), also known as similar to NAP1 TBK1 adaptor (SINTBAD), and TRAF family member-associated NF-kappa-B activator (TANK) are expected to be essential subunits for IKKε and TBK1 scaffolding (211, 235, 243, 244). However, there are many unanswered questions regarding the formation of IRF3-activation complexes, including the exact mechanism by which scaffold proteins interact with IKKε and TBK1 and their detailed functions.

1.1.5.1 Structural basis of IRF3 activity

In 1995, bioinformatic homology screening of IRF1 and IRF2 enabled the discovery of IRF3, which defined it as a 50 kDa ISRE-binding protein (245). At a transcriptional level, nuclear-translocated IRF3 was found to interact with the regulatory elements of IFN gene promoters via its DNA-binding domain (DBD). Such interactions include the positive regulatory domains I and III (PRDI and PRDIII) of the IFNβ promoter (**Fig.1.1.1**), by which antiviral IFNβ is induced (65, 246, 247). IRF3 can also bind directly to ISREs within

ISG promoters leading to an IFN-independent induction of a subset of ISGs that include the expression of the chemokine IP-10, ISG15 (**Section 1.1.1**) and ISG54, a protein that can inhibit viral mRNA translation (213, 248, 249). Although the IRF3-DBD shares more than 30% homology with other IRF members (245), the identification of its crystal structure indicated that it differs in its DNA binding affinity due to the flexibility of loop 1 (L1) (250). Additionally, the mobile nature of the IRF3-DBD loops appears to be responsible for the efficient binding (251). The IRF3-DBD is connected to an IRF-associated domain (IAD) by a proline-rich linker. This linker has been shown to act as a suppressor of IRF3 transactivation upon its phosphorylation by glycogen synthase kinase 3 (GSK3) (252).

The C-terminal domain of IRF3 contains serine/threonine phosphorylation sites that are critical for its activation (253) (**Fig.1.1.6**). Inactive IRF3, which is located in the cytoplasm of most cells, is exposed to both phosphorylation and dimerization upon viral infection that allow for its nuclear translocation and subsequent transactivation of TI-IFN genes (62, 254). IRF3 phosphorylation was reported for the first time in 1998 in human embryonic kidney 293(HEK293) cells that were infected with Sendai virus (SeV) (255). On the other hand, the dimerization mechanism by which IRF3 is transcriptionally activated has not yet been confirmed. There is a well-established model of IRF3 dimerization that depends on the interaction between two phosphorylated IRF3 molecules to form a homodimer (60, 65, 256-258). Alternatively, the autoinhibition model proposes an ability of IRF3 to bind to another homologous pair, mostly IRF7, to form a heterodimer by which phosphorylation can also release the autoinhibition structure for heterodimerization. It has been demonstrated that IRF3 interacts with IRF7 at their C-terminal domains in virus-infected HEK293T cells (259, 260). In any event, both models agree on IRF3 nuclear translocation following dimerization (65). Dimerization also allows the active form of IRF3 to bind

transcriptional coactivators, including p300/CREB binding protein (CBP). IRF3 serine residues 386 and 396 were shown to be critical for IRF3 phosphorylation and mutations of residues, such as arginine residue 385, that interact with phosphorylated 386 serine residue upon dimerization disrupt IRF3 activation and nuclear translocation (254, 261). Additionally, serine 396 mutation abolished IRF3 interaction with p300/CREB following SeV infection (255).

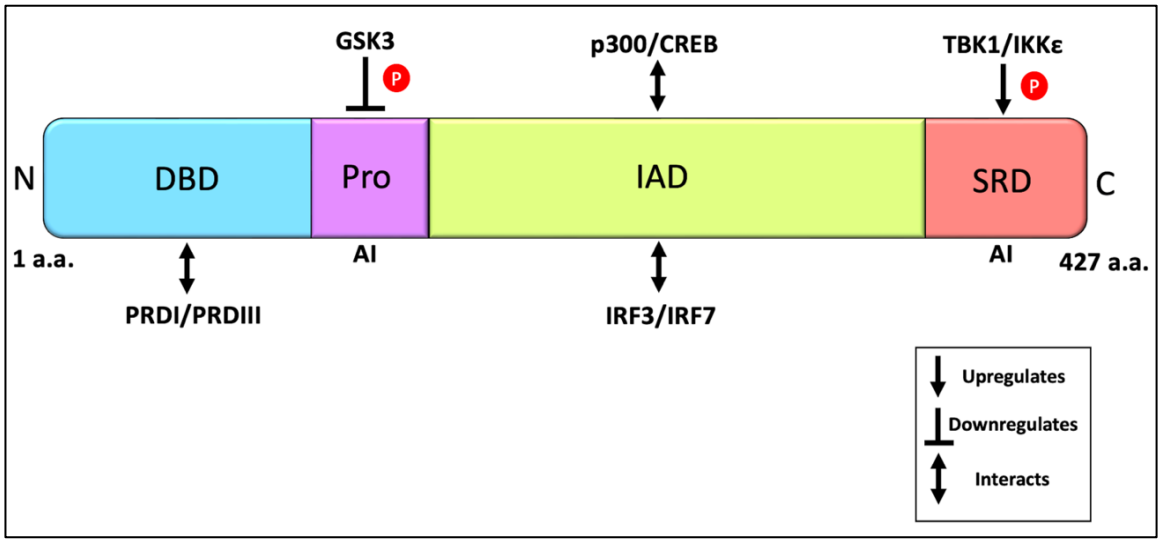

Figure 1.1.6 Schematic illustration of the molecular organization of IRF3. The IRF3 protein consists of 427 amino acid residues. From the N-terminus (N) to the C-terminus (C): DNA-binding domain (DBD) to bind to PRDI/PRDIII within ISREs of the target gene promoter, proline-rich linker (Pro) that is targeted by GSK3 for inhibition through phosphorylation (P), IRF-associated domain (IAD) to interact with IRFs and cofactors and signal response domain (SRD) sites containing sites for phosphorylation (P), such as Ser386 and Ser396. Autoinhibitory (AI) sites are accommodated at proline linker and SRD.

Analysis of the crystal structure of the C-terminal domain of IRF3 suggests that IRF3 originates from the Smad family due to its resemblance with their MAD homology 2 (MH2) domain (256). The Smad proteins are involved in the mediation and regulation of transforming growth factor beta (TGFβ) cytokines which have multiple roles in modulating cell growth, immunoregulation and tumour suppression. Comparable with IRF3, the Smads are activated upon phosphorylation of serine/threonine residues at the MH2 domain that is required for their translocation from the cytoplasm to the nucleus (262, 263). Interestingly, members of the Smad proteins are associated with antiviral immunity. For example, TGFβ and Smad3 regulate IFNβ-driven IRF7 activation via the interaction between IRF7-IAD and Smad3-MH2 (264, 265). Additionally, a study published in 2016 revealed the need for TGFβ and Smad 2/3 for the optimal secretion of IFNβ upon infection with human respiratory syncytial virus (RSV) (266). The direct association in signaling between Smads and IRF3 was reported and showed IRF3 as a negative regulator of the TGFβ-dependent Smad3 activation (267). This indicates a cross-regulation between IRF3 and IRF7 in the TGFβ-dependent Smad3 pathway.

1.1.5.2 The antiviral IRF3 signaling pathways

The roles of IRF3 have been expanding through the years to include antibacterial immunity, anticancer immunity and T cell-mediated immunity (268-270). However, the best-characterized pathways leading to IRF3 activation are those related to antiviral immunity. Like canonical antiviral NF-κB activation, the virion constituents, particularly viral nucleic acids, are sensed by PRRs that include TLR3/7/8/9, RIG-I, MDA5 and the specialized sensor of DNA cGAS. These receptors use adaptor proteins to stimulate signal transduction pathways that sequentially trigger the next molecule downstream in the pathway ultimately culminating in the activation of IRF3 and the expression of TI-IFN genes (194, 244, 271-273) (**Fig.1.1.7**).

One of the major PRRs leading to IRF3 activation is toll-like receptor 3 (TLR3), which is a critical receptor for viral double-stranded RNA (**Table 1**). The binding of TLR3 to its ligand in the endosomes of innate immune cells leads to the dimerization of its cytosol-facing toll-interleukin-1 (TIR) domains. In turn, the TLR3 TIR domain interacts with its adaptor molecule TRIF through a homotypic TIR-TIR association (274-278). TRIF then binds to an essential regulator of the TLR3-based IRF3 pathway, TNF receptor-associated factor 3 (TRAF3). TRIF was suggested to interact with TRAF3 via its 160-181 amino acid residues (160-181 a.a.) located at the N-terminal domain (279). This allows the recruitment and activation of the IRF3-activation complex components through ubiquitination (280-282).

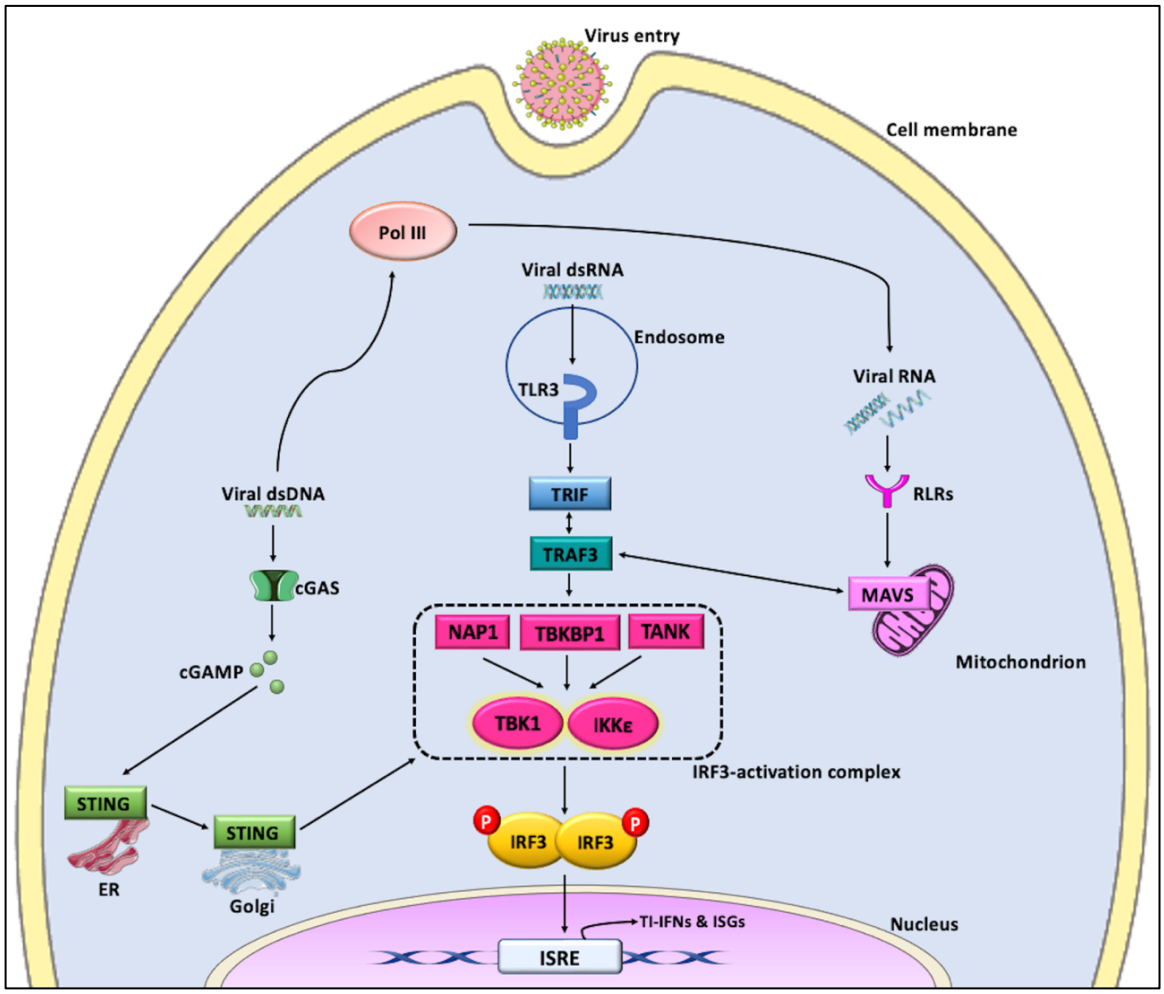

Figure 1.1.7 Antiviral PRR signaling pathways to IRF3 activation. Upon viral infection, the innate immune sensors cGAS, TLR3 and RIG-I-like receptors (RLRs) interact with their viral ligands leading to the activation of their adaptor proteins STING, TRIF and MAVS, respectively. RNA polymerase III (Pol III) transcribes cytosolic DNA into 5′- triphosphate dsRNA for recognition by RLRs. cGAS catalyzes the formation of the isomer 2′,5′ cGAMP, which in turn, binds to STING in the endoplasmic reticulum (ER). Activated STING migrates to the Golgi and triggers the activation of IRF3 kinases. Both TRIF and MAVS use TRAF3 to activate TBK1 and IKKε. The kinases are recruited and regulated via complexing with NAP1, TBKBP1 and TANK. IRF3 is next activated through phosphorylation and dimerization that result in its nuclear translocation. In the nucleus, the active form of IRF3 dimers binds to ISRE-containing promoters resulting in the

transcription of TI-IFNs, for example, IFNβ, and ISGs. Servier Medical Art (https://smart.servier.com/) was used to construct the illustration.

In vitro studies have shown the ability of TRAF3 to interact with TRAF family member-associated NF-kappa-B activator (TANK) in IFNβ induction (283). Since TANK is a scaffold protein of IKKε and TBK1, TRAF3 is predicted to mediate the formation of the IRF3-activation complex. However, the exact mechanism by which TRAF3 activates IKKε and TBK1 is still debated. It has been suggested that upon its activation, TRAF3 modifies the IRF3 kinases through ligation of polyubiquitin chains that are required for their association with scaffold proteins (284). Regardless, the role of TRAF3 in activating IRF3 downstream has been highlighted in multiple studies of viral inhibitors that target it, TRAF3 deficiency and TRAF3 knockout mice. VP3 protein derived from infectious bursal disease virus (IBDV) has been found to inhibit IRF3 activation by blocking the formation of the TRAF3-TBK1 complex through the reduction of TRAF3 polyubiquitination (280). Another virus that mimics IBDV in targeting TRAF3 ubiquitination is Influenza A virus (IAV) through the viral inhibitor non-structural protein 1 (NS1) (285). The difference between the two inhibitors is that VP3 targets K33-linked polyubiquitination, while NSI targets an E3 ubiquitin ligase (280, 285). Additionally, patients with human TRAF3 deficiency have been proven to be more susceptible to encephalitis caused by herpes simplex virus (HSV) due to the prevention of TLR3-dependent IFN production (237, 286). Following infection with Indiana vesiculovirus, mouse embryonic fibroblasts (MEFs) isolated from TRAF3 knockout mice showed a significant reduction in the phosphorylation of both TBK1 and IRF3 (287). In addition, studies in mice have shown that the secretion of TI-IFNs through TRAF3 occurs in dendritic cells and MEFs but not macrophages. This

cell-type specificity of the TRAF3 activity could add to the complexity of its role in the antiviral IRF3 pathways (287).

TRAF3 also acts as a mediator for the adaptor protein MAVS (288). Recruitment of TBK1 and IKKε to the mitochondria for IRF3 phosphorylation by MAVS has been noted as a role of TRAF3 in this system (289). This is due to TRAF3 accumulation, facilitated by TRAF3 interacting protein 3 (TRAF3IP3), in the mitochondria upon RIG-I sensing of negative-strand RNA viruses (−ssRNA viruses) and MDA5 sensing of positive-strand RNA viruses (+ssRNA viruses) (104, 288) (**Section 1.1.2**). It has been documented that TI-IFN induction in mice lacking TRAF3IP3 is significantly reduced upon RNA virus infection (288). In vitro, RIG-I and MDA5 can bind to short and long 5′-triphosphate single-stranded RNA, respectively. Both receptors have been found to function in length-based detection of double-stranded RNA generated by Indiana vesiculovirus (290). Working through the RIG-1 sensing system, RNA polymerase III (Pol III) can activate the MAVS-based IRF3 pathway by transcribing cytosolic DNA into 5′-triphosphate double-stranded RNA (291).

MAVS is composed of 540 amino acid residues, and it is mainly found on the outer mitochondrial membrane. The functional domains of MAVS include a caspase recruitment domain (CARD), a proline-rich linker and a transmembrane domain (TMD), from the N-terminus to the C-terminus, respectively (292, 293). Upon MAVS discovery in 2005, it was named CARD adaptor inducing IFN-β (Cardif) that uses its CARD to interact with RIG-I receptors. In the same study, MAVS was found to specifically recruit IKKε, but not TBK1, in HEK293T cells (294). Therefore, it was proposed that IKKε might be favored by MAVS for IRF3 activation in contrast to TRIF which is associated with TBK1, but not IKKε, in HEK293T cells. However, the identity of the IRF3 kinase chosen by the adaptor proteins

could also be virus or cell-type specific (294, 295). For example, MAVS was found to recruit both TBK1 and IKKε pre-complexed with TRAFs, namely TRAF2/3/6, in HEK293T cells upon SeV infection (289). Both kinases were also demonstrated to phosphorylate MAVS upon SeV infection at serine 442 residue to recruit IRF3 to the adaptor protein for activation by TBK1 and IKKε (296).

IRF3 kinases can also be activated directly through the cGAS-STING DNA sensing pathway. As mentioned in **section 1.1.1**, cGAS is an essential sensor of viral double-stranded DNA in the cytosol that catalyzes the formation of cGAMP to activate its adaptor protein STING causing it to translocate from the endoplasmic reticulum (ER) to the Golgi following oligomerization. STING oligomerization is required for the activation of TBK1 and the consecutive phosphorylation of IRF3 (115, 297-299). The interaction between STING and TBK1 has been recently shown to occur through a motif at the C-terminus of STING, named PLPLRT/SD (300). Several viruses have been shown to target cGAS/STING-dependent IRF3 activation including pseudorabies virus (PRV) using the viral inhibitor UL13 (301), herpes simplex virus 1 (HSV-1) with the viral inhibitor UL46 (302) and the poxvirus immune nucleases (poxins) that target cGAMP for degradation (303).

PRR-regulated TRIF, MAVS and STING result in the activation of TBK1 and IKKε required for IRF3 phosphorylation. The production of TI-IFNs via IRF3 at an early stage of viral infection triggers the expression of ISGs through the binding to ISREs in their promoters. ISG induction in nearby cells is mediated in a positive feedback manner through crosstalk with the Janus kinas- JAK-STAT pathway (**Figure 1.1.5**). This leads to an IFN-induced antiviral state in infected cells that limits virus spread and assists in triggering the

emergence of adaptive immunity (21, 67, 197, 202, 225, 304-307). Given the importance of rapidly establishing the antiviral state after infection, it is unsurprising that some systems have evolved to fast-track transference of the interference state across infected tissue. For example, cGAMP has been shown to passively diffuse into adjacent cells through gap junctions and can be inadvertently transported inside virions to uninfected cells (131, 308).

1.1.5.3 Regulation of antiviral IRF3-activation components

In vitro studies initially identified IκB kinase epsilon (IKKε) and TANK-binding kinase-1 (TBK1) as activators of the NF-κB pathway (309-311). IKKε was discovered to phosphorylase IκB kinase alpha (IKKα) (309, 310), while TBK1 was shown to phosphorylase both IKKα and IκB kinase beta (IKKβ) (311). IKKα and IKKβ form together with NEMO the IKK- activation complex of the canonical NF-κB pathway (312) (**Fig.1.1.4A**). However, the role of IKKε and TBK1 in the NF-κB pathway was later shown to involve the regulation of NF-κB mediators, rather than the direct activation of NF-κB kinases (313-315). The non-canonical NF-κB pathway depends on the interaction between the transcription factors p52 and RelB mediated by the NF-κB protein p100. NIK targets IKKα for phosphorylation, by which the latter activates and phosphorylases p100 exposing it to ubiquitination. This leads to the formation of the heterodimer p52/RelB that activates NF-κB (316, 317) (**Fig.1.1.4B**). TBK1 was found to target NIK degradation for the negative regulation of NF-κB activation (313). On the other hand, IKKε has been linked to the phosphorylation of NF-κB transcription factor p65, in T cell-dependent costimulation, which along with NF-κB p50, co-transactivate NF-κB genes (181, 314, 315, 318).

In 2003, it was discovered that IKKε and TBK1 rather play a pivotal role in the IRF3 signaling pathways, specifically in the direct phosphorylation of IRF3 (319). Both kinases

are capable of phosphorylating IRF3 at the C-terminal domain resulting in its dimerization and transcriptional activity (320-322). IKKε and TBK1 also activate IRF7, which as mentioned in **section 1.1.4**, is another regulator of TI-IFNs, in the same manner as IRF3 (322-324). IRF3 can operate in a consecutive corporation with IRF7 to drive waves of TI-IFNs. For example, PRRs activate IRF3 to drive IFNβ induction, which in turn triggers IRF7 expression to drive IFNα induction in monocytes (325).

A previous study conducted in mouse embryonic fibroblasts (MEFs) derived from TBK1-deficient mice showed their inability to drive the expression of IRF3-dependent TI-IFNs upon RNA virus infection in comparison to the wild-type MEFs. Additionally, IRF3 phosphorylation and translocation were prevented following infection with Sendai virus (SV) (326). IKKε-knockout mice have been observed to be more prone to viral infection, showing a reduction in the induction of ISG expression, including adenosine deaminase acting on RNA 1(ADAR1) (327). This supports the essential role of IKKε in activating ISG expression through phosphorylation of the transcription factor STAT1. Both TBK1 and IKKε can phosphorylate IRF3, but only IKKε can phosphorylate STAT1(327-329). An interesting finding from a recent study on myeloid TBK1-deficient mice revealed an exceptional reduction in TI-IFN induction upon influenza A virus (IAV) infection coincident with an upregulation of IKKε. This suggests that myeloid-specific loss of TBK1-dependent TI-IFN induction might be compensated by the upregulation of IKKε in lung myeloid cells (330).

The activation of IKKε and TBK1 involves three scaffold mediators that provide a platform for their assembly and subsequent IRF3 phosphorylation. These proteins are NAP1, TBKBP1/SINTBAD and TANK. Similarly, they act as scaffold proteins for IRF7

activation. The exact mechanism by which NAP1, TBKBP1 and TANK interact with IKKε and TBK1 remains unclear (282, 331-335). In many respects, research on IRF3 activation has traditionally proceeded on the presumption of analogy to the well-characterized NF-κB-activating IKK complex, largely due to the similarity of the respective kinases and the involvement of adaptor proteins associated with their activation. However, as will be discussed, though there are analogies, it is still not entirely clear if the IRF3-activating system operates in the same manner as the IKK complex. Indeed, there is evidence that it may be more complex and stimulus-dependent.

To understand the regulation of IKKε and TBK1, it is necessary first to look at their structures (**Fig.1.1.8B**). Both kinases share around 28% similarity with the canonical kinases IKKα and IKKβ (**Fig.1.1.8A**), including having a kinase domain (KD), a ubiquitin-like domain (ULD) and a scaffold dimerization domain (SDD), respectively from the N-terminus to the C-terminus. Despite these similarities, the relative orientation of these domains differs between canonical and non-canonical NF-κB kinases. The crystal structure of active TBK1 indicated that the stability of TBK1 dimer is higher than that of IKKβ due to a large-scale of TBK1 dimerization interfaces. This suggests the requirement of TBK1 dimer stabilization for its regulation which could be achieved through complexing with scaffold proteins (310, 329, 336, 337).

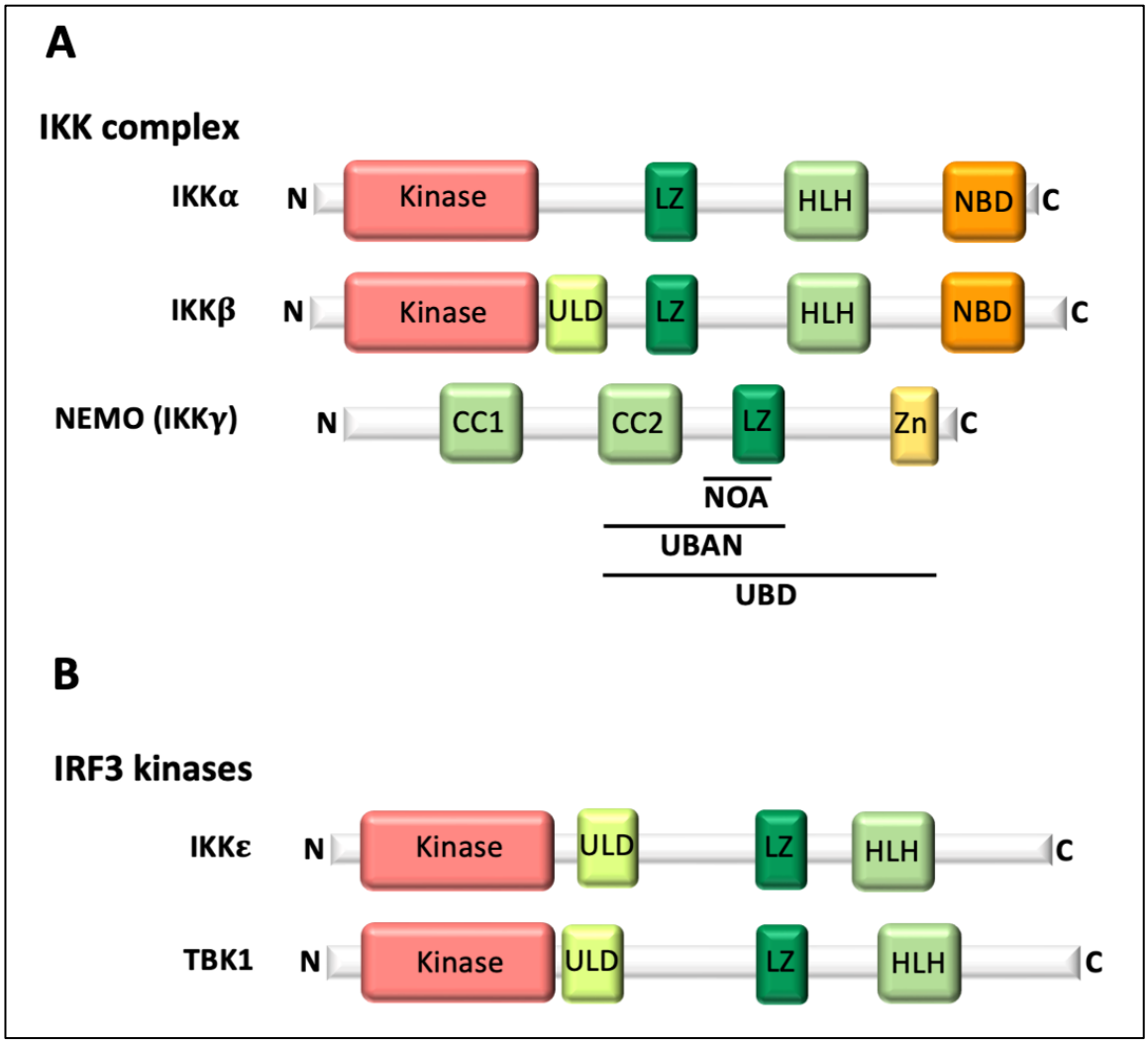

Figure 1.1.8 Domain organization of the components of the IKK complex and IRF3 kinases. (A) NF-κB proteins are activated by the IKK complex composed of the kinases of IκB inhibitors, IKKα and IKKβ, and the regulator of IκB kinases nuclear factor κB (NF-κB) essential modulator (NEMO). IκB kinases gain their catalytic activity from their kinase domain. Unlike IKKα, IKKβ requires a ubiquitin-like domain (ULD) for an efficient catalytic activity. They both have a scaffold dimerization domain (SDD) by which they dimerize via their helix-loop-helix (HLH) motif and bind to NEMO through their NEMO binding domain (NBD). NEMO dimerizes via its coiled-coil motif, CC1 and CC2, and it is exposed to ubiquitination through its ubiquitin-binding domain including multiple ubiquitination sites: zinc (Zn) finger, NEMO optineurin ABIN2 (NOA), A20 binding and inhibitor of NF-κB (ABIN) and NEMO (UBAN). (B) IRF3 kinases IKKε and TBK1. From

the N-terminus (N) to the C-terminus (C): a kinase domain exerting the catalytic activity, a ubiquitin-like domain (ULD) and a scaffold dimerization domain (SDD) containing a leucine zipper (LZ) motif and a helix-loop-helix (HLH).

IKKε and TBK1 are highly homologous sharing around 65% similarity, which could indicate the formation of a heterodimer upon activation (318). However, in vitro attempts to show their interaction have not been successful. This, in turn, could support the homodimerization or a homo-oligomerization model of IKKε and TBK1 upon activation. Indeed, IKKε dimers have been observed through co-immunoprecipitation (310). In addition, both kinases use auto-transphosphorylation at the serine-172 residue of the kinase domain as a mode of activation (329, 336, 338). The kinase domain requires the ubiquitin-like domain (ULD) for its functionality as ULD deficiency has been shown to abolish, not only IRF3 activation, but also autophosphorylation of TBK1 and IKKε (339).

A NEMO-binding domain (NBD) in IKKα and IKKβ appears to lack an equivalent in IKKε and TBK1 (**Fig.1.1.8**). Instead, IKKε and TBK1 possess α-helical coiled coils at the C-terminal domain that mediate their association with adaptor scaffold proteins via coiled coil 2 (CC2). The structural similarity between NAP1, TBKBP1 and TANK to NEMO predicts a similar role of these pathway components in IRF3 activation (329, 335). NEMO dimerizes via its coiled-coil motif and uses its ubiquitin-binding domain (NOA/UBAN) to interact with lysine-63 (K63)-linked polyubiquitin (**Fig.1.1.8A** & **Section 1.1.3**). Through association with TRAF-regulated ubiquitination, NEMO acts as a recruiter and regulator of canonical kinases that allows for their oligomerization, auto-trans-phosphorylation and activation (340-342). In the same manner as NEMO, the predicted model of the interaction

between the aforementioned scaffold proteins and IKKε or TBK1 is expected to be based on ubiquitination-induced oligomerization (329, 335) (**Fig.1.1.9**).

All three scaffold proteins target the same binding site at the kinases, suggesting a competitive mode of binding. This model of interaction is supported by a study that reported the presence of exclusive TBK1-complexes at different cellular sites rather than inclusive TBK1-complexes (102). An indication that what determines which scaffold protein will bind to the kinases is based on the signal transduction triggered by the stimulator, by which NAP1, TBKBP1 and TANK recruit IKKε or TBK1 and direct their functional specificity. This might also explain why certain scaffold proteins have been detected to interact with IKKε or TBK1 in different IRF3 activation pathways (282, 333, 335, 343, 344).

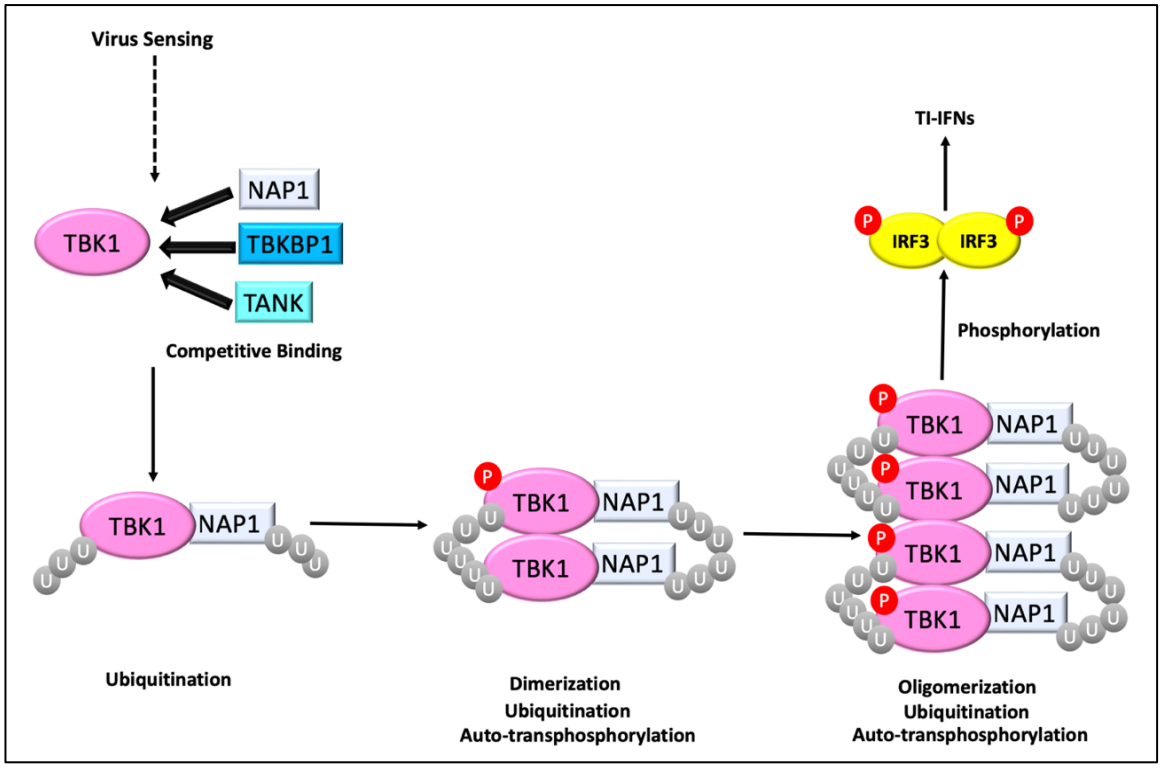

Figure 1.1.9 Proposed model of TBK1 or IKKε interaction with scaffold proteins in IRF3 activation. Cellular signaling upon virus detection recruits the scaffold proteins NAP1, TBKBP1 and

TANK to TBK1 for competitive binding to coiled-coil 2(CC2) of the kinase's helix-loop-helix (HLH) motif. Based on the induced signaling, alternative complexes, such as TBK1-NAP1, are formed to recruit TBK1 towards a certain subcellular location. The TBK1-NAP1 complex is ubiquitously modified by adaptor proteins, such as TRAF3, leading to dimerization. TBK1 homodimers form in a specific orientation by which the kinase domains are facing each other for transphosphorylation. Ubiquitination allows for further homodimers to recruit, which results in a further transphosphorylation through oligomerization. Overexpression of TBK1-NAP1 complexes causes the dimerization and phosphorylation of IRF3. In turn, IRF3 homodimers migrate to the nucleus and bind to IFN gene promoters for TI-IFN induction. IKKε is predicted to follow the same model of complexing with scaffold proteins. P: phosphorylation, U: ubiquitination.

NAP1 has been related to TLR3/RIG-I-driven IRF3 activation as NAP1 knockdown resulted in a reduction of IFNβ induction upon RNA virus infection and poly I:C stimulation (345). In agreement with this, tripartite motif-containing protein 38 (TRIM38) has been found to inhibit TLR3/RIG-I-driven IRF3 activation by targeting NAP1 for degradation (346). The role of NAP1 as a mediator of the negative regulation of IRF3 activation has been also seen through the interaction with tax1-binding protein 1 (TAX1BP1), which can inhibit the activation of IKKε and TBK1 (347, 348). TBKBP1 and TANK have been also associated with RNA sensing. The viral inhibitor non-structural protein 3 (Nsp3) derived from severe acute respiratory syndrome coronavirus 2 (SARS-CoV-2) has been found to inhibit TBK1 through binding to TBK1-TBKBP1 complexes, which inhibited IRF3 activation (349, 350). Upon poly I:C stimulation, TBK1-TANK complexes have been implicated in the control of IRF3-dependent IFNβ induction with suppression of IFNβ production in TANK knockout mice (351). All three scaffold

proteins were targeted by the vaccina virus protein C6 (VVC6) for the inhibition of IRF3 and IRF7 activation (352).

Interestingly, there is currently no evidence of NAP1/TBKBP1/TANK interaction with IRF3 kinases upon activation of the cGAS-STING pathway. This could be attributed to the ability of STING to directly recruit TBK1 for IRF3 phosphorylation or the requirement of IKKε/TBK1 ubiquitination by TRAF3 for recognition by the scaffold proteins (115, 284). It also supports previous studies on the requirement of scaffold proteins for the activity of IRF3 kinases by upstream stimuli (335). However, the role of these three scaffold proteins in recruiting TBK1 downstream for STING-driven IRF3 activation cannot be excluded until further exploration of their potential functions in the cGAS-STING pathway. Although, NAP1 and TBKBP1 have been indicated to follow a punctate subcellular localization, they have been also partially detected at the Golgi compartments, which can refer to a role in TBK1 recruitment to the Golgi where active STING resides (335, 353). In addition, the NEMO homologue optineurin (OPTN), which is also partially located at the Golgi, has been found to recruit TBK1 to the Golgi upon RNA sensing for optimal activation (353-355). This may suggest that other scaffold proteins can act in the same manner upon DNA stimulation. Scaffold proteins could also have another role in relation to DNA sensing. For example, TANK has been discovered to migrate from its perinuclear localization to autophagy-related vesicles upon DNA stimulation (335). Investigating the closely associated proteins with each scaffold protein and kinase might provide insights into the assembly of the IKKε or TBK1 complexes.

1.1.5.4 Viral inhibitors of the components of IRF3-activation complex

Viruses evolve mechanisms to target human antiviral immunity after long periods of host-virus coevolution. Studying viral inhibitory strategies can provide key insights into antiviral immunity and therapeutics and vaccine development by understanding how viruses target key-rate limiting steps in innate immune signaling. It also boosts our understanding of the human immune system to treat immune-mediated diseases and disorders. This specifically applies to the antiviral IRF3 signaling pathways as many immune conditions have been related to them including type-I interferonopathies, such as systemic lupus erythematosus (SLE), rheumatoid arthritis (RA) and multiple sclerosis (MS) (203, 242) (**Section 1.1.5.5**). The IRF3 signaling pathways have been also associated with antitumor immunity through the detection of damage-associated molecular patterns (DAMPs), for example, activating the cGAS/STING-driven IRF3 pathway via damaged self-DNA (211, 356). Different viral inhibitors have been discovered to inhibit IRF3 activation by targeting the components of the IRF3-activation complex. The mode of targeting varies to include direct interaction with the kinases or their scaffold proteins, acting as a substrate for IKKε/TBK1 or causing their degradation via viral proteases. **Table 4** presents multiple IRF3 viral inhibitors that target IRF3 kinases and their scaffold proteins.

Table 4. IRF3-based viral inhibitors of IKKε, TBK1, NAP1, TBKBP1 and TANK.

Viral inhibitor	Virus	Target for IRF3 inhibition	Mode of targeting	Reference(s)
MC159	Molluscum Contagiosum	TBK1/ IKKε	Direct interaction	(225)
MC160	Molluscum Contagiosum	TBK1	Unknown	(225)
VVN1/VVN2	Vaccinia Virus	TBK1	Unknown	(344, 345)
VVC6	Vaccinia Virus	NAP1/TBKBP1/TANK	Direct interaction with scaffold proteins	(339)
Nsp3	SARS-CoV-2	TBK1/TBKBP1	Direct interaction with the TBK1-TBKBP1 complex	(336)
SPI-2	Vaccinia Virus	TBK1/IKKε	Direct interaction	(346)
$\gamma_1$34.5	Herpes Simplex Viruses	TBK1	Direct interaction	(347)
HIV-1 protease	HIV-1	TBK1	Cleavage	(348)
BFRF1	Epstein-Barr Virus	IKKε	Direct interaction	(349)
Paramyxovirus V proteins	Rubulavirus	TBK1/IKKε	Alternative substrates	(350)
UL46	Herpes Simplex Virus 1	TBK1	Direct interaction	(351)
VP35	Ebola Virus	TBK1/IKKε	Direct interaction	(352)

Abbreviations: Nsp3, Non-structural protein 3; SARS-CoV-2, severe acute respiratory syndrome coronavirus 2; SPI-2, serine proteinase inhibitor 2, HIV-1; Human immunodeficiency virus 1.

1.1.5.5 The IRF3 pathways in diseases and disorders

Because IRF3 is a major inducer of TI-IFNs and ISGs, it has been associated with type-I interferonopathies which are autoimmune and autoinflammatory disorders resulting from abrogated TI-IFN activation. Examples of the pathogenesis of TI-interferonopathies

include the aberrant recognition of self-DNA, defects of nucleic acid receptors and abnormalities of signaling components within the IRF3 pathways (357).

RIG-I pathway abnormalities have their share in TI-interferonopathies, for instance, mutations of interferon induced with helicase C domain 1 (IFIH1) gene responsible for encoding MDA5 have been found to increase the susceptibly to TI-diabetes (358). The involvement of IFIH1 mutations in TI-diabetes remains unclear but IFIH1 single-nucleotide polymorphisms (SNPs), such as A946T SNP, were shown to increase TI-IFN production in peripheral blood mononuclear cells (PBMCs) in mice in parallel with being resistance against a lethal encephalomyocarditis virus (EMCV) infection (359, 360). Interestingly, IFIH1 A946T SNP was also observed to increase the risk of developing other TI-interferonopathies like systemic lupus erythematosus (SLE) (358).

SLE is a complex autoimmune disorder caused by multiple genetic variants and environmental factors. Symptoms of SLE differ among patients and can include arthritis, rash, ulcers and neurological disorders. Although around 50% of SLE patients show high levels of TI-IFN secretion, such as IKKα, other patients rather have low IFN activity (361-363). A study published in 2011 revealed that an SNP mutation of MAVS (C79F) accounted for the reduction in TI-IFN expression, exclusively, in African American SLE patients. The C79F MAVS mutation disrupted antiviral MAVS-dependent responses against viral infections, such as SeV and influenza A (IAV), as well as MAVS-TRAF3 interaction (362). MAVS could also play a role in the SLE TI-interferonopathy variant as it was shown to interact with eyes absent 4 (EYA4) protein, a predicted stimulator of SLE (362, 364). Additionally, MAVS was found to induce autoreactive antibodies in bone marrow-derived cells of the SLE mouse model (FcγRIIb-deficient mice) (365). Therefore,

genetic variants and ancestral background are taken into consideration for effective targeting of SLE immune drivers.

A major factor in obesity is the increase in inflammatory mediators, such as C-reactive protein (CRP) (AKA low-grade inflammation), induced from the accumulation of nutrients, such as fats, in white adipose tissue (WAT) where macrophages predominantly resided (366-368). In an obese mouse model, the expression of IKKε has been found to increase significantly in white adipose tissue macrophages (ATMs) in a positive correlation with the number and density of ATMs (369, 370). In obese mice, both IKKε and TBK1 were able to phosphorylate phosphodiesterase 3B (PDE-3B), an essential enzyme for regulating energy metabolism and insulin in cardiovascular cells and WAT. The activated PDE-3B cleaves cGAMP preventing it from activating proteins important for lipolysis (371). Because IKKε and TBK1 can both activate PDE-3B, they can also be therapeutic targets for other disorders linked to the phosphodiesterase isoform, such as TII-diabetes. Indeed, the IKKε /TBK1 inhibitor amlexanox was shown to increase insulin sensitivity and fat oxidation in a clinical trial (372).

Table 5. Examples of diseases/disorders linked to IRF3 pathways.

IRF3 signaling component	Disorder/Disease	Reference(s)
RIG-I	Dermatomyositis and Sjögren's syndrome	(373)
MDA5	TI-diabetes, SLE, RA, MS and AGS	(358-360, 373)
TLR3	Cardiovascular diseases	(374)
cGAS-STING	Cancer, Inflammatory bowel disease and NASH	(375, 376)
MAVS	SLE, Diabetic kidney disease, cardiovascular diseases and cancer	(362, 364, 365, 377-379)
TRIF	ALS and Cancer	(380, 381)
TRAF3	B cell malignancy, Cardiovascular and neurological diseases	(382, 383)
IKKε /TBK1	Cancer and metabolic disorders: Obesity and TI-diabetes.	(331, 369, 370, 372)
IRF3	Cancer	(384-386)

Abbreviations: SLE, Systemic lupus erythematosus; RA, Rheumatoid arthritis; MS, Multiple sclerosis; AGS, Aicardi-Goutières syndrome; NASH, Nonalcoholic fatty liver disease; ALS, Amyotrophic lateral sclerosis.

TI-IFNs are believed to be an essential tumour marker since cancerous cells constitutively express them and they can be killed if TI-IFN genes, such as the IFNβ gene, are knocked out (387). In fact, IRF3 has been linked to multiple types of cancer, such as renal cell carcinoma and colorectal cancer, in which IRF3 was overexpressed and associated with a poor prognosis through the mediation of tumour-infiltrating immune cells (TIICs) and overexpression of immune-related genes (384, 385). Additionally, although deadly malignant pleural mesothelioma grew rapidly in IRF3 knocked-out mice, after 20 days, the size of the tumour was significantly smaller than in wild-type mice with the lattice radiation therapy (LRT) accelerating the shrinking indicating a positive response to treatment.

Tumour-infiltrating macrophages were also significantly less in IRF3 knocked-out mice in comparison to the control (386). Therefore, targeting IRF3 activation and regulation is an optimistic field for developing potential therapeutics for multiple types of cancer and interferonopathies.

1.2 Viruses

Viruses are microscopic infectious organisms that are conditioned to replicate through a host. The virus particle, known as virion, is composed of a genetic core of nucleic acid (DNA or RNA) coated by a protein shell called the capsid. An outer lipid membrane surrounding the capsid distinguishes enveloped viruses from non-enveloped viruses, also known as naked viruses (388) **(Fig.1.2.1)**. Through the capsid, the viral genetic material is protected and delivered into the host cell via disassembly (389, 390). Over time, if the virus does not find a suitable host, which includes mammals, plants, fungi, bacteria (bacteriophages) and unicellular organisms, the capsid will break down leading to virus disruption (389, 391, 392). Therefore, viruses have adapted a survival mechanism of rapid genetic evolution allowing it to become one of the most successful ancient inhabitants to be known (393-397). Recently, researchers identified multiple families of the giant DNA pandoraviruses that infect amoebae, the largest known viruses yet (~ 1 μm in length), dated back to more than 48,500 years ago at the Arctic thawed region indicating that old infectious viruses can be revived (398, 399).

The International Committee on Taxonomy of Viruses (ICTV) classifies viruses into different families based on similarities in genome, size, structure, and ancestral relationships. According to the ICTV database, there are currently 264 virus families including 11273 species (https://ictv.global/taxonomy/).

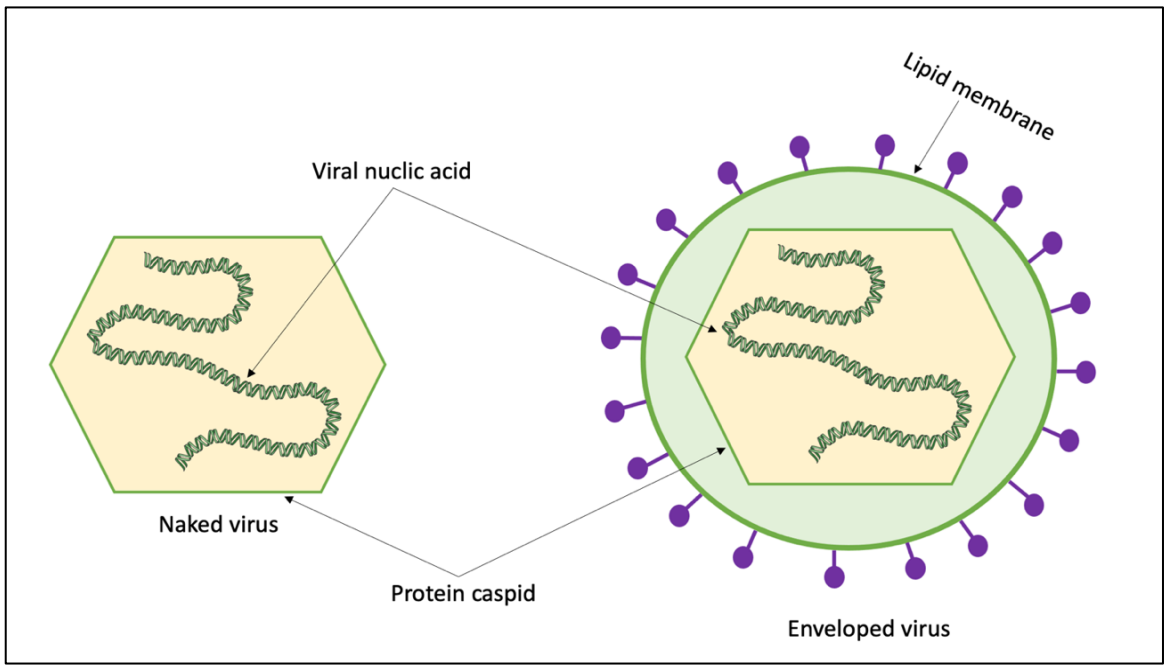

Figure 1.2.1 Basic structure of naked (non-enveloped) virus and enveloped virus. The core part of a virus relies on the genetic material (nucleic acid) surrounded by a protected shell of proteins known as the capsid. Enveloped viruses contain an outer lipid bilayer membrane. Servier Medical Art (https://smart.servier.com/) was used for the nucleic acid illustration.

A key criterion of virus classifications is the identity of the viral genome, which mainly falls into four categories: single-stranded-DNA (ssDNA), single-stranded RNA (ssRNA), double-stranded DNA (dsDNA), and double-stranded RNA (dsRNA). Whilst most viruses contain double-stranded nucleic acid, there are viruses with either positive or negative single-stranded genome (400). Regardless of the virus species, they share a similar concept for replication using the host's cellular processes. Human viruses penetrate the body through the mucosal barriers or the skin, they attach to the cell and penetrate the cell membrane. They disassemble their capsids to transport their genetic material, either to cytoplasm or nucleus, for genome replication and synthesizing of viral proteins that are together, assembled into a new virion. The replication of most RNA viruses occurs in the cytoplasm, while DNA viruses, with the exception of poxviruses, replicate in the nucleus

(3, 401-403). To propagate, viruses rely on encoding protein inhibitors that suppress the host antiviral sensing pathways.

1.3 Poxviruses

Poxviruses are a large family of enveloped double-stranded DNA viruses, known as the Poxviridae, that infect vertebrates (chordopoxvirinae) and invertebrates (entomopoxvirinae) (235, 404). Poxviruses have a spherical brick-like structure and they replicate in the cytoplasm with the ability to generate generalized or localized lesions of the skin or the mucosal membranes (405, 406). There are ten genera within the Chordopoxvirinae subfamily including orthopoxviruses of the famous deadly smallpox virus (variola virus) and molluscipoxviruses where the human molluscum contagiosum virus (MCV) belongs. Poxviruses were the reason for developing the first known vaccine when Edward Jenner noticed the viral interference phenomenon (**Section 1.1.1**) of cowpox virus preventing smallpox virus infection. He named the virus used for the inoculation process, vaccine virus, and thus the concept of vaccination emerged (404, 407, 408).

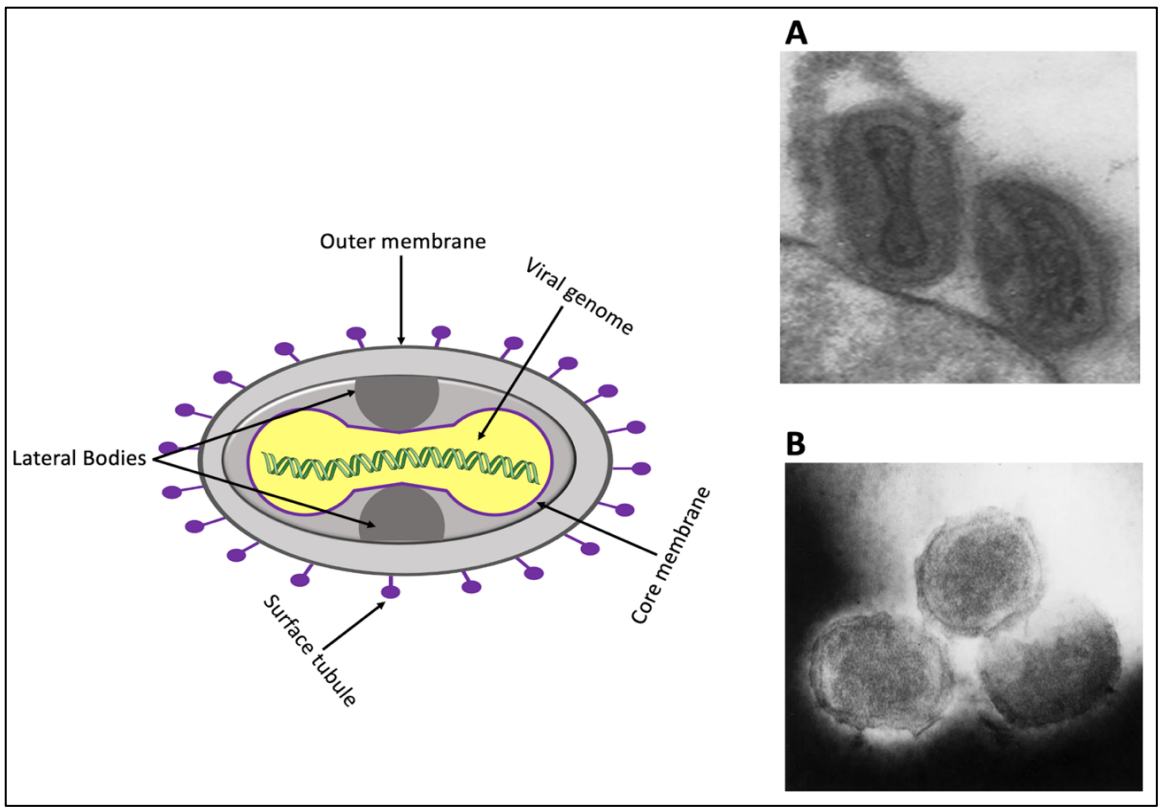

Figure 1.3.1 The main structure of poxviruses. Poxviruses have a spherical brick-like shape with three major components: a core of viral genome enveloped by a membrane, lateral bodies of immunomodulatory proteins and an outer membrane with structural proteins called surface tubules. (A) Electron microscope image of vaccinia virus. Image from Dales & Siminovitch, 1961 (409), license under The Rockefeller Institute Press (B) Electron microscope image of molluscum contagiosum virions, Image from the Centers for Disease Control and Prevention (CDC) (410), free under the public domain.

Poxviruses are thought to be ancient, and their large complex genomes account for successful adaptation to their hosts to evolve potent immunomodulatory inhibitors of antiviral defense systems. Those viral proteins are mostly contained within structures, called lateral bodies, and delivered upon virus entry into the host cell cytoplasm (**Fig.1.3.1**). Because NF-κB and IRF transcription factors are critical components of antiviral immunity, poxviral inhibitors target their activating pathways (404, 411). An example is

the vaccinia virus (VACV), the source of the modern smallpox vaccine, which can inhibit IRF3/IRF7 activation through the C6 viral protein that binds to the scaffold proteins of the IRF3 activation complex NAP1, TBKBP1 and TANK (352). It can also inhibit NF-κB activation by encoding the viral proteins C4, A49, C2 and F3 (412-414). Another example is the goats and sheep Orf virus (ORFV) that can suppress RIG-I-dependent TI-IFN and NF-κB activation through the viral proteins ORF020 and ORFV073, respectively (415-417). To date, MCV is only the second known human-specific poxvirus, with the deadly eradicated smallpox virus being the first, making it a unique model for investigating its potent inhibitors of human antiviral pathways.

1.3.1 Poxvirus replication

VACV (191,636 bp DNA genome) has become a model virus for investigating replication and biology of poxviruses since developing the modern smallpox vaccine from living attenuated VACV (418-421). Although it was first believed that it is the same virus used in Jenner's vaccine from cowpox inoculation, it was later discovered that it is rather a closely related virus from the same family that originated from another animal (422). VACV has been routinely cultivated in laboratories multiple times during the years but the exact mechanism by which the virus propagates and interacts with the host is still not fully understood (420, 423). However, it is known that VACV infection produces two distinct virions: the intracellular mature virus (IMV) and the extracellular enveloped virus (EEV), of which IMV accounts for most of the virus infectious progeny while EEV works on virus propagation and host immune evasion via its extra viral proteins and protective membrane. Therefore, IMV is only released from the host cell upon cell lysis in alternative to EEV which is microtubule-transported to the cell surface to be discharged upon assembly (424, 425).

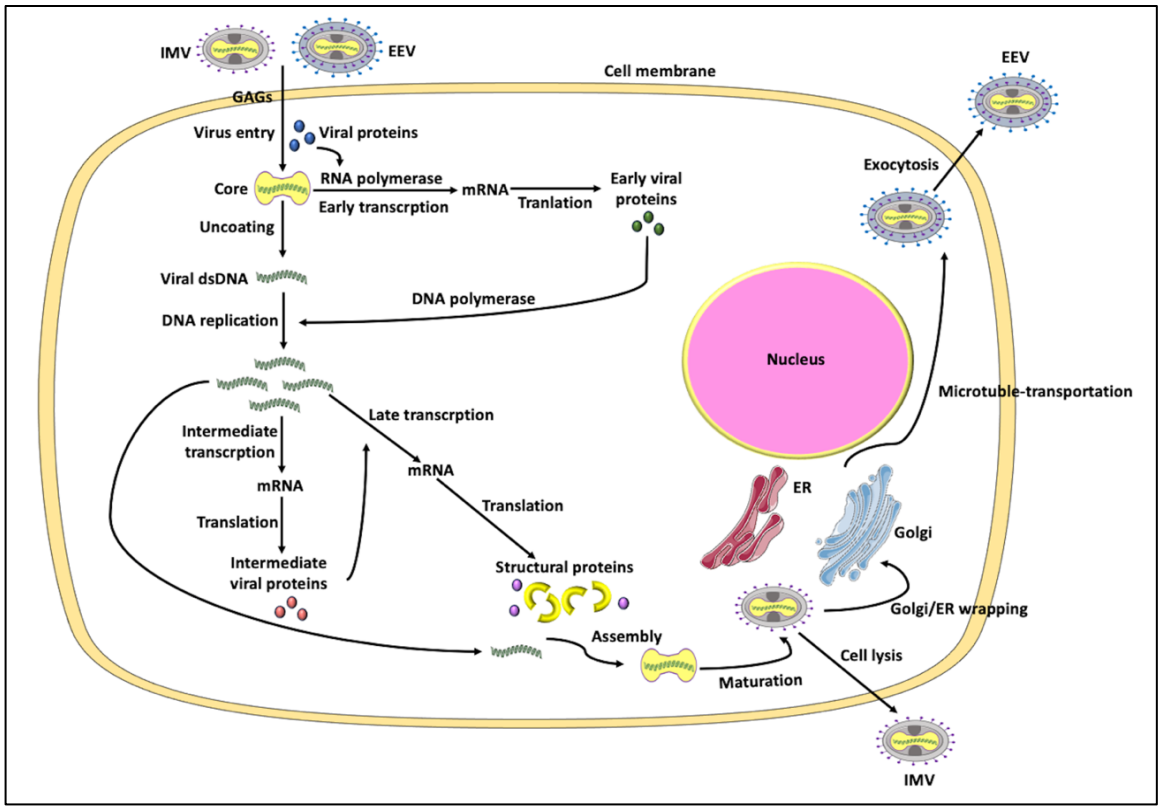

Figure 1.3.2 The replication cycle of poxviruses. An outline of poxviruses replication in human cells based on the VACV model. The poxviral infection produces two virus forms: intracellular mature virus (IMV) and extracellular enveloped virus (EEV). VACV interacts with glycosaminoglycans (GAGs) located on the host cell membrane, thus, fusing into the cytoplasm. Upon entry, the viral DNA-dependent RNA polymerase initiates the early expression of viral genes that include DNA polymerase and immunomodulatory proteins. The virus is uncoated inside the cell where the viral DNA genome is replicated via the early phase DNA polymerase and expressed into intermediate viral proteins. The late phase of gene expression is mediated by intermediate protein and translated into late viral proteins that include structural proteins of the capsid, lateral bodies and membrane proteins, which can also act as suppressors of antiviral immunity. The viral particles are assembled into an IMV that is released upon cell lysis. Some of the IMVs are coated with an additional envelope from membrane cell compartments like the Golgi or the endoplasmic reticulum

(ER) before being ejected outside the cell by exocytosis, termed EEV. Servier Medical Art (https://smart.servier.com/) was used in the illustration.

VACV enters and penetrates the host cell through viral fused proteins, termed entry-fusion complex (EFC), that are conserved among poxviruses and composed of around 11 proteins (426, 427). The EFC is believed to interact with the polysaccharides glycosaminoglycans (GAGs) on the host cell membrane where the virus is then brought to the cytoplasm through endocytosis and viral shedding of IMV and EEV, respectively (428, 429). The replication is then initiated at different sites of the host cytoplasm, such as near the ER, at which it releases its genome and viral enzymes that include DNA-dependent polymerases, DNA helicases, DNA primases and ligases (423, 430). The expression of poxviral genes occurs through three phases of the infection: early (~20 minutes), intermediate (~ 2 hours) and late expression (~ 3 hours) (431). In the early phase, proteins essential for replication and immunomodulation are expressed. Many of the proteins expressed during the poxviral late phase are structural proteins, but late-expressed proteins can also be immunoevasins. For example, the poxviral protein F17 of the lateral bodies (LB) is expressed during the late phase that localizes to the mitochondria and targets mammalian target of rapamycin (mTOR) to inhibit cGAS-ISG induction (432, 433). The viral particles are then assembled, and the mature virion can be released by cell lysis or in the case of EEV, it can go through an additional envelope coating process before being released by exocytosis (425). The exact mechanism by which EEV gains its extra membrane remains unclear but is speculated to be either from lipid and viral proteins or from the host membrane cellular compartments like the Golgi or the ER (434) (**Fig.1.3.2**).

1.4 Molluscum contagiosum virus (MCV) as a human-adapted poxvirus

Molluscum contagiosum (MC) was first described in detail in 1816 by the British physician Thomas Bateman. It was defined as a tubercular disease of the skin that can be characterized by the appearance of small singular non-inflammable tumours (435). In 1841, W. Henderson and R. Paterson noticed a classic pattern within the center of the lesions represented by microscopic globular elements (436, 437). These phenomenal inclusions, known as Henderson- Paterson bodies, have been considered since their discovery to be a characteristic feature in histopathology for diagnosing molluscum contagiosum infection (438, 439). However, it would take more than half a century to report that Henderson-Paterson bodies are in fact virions. This was when M. Juliusberg attempted successfully in 1905 to infect human participants with molluscum contagiosum using a molluscum lesion extract (439, 440). MCV was linked to poxviruses for the first time in 1931 by EW. Goodpasture and CE. Woodruff when they reported the similarity in nature between molluscum bodies and Borrel bodies in fowl-pox (441). The attempt to grow MCV in vitro has not been successful yet, but given the strong conservation of the core virus life cycle genes in MCV, it is expected to follow a similar replication cycle to VACV in vivo (442).

As part of the Poxviridae, MCV has a linear double-stranded DNA genome. It also shares with the rest of the family members having an enveloped virion structure that measures around 360 nm × 210 nm (443, 444). Additionally, previous electron microscopy studies showed that MCV has a spherical or ellipsoidal morphology (445, 446) (**Fig.1.3.1B**). Since the 1980s, four subtypes (I-IV) of MCV have been discovered using restriction enzyme mapping, of which MCV-I is the dominant infection (447-449). MCV-II has been mainly recorded in immunosuppressed patients, whereas MCV-III and MCV-IV are considered to be rare (444). The complete sequence of the MCV-I genome (190, 289 bp) was made

available in 1997 (444, 450). The MCV and VACV genomes are comparable in length and predicted encoding proteins, 182 proteins and 198 proteins , respectively, but they differ in their nitrogenous base composition where MCV has a high guanine (G)-cytosine (C) content of around 64% and VACV has a high adenine (A)-thymine (T) content of approximately 66 % (418, 444, 450). The rich GC content of the MCV genome increases the frequency of long overlapped open reading frames (ORFs) due to the frequency decrease of stop codons (450). The rich GC-content and ORF overlap have been suggested to play a role in the evolution and flexibility of viral and microbial genomes (451-453). Overall, 105 of the 182 predicted MCV-encoding proteins are homologous to VACV and mostly associated with replication, such as polymerases and ligases. The remaining gene-encoding proteins are unique to MCV and are believed to have roles in immune evasion (450).

A recent study reported the discovery of an equine molluscum contagiosum-like virus (EMCLV) isolated from horse skin lesions. A screen of the EMCLV genome (166, 843 bp) identified 159 possible open reading frames (ORFs), of which 139 ORFs are homologous to MCV and 20 ORFs are unique to EMCLV. However, the conserved core region of MCV and EMCV shows a low sequence identity compared to other poxvirus genera. Similar to MCV, the EMCLV genome contains a high GC content (66.8%) and it is predicted to encode multiple immunomodulators, including EMCLV007L and EMCLV157R homologous of immune mammalian proteins secreted and transmembrane protein 1 (SECTM1) and insulin growth factor-like receptor 1 (IGFLR1), respectively (454).

MCV primarily infects keratinocytes, the major cell type of epidermis, causing benign rounded skin-colored skin lesions, known as mollusca, that are presented with minimal or no inflammation (455-457) (**Fig.1.4.1A**). The mollusca are small (2-5 mm) and vary in

number from one to less than 100 lesions. MCV can be transmitted by direct skin contact either from one person to another or from one site of infection to another (autoinoculation). It can also be transmitted by fomites which may explain the higher infection frequency in children (457, 458). The infection normally revolves without the requirement of treatment, and it only appears severe in immunocompromised patients, such as HIV and cancer patients. The size of atypical MCV lesions can reach up to 15 mm (giant mollusca) resulting in disfigurement and showing no signs of auto-resolving (456, 457, 459, 460) (**Fig.1.4.1B**). Because MCV infection is normally a self-limiting viral infection (6 months- 5 years), intervention is not usually required but rather determined by status (461). Physical treatments of MCV lesions include cryotherapy and laser but they tend to be painful and could cause scarring. The topical cantharidin (YCANTH™), a phosphodiesterase inhibitor, was demonstrated in clinical trials to treat MCV lesions within 3 months, however, the efficacy rate of chemical drugs, such as cantharidin and potassium hydroxide, varies among different studies (462, 463). Immunotherapeutic treatments have been also developed to induce antiviral immunity to eliminate MCV infection. An example is the tropical drug imiquimod, a TLR7 agonist that stimulates the secretion of IFNα and proinflammatory cytokines, which has been shown to achieve 69% clearance in a clinical study after 4 months. However, another study indicated that the efficacy of imiquimod was not significantly different in comparison to placebo and could rather be painful with adverse effects, such as irritation (457, 464).

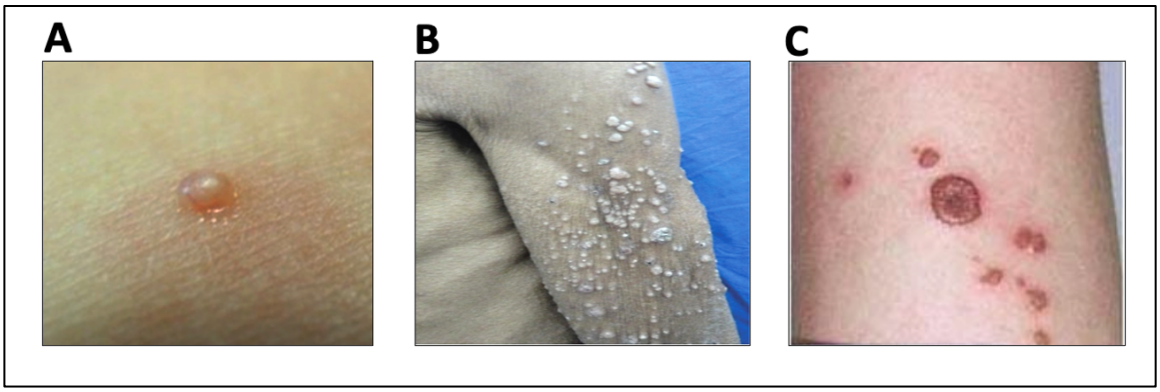

Figure 1.4.1 Typical and atypical molluscum contagiosum lesions versus vaccinia virus lesions. (A) Typical umbilicated mollusca. Image from Meza-Romero et al, 2019 (457), licensed under CC-BY-NC-3.0. (B) Atypical giant mollusca in an HIV patient. Image from Vora et al, 2015 (459), licensed under CC BY-NC-ND 4.0. (C) Inflamed lesions post vaccina virus vaccination. Image reproduced from Frey et al, 2002 (465), license under Copyright Massachusetts Medical Society.

Keratinocytes drive efficient antiviral innate responses through multiple PRRs (466), however, MCV can last from months to years through immunomodulation of human antiviral sensing pathways (467). Alternatively, a non-adapted human poxvirus, like in the case of VACV, inflamed ulcerated lesions develop that heal over several weeks (468) (**Fig.1.4.1C**). MCV immune escape mechanisms include encoding multiple inhibitors, each specialized to target a specific part of the human antiviral signaling pathways. To date, most of the discovered MCV-derived inhibitors target NF-κB activation (**Table 6 & Fig.1.4.2**), including three inhibitors, MC005, MC008 and MC159, that target NEMO-dependent NF-κB activation by disrupting ubiquitin-based NEMO activation (469-471). MC132 inhibits NF-κB activation at the level of the transcription factor p65 at which it interacts with p65 and targets it for ubiquitin-mediated proteasomal degradation (472). Other MCV-derived inhibitors associate with the IKK kinases, like in the case of MC160 interacting with heat shock protein 90 (Hsp90) required for IKKα stabilization and thus,

causing its degradation (473). Because IRF3 pathways are essential components of antiviral immunity, discovering MCV viral proteins that inhibit their activation will extend our understanding of IRF3 antiviral activation and the molecular mechanisms of MCV infection. However, until now only two MCV proteins, MC159 and MC160, have been linked to IRF3 inhibition. Both proteins are FLICE-inhibitory proteins (FLIPs) that possess death-effector domains (DEDs) allowing them to suppress apoptosis mediated by death receptors, such as TNF receptors. Regarding the inhibition of IRF3 activation, MC159 was found to interact with both TBK1 and IKKε, while MC160 targeting of IRF3 activation remains unclear but was demonstrated to prevent TBK1 phosphorylation without interacting with either TBK1 or IKKε (236).

Table 6. MCV-derived inhibitors of NF-κB and IRF antiviral pathways.

MCV inhibitor	Transcription factors	Target for inhibition	Reference(s)
MC159	IRF3/NF-κB	TBK1-IKKε /NEMO	(236, 471)
MC160	IRF3/NF-κB	TBK1/IKKα	(236, 473)
MC132	NF-κB	P65	(472)
MC005	NF-κB	NEMO	(469)
MC163	NF-κB	IKK complex	(474)
MC008	NF-κB	NEMO	(470)

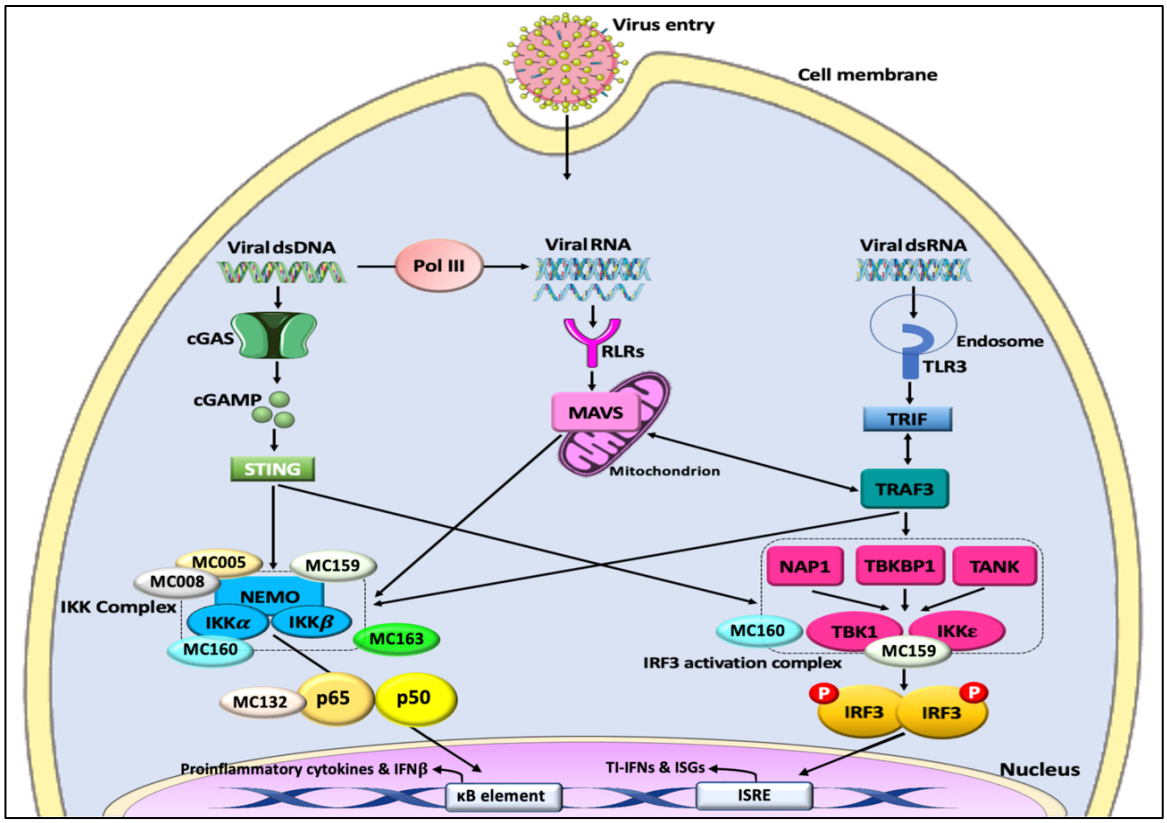

Figure 1.4.2 Discovered MCV-derived inhibitors of NF-κB and IRF3 activation. MC005 and MC008 target NEMO for NF-κB suppression. MC163 inhibits NF-κB activation at the level of the IKK complex. MC132 targets the transcription factor p65 for degradation. Both MC159 and MC160 lead to bifurcated inhibition of NF-κB and IRF3 activation: MC159 targets NEMO and IRF3 kinases to block the positive regulation of NF-κB and IRF3, respectively, while MC160 inhibits IKKα-dependent NF-κB activation and TBK1-induced IRF3 activation. Servier Medical Art (https://smart.servier.com/) was used in the illustration.

Other MCV inhibitors have been found to directly associate with proinflammatory cytokines and chemokines, namely MC053, MC054 and MC148. Both MC053 and MC054 act as IL-18 antagonists and inhibit IL-18-induced IFNγ production (475). MC148 disrupts the interaction between the chemokines CXCL12α and CXCR4 to inhibit the chemotaxis of immune cells (476). Adaptive immunity can also be targeted by MCV inhibitors which

has been evident by MC080 prevention of human leukocyte antigen (HLA) presentation to cytotoxic T cells by interacting with tapasin, a molecule important for the efficient assembly of major histocompatibility complex (MHC) class I (477, 478). There are also MCV proteins, MC163 and MC007, that function at the level of mitochondria, an organelle that mediates antiviral signaling cascades, for example, through MAVS, and thus, it serves as a target for viruses (479). MC163, which can also inhibit NF-κB activation, localizes to the mitochondria to prevent mitochondrial membrane permeabilization (MMP) needed for apoptosis (480). MC007 displaces the retinoblastoma protein (pRb) at the mitochondrial membrane leading to the activation of the E2F transcription factor essential for cell proliferation (481). There are still many proteins unique to the MCV genome that are yet to be discovered and identifying them will not only uncover new MCV strategies of immunomodulation but will also expand our knowledge on human antiviral signaling pathways.

1.5 Research Objectives

A high-throughput luciferase screen of MCV open reading frames (ORFs) was performed in the host laboratory to identify novel inhibitors of human antiviral signaling pathways. A number of MCV proteins emerged as possible candidates including MC132, MC005 and MC008 which, as previously discussed, were later characterized as specific inhibitors of NF-κB activation. Among those potential MCV inhibitors, MC089 appeared to specifically target IRF activation. To date, most of the MCV-discovered inhibitors of innate signaling pathways target NF-κB activation with FLICE-inhibitory MCV proteins suppressing both NF-κB and IRF activation. Therefore, specific MCV inhibitors of IRF activation are yet to be discovered. Additionally, NF-κB signaling pathways are better understood compared to antiviral IRFs, and although IRF3 is the most studied member of IRFs, many unsolved questions regarding the regulation of IRF3 activation are yet to be answered. For these reasons, identifying MC089 as a novel inhibitor of IRF activation may reveal new insights into MCV pathogenesis and contribute to the knowledge of antiviral IRF3 regulation. This, in turn, could lead to potential therapeutic strategies involving type I interferonopathies and viral infections. This thesis aims to investigate the role of MC089 in MCV evasion of human innate antiviral signaling pathways and characterize its inhibitory effect in IRF activation.

:

Chapter 2: Materials & Methods

2.1 Materials

Table 7. List of materials used in the experiments.

Material	Source	Code
Acetyl coenzyme A sodium salt	Sigma-Aldrich	A2181
Alexa Fluor 488 FLAG tag antibody	Invitrogen	MA1142A488
Alexa Fluor 647 HA tag antibody	Invitrogen	26183A647
Anti-β-actin	Sigma-Aldrich	A5316
Anti-FLAG M2 beads	Sigma-Aldrich	A2220
Anti-HA	Biolegend	901515
Anti-IRF3 (phospho S386)	Abcam	76493
Anti-Rabbit HRP-linked IgG antibody	Cell Signaling Technology	7074
Anti-TBKBP1 antibody	Sigma-Aldrich	ZRB1932
Aprotinin	VWR	CAYM14716
ATP disodium salt	Sigma-Aldrich	A2383
β-Glycerophosphate	Sigma-Aldrich	G9422
Benzonase	Sigma-Aldrich	70746-3
Blasticidin	InvivoGen	ant-bl
Bovine serum albumin	Merck	12659
Bromophenol blue	Sigma-Aldrich	114391
Cadmium Chloride ($CdCl_2$)	Sigma-Aldrich	655198
Cell culture dishes (10 cm)	Merck	CLS430599
Cell culture flasks (T175)	SARSTEDT	83.3912.002
Cell culture plates (6-well)	Thermo Scientific	10146810
ChemiDoc™ MP Imaging System	Bio-Rad	12003154
Coelenterazine	Biotium	10110
Cooling centrifuge (MICRO 17R)	Thermo Scientific	75002404
CTDA monohydrate	Merck	319945
Dimethyl sulfoxide (DMSO)	Sigma-Aldrich	D5879
Dithiothreitol (DTT)	Fisher Scientific	10592945
D-luciferin	Carbosynth	FL08607
Dulbecco's Modified Eagle Medium	Gibco	61965026
EDTA	Thermo Scientific	15575020
Fetal bovine serum	Sigma-Aldrich	F9665
FLAG tag peptide	Sigma-Aldrich	F3290
Flat bottom TC microplates	Scientific Laboratory Supplies	3596

GeneJuice reagent	Merck	70967
Gentamicin	Sigma-Aldrich	G1397
Glass chamber slides	Thermo Scientific	154534
Glycerol	Fisher Scientific	10336040
Goat anti-mouse (IRDye 680RD)	LI-COR	92668070
Goat anti-rabbit (IRDye 680RD)	LI-COR	92668071
Goat anti-rabbit (IRDye 800CW)	LI-COR	92632211
HEK-blue IFN-α/β cells	InvivoGen	hkb-ifnab
Hemacytometer	Merck	Z359629
Hydrochloric acid (HCL)	Fisher Scientific	15693640
Hygromycin B gold	InvivoGen	ant-hg
Immunoassay microplates	VWR	735-0465
IP-10 ELISA kit	R&D Systems	DY266-05
Isopropanol	Fisher Scientific	17140576
Lecia SP8 confocal microscope	Lecia	-
lipofectamine 2000 reagent	Invitrogen	11668019
Luminoskan™ microplate luminometer	Thermo Scientific	-
Luria-Bertani agar	Fisher Scientific	11758902
Luria-Bertani broth	Fisher Scientific	12801660
Magnesium carbonate hydroxide pentahydrate	Sigma-Aldrich	56378-72-4
Magnesium sulfate heptahydrate	Sigma-Aldrich	10034-99-8
MAVS antibody	Cell Signaling Technology	3993
Maxi Plasmid Purification Kit	Invitrogen	A31231
Mini-PROTEAN Electrophoresis system	Bio-Rad	1658006FC
Mini shaking incubator	Benchmark Scientific	H1001-M-E
MitoTracker deep red FM	Cell Signaling Technology	8778
Multiskan FC microplate photometer	Thermo Scientific	N07710
NanoDrop 8000 spectrophotometer	Thermo Scientific	-
Nitrocellulose membranes	VWR	10600012
Normocin	InvivoGen	ant-nr
NP-40	Thermo Scientific	28324
Paraformaldehyde (PFA) (4%)/PBS	Thermo Scientific	J19943-K2
PBS	Gibco	10010015

Penicillin-streptomycin	Gibco	15140122
Phenylmethylsulfonyl fluoride	Sigma-Aldrich	P7626
Phosphate-buffered saline	Gibco	10010056
Poly(dA:dT)	Sigma-Aldrich	P0883
Prestained Protein Marker	Thermo Scientific	26619
ProLong Gold reagent with DAPI	Thermo Scientific	P36931
QUANTI-blue	InvivoGen	rep-qb
Rabbit IgG Phospho-IKKε (Ser172) (D1B7)	Cell Signaling Technology	8766
Rabbit IgG Phospho-IRF-3 (Ser396) (4D4G)	Cell Signaling Technology	4947
Recombinant human IFNβ standard	R&D Systems	8499-IF-010/CF
RIG-I pathway sampler kit	Cell Signaling Technology	8348
SignalFire ™ ECL (Reagent A)	Cell Signaling Technology	46935P3
SignalFire ™ ECL (Reagent B)	Cell Signaling Technology	74709P3
Sodium dodecyl sulfate	Sigma-Aldrich	L4509
Sodium fluoride	Merck	GSK5130
Sodium hydroxide	Sigma-Aldrich	1310-73-2
Sodium orthovanadate	Sigma-Aldrich	13721-39-6
STERI-CYCLE i160 CO_2 incubator	Thermo Scientific	-
Subcloning Efficiency™ DH5α Competent Cells	Invitrogen	18265017
Tricine	Sigma-Aldrich	T0377
Tris base	Fisher Scientific	10376743
Trypan Blue Stain	Gibco	15250-061
Trypsin-EDTA	Gibco	25300054
Tube roller	Benchmark Scientific	R3005
Tween 20	EC-607	Sparks Lab Supplies
Vortex mixer	Benchmark Scientific	BV1003
X-100 Triton	Sigma-Aldrich	T8787
Zeocin	InvivoGen	ant-zn

2.2 Methods

Cell culture. Human embryonic kidney 293T (HEK293T) cells were maintained in Dulbecco's Modified Eagle Medium (DMEM) (1x) (Gibco # 61965026) supported with 10% (vol/vol) fetal bovine serum (FBS) (Sigma-Aldrich # F9665). The antibiotic used was alternated between 1% (vol/vol) penicillin-streptomycin (Gibco # 15140122) and 0.1% (vol/vol) gentamicin (Sigma-Aldrich # G1397) to maintain sterilization. Cells were trypsinized using 0.05% trypsin-EDTA (Gibco # 25300054) following a double washing step with sterile phosphate-buffered saline (PBS) (Gibco # 10010056). Incubation conditions were 37 ℃ / 5% CO_2.

Plasmids and oligonucleotides. Prior to commencing this research, a library of ORFs from MCV subtype 1 MC089L was custom synthesized by GenScript and subcloned into KpnI and NotI sites of the pCEP4 expression vector (Invitrogen # V04450) (**Fig.2.2.1A)** with a C-terminal FLAG (DYKDDDDK) or an HA (YPYDVPDYA) epitope tag. Similarly, MCV subtype 1 MC020L was cloned into the pCEP4 vector. For $CdCl_2$-conditional expression, MC089L was subcloned into KpnI and NotI restriction sites of the pMEP4 vector (Invitrogen) (**Fig.2.2.1B)** fused with a C-terminal flag-tag. Other plasmids were acquired as referred to previously (352, 469, 472). The vaccinia virus protein VVC6-cloned into pCMV-HA (Clontech) was a kind gift from Professor Andrew Bowie (Trinity College Dublin) and was constructed as described previously (352).

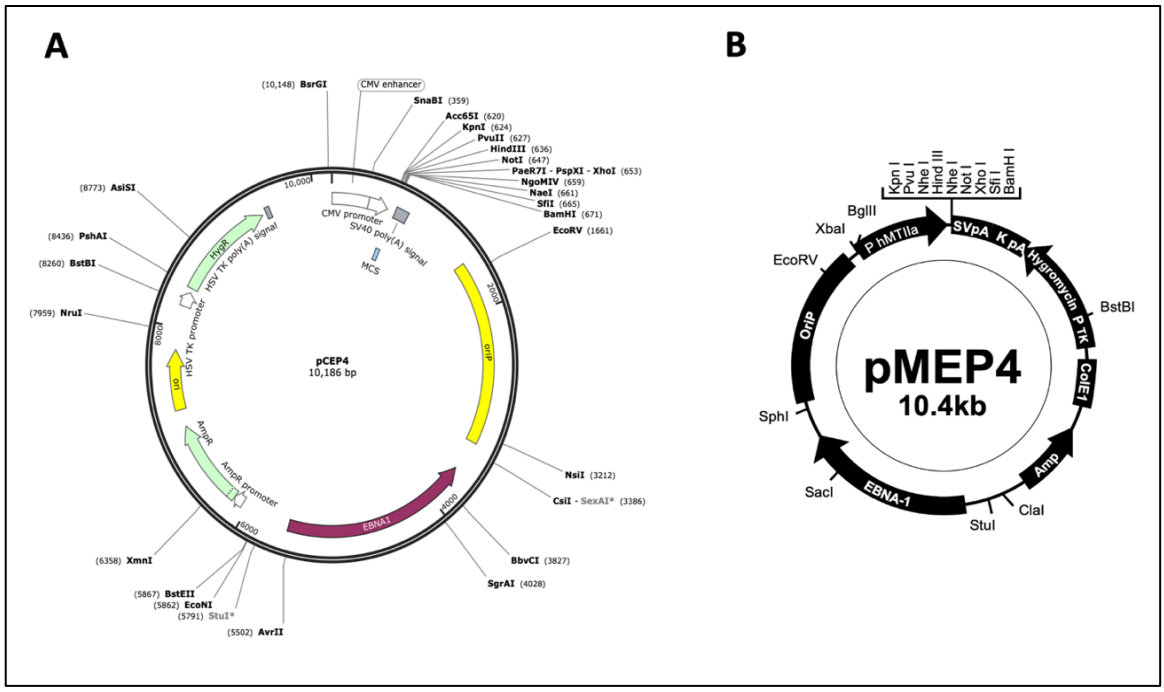

Figure 2.2.1 Mammalian vectors for MC089 gene expression. (A) The pCEP4 vector from InvivoGen contains the human cytomegalovirus (CMV) promoter for high-level transient expression. Map generated by SnapGene (Available at snapgene.com). (B) The pMEP4 vector from InvivoGen includes the human metallothionein II (hMTII) promoter that allows for inducible stable gene expression upon the addition of metals, such as cadmium chloride. Map obtained from InvivoGen (Adopted from thermofisher.com).

Antibodies. The primary antibodies used for immunoblotting were anti-FLAG M2 (Sigma-Aldrich # F3165), anti-HA (Biolegend # 901515) and anti-β-actin (Sigma-Aldrich # A5316). Goat anti-mouse (IRDye 680RD) (LI-COR # 92668070), goat anti-rabbit (IRDye 680RD) (LI-COR # 92668071) and goat anti-rabbit (IRDye 800CW) (LI-COR # 92632211) were utilized as secondary antibodies. Phosphospecific antibodies were obtained from the RIG-I pathway sampler kit (Cell Signaling Technology # 8348), except for anti-IRF3 (phospho S386) (Abcam # 76493). Other antibodies used include an anti-MAVS antibody (Cell Signaling Technology # 3993) and an anti-TBKBP1 antibody (Sigma-Aldrich # ZRB1932). For confocal microscopy, Alexa Fluor 488 FLAG tag antibody (Invitrogen #

MA1142A488) and Alexa Fluor 647 HA tag antibody (Invitrogen # 26183A647) were used.

Bacterial transformation and plasmid DNA isolation. Luria-Bertani (LB) agar (Fisher Scientific # 11758902) and Luria-Bertani (LB) broth (Fisher Scientific # 12801660) were dissolved in deionized water and autoclaved at 121℃ for 15 minutes. Ampicillin (50 µg/ml) was added to the cooled LB agar as a selective antibiotic. Around 20 ml of sterilized LB agar was poured into Petri dishes (10 cm) and left for solidification. 1 µl of each plasmid was mixed with 10 µl of chemically competent *E. coli* cells (Invitrogen # 18265017). The plasmid-cell mixture was incubated on ice for 30 minutes before being heat-shocked at 42℃ for 45 seconds. Another ice incubation step was followed for 5 minutes. LB broth (150 µl) was added to the plasmid-cell mixture and left in the shaking incubator for 1 hour at 37℃/ 225rpm. The bacterial cells were streaked on the LB agar Petri dishes and were left on a stationary incubator invertedly at 37℃. The following day, for subculture, one bacterial colony was inoculated in LB broth (5 ml) with ampicillin (50 µg/ml) in a sterile falcon tube (15 ml). The tubes were closed loosely with an autoclave tape and incubated for 8 hours in the shaker incubator (225 rpm) at 37℃. Bacterial culture amplification was achieved by mixing 2 ml of the subculture broth with 200 ml of LB broth in a sterile canonical flask covered with tin foil and autoclave tape. Following overnight incubation at 37℃/ 140 rpm, the 200 ml bacterial culture LB broth was divided into falcon tubes (50 ml) and centrifuged at 3,500 x g for 15 minutes. The supernatants were discarded, and pellets were harvested for DNA Maxiprep DNA isolation according to the manufacturer's instructions (Invitrogen # A31231). All the bacterial culture steps were performed in a sterilized Bunsen flame zone. The DNA concentration and purity were measured using a NanoDrop 8000 spectrophotometer (Thermo Fisher Scientific).

Reporter gene assays. HEK293T cells were seeded at $2x10^5$ cells/ml in 96-well culture plates. The cells were transfected 24 hours later with 80 ng/well of the indicated firefly luciferase reporter gene (NF-*κ*B, ISRE & IFNβ), 40 ng/well of pGL3-*Renilla* control and the indicated amounts of signaling element constructs and MCV ORFs. The final volume of plasmids added was adjusted to 220 ng/well using the empty vector control (pCMV-HA). The next day, cells were transfected with 1 µg/ml of Poly(dA:dT) for 16 hours, or directly lysed using passive lysis buffer (Promega technical bulletin # TB281) made from dithiothreitol (DTT) (2mM), glycerol (10% (vol/vol)), X-100 Triton ((1% (vol/vol)), Tris phosphate (25 mM, pH 7.8) and CTDA monohydrate (2 mM). GeneJuice reagent (Merck # 70967) was used to transfect the cells with the plasmids, while lipofectamine 2000 reagent (Invitrogen # 11668019) was used for Poly(dA:dT) transfection. Supernatants were aspirated, and cells were incubated with 50 µl/well of passive lysis buffer for 15 minutes on the shaker. Using white luminometer plates, 20 µl/well of lysates was mixed with 40 µl/well of luciferase assay mixture (LAM 1x) or 40 µl/well of coelenterazine (0.1% (vol/vol)) (Biotium # 10110). LAM was prepared using 20 mM tricine, 2.67 mM magnesium sulfate heptahydrate, 0.1 mM EDTA, 33.3 mM dithiothreitol (DTT), 530 µM ATP disodium salt, 270 µM acetyl coenzyme A sodium salt, 420 nM D-luciferin, 5µM sodium hydroxide, 9.7 mM magnesium carbonate hydroxide pentahydrate. LAM (D-luciferin) measured firefly luciferase activity, while coelenterazine measured *Renilla* luciferase activity through light emission. *Renilla* luciferase cannot catalyze the oxidation of firefly luciferin and, therefore, it was used as an internal control in which *Renilla* luciferase was constitutively expressed and firefly luciferase was expressed under the control of the promoter of interest (482-484). By normalizing firefly luciferase activity to *Renilla* luciferase activity, transfection efficiency can be maintained. For the Ras-

dependent Elk1-Gal4 reporter assay, 80 ng of the pFR luciferase plasmid containing Gal4 binding sites, 5 ng of the pFA-Elk1-Gal4 expression vector and 50 ng of HA-tagged Ras were employed. Luciferase activity was read using a Luminoskan™ microplate luminometer (Thermo Scientific).

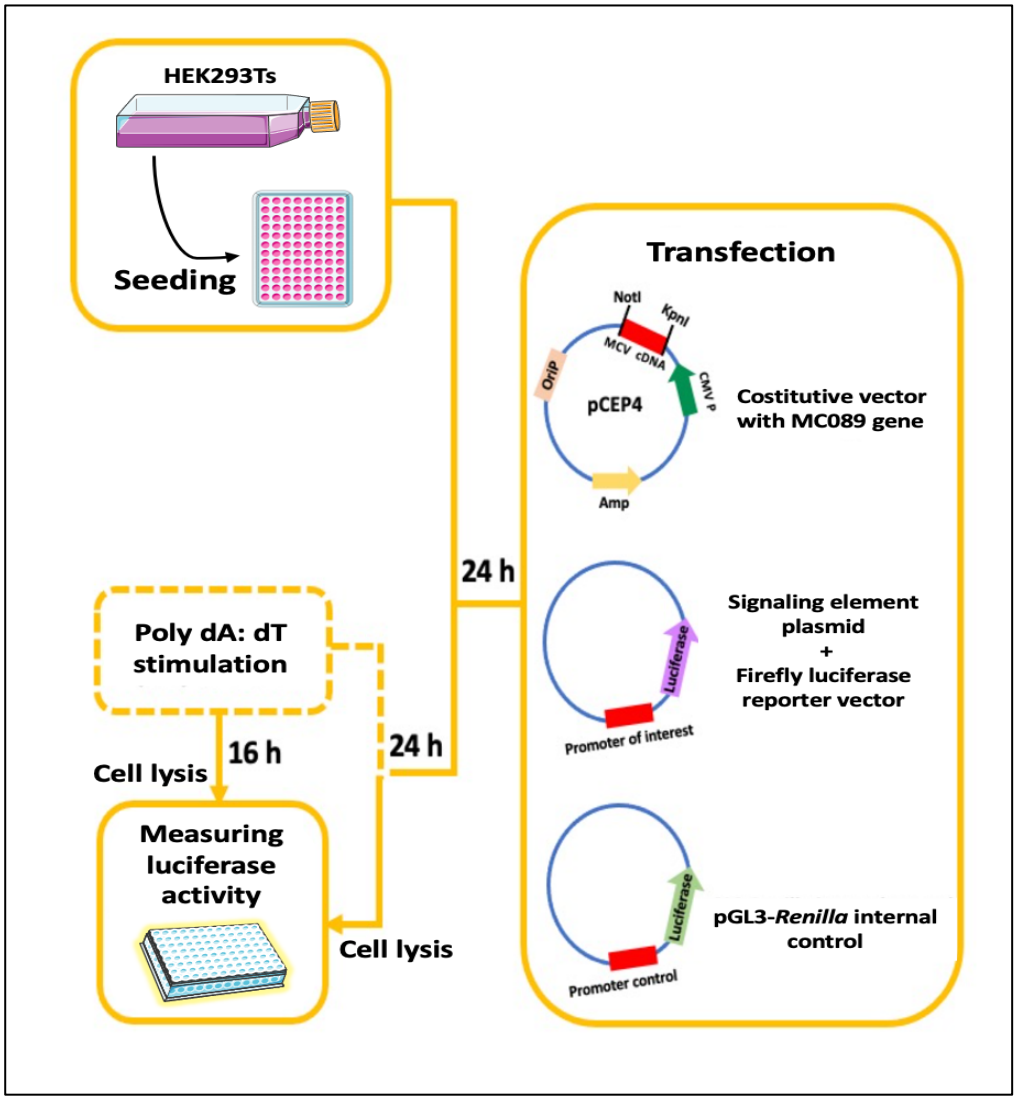

Figure 2.2.2 Schematic overview of the luciferase assay protocol. On day 1, HEK293T cells were seeded in 96-well plates. The following day, the cells were transfected with pCEP4-MC089 plasmid, signaling element expression plasmid, firefly luciferase reporter vector and pGL3-*Renilla* internal control. Overexpression of signaling elements, such as cGAS and STING, or stimulation with DNA transfection (Poly(dA:dT)), activates the transcription factor (TF)

promoter/enhancer, for example, NF-κB, to induce firefly luciferase gene expression. The cells were next lysed, and substrates were added to be catalyzed by the luciferase enzymes, firefly and *Renilla* luciferases, resulting in the production of light which can be measured by a luminometer. pGL3-*Renilla* does not catalyze the firefly luciferase substrate and, thus, was used as an internal control. Servier Medical Art (https://smart.servier.com/) was used in the illustration.

Immunoblotting. HEK293T cells were seeded at $5x10^5$ cells/well in six-well plates and transfected 24 hours later with a total of 3 μg of plasmids via GeneJuice. The next day, supernatants were aspirated, and the cells were lysed with 180 μl/ well of sample lysis buffer (1 M Tris-HCl (pH 6.8), 2% (wt/vol) sodium dodecyl sulfate, 10% (vol/vol) glycerol, 0.1% (wt/vol) bromophenol blue, 100 mM dithiothreitol (DTT), 1 ul/ml benzonase and dH_2O) for five minutes on ice. Lysates were then boiled for another five minutes. Lysates (20 μl/ well) were resolved by 10-15% SDS-PAGE and Western blotting was performed using nitrocellulose membranes (VWR # 10600012). Membranes were blocked for non-specific bindings for one hour using 3% (wt/vol) bovine serum albumin (BSA) dissolved with PBS (1x) and 0.05% (vol/vol) tween 20, except for phosphorylation antibodies as BSA was dissolved with Tris-buffered saline (TBS) and tween 20 to minimize non-specific bindings form phosphate ions in PBS. Probing with primary antibodies was performed according to the manufacturer's specifications using blocking buffer for dilution; anti-FLAG (1/5000), anti-HA (1/1000) and anti-β-actin (1/10000). Following overnight incubation at 4°C, membranes were washed with PBS (1x) and 0.05% (vol/vol) tween 20, probed with secondary antibodies for one hour at room temperature and followed with a further triplicate wash. TBS and 0.05% (vol/vol) tween 20 buffer were used to wash blots

with phosphorylation events. Blots were scanned using ChemiDoc™ MP Imaging System (Bio-Rad # #12003154).

Immunoprecipitation (IP). HEK293T cells were seeded at $3x10^6$ cells/culture dish and transfected 24 hours later with a total of 8 µg of plasmids using GeneJuice. The next day, supernatants were aspirated, and the cells were scraped on ice with 500 µl/well of cold IP lysis buffer as described previously (469, 472). Lysates were centrifuged at 17,000 x g / 4℃ for 10 minutes using a cooling centrifuge (Thermo Scientific # 75002404). Around 350 µl and 50 µl of cell lysates were added into pre-cooled IP and control eppendorfs, respectively. Lysate controls were frozen until immunoblotting. Around 10 µl/sample of anti-FLAG M2 affinity gel beads (Sigma-Aldrich # A2220) was added into pre-cooled eppendorfs, centrifuged at 3,000 x g for one minute and then washed with cold IP lysis buffer. This step was repeated three times for the equilibration of anti-FLAG beads. Next, the beads (60 µl/sample) were mixed with lysis buffer and left for an overnight incubation at 4℃. The samples were centrifuged at 3,000 x g/4℃ for one minute and then washed with cold IP lysis buffer. The triplicate washing step was repeated and followed by the addition of 3 µg of FLAG tag peptide (Sigma-Aldrich # F3290) diluted with 80 ul of PBS (1x) per sample. The samples were rolled on a shaker at 4℃ for 30 minutes and then centrifuged at 3,000 x g/ 4℃ for one minute for separation from the beads. Around 80 ul of each sample suspension was collected in pre-cooled eppendorfs. Beads were preserved as diagnostics of the elution stage in case of troubleshooting. Sample lysis buffer was added into controls (30 µl), IP samples (30 µl) and beads (50 µl) for immunoblotting with the indicated antibodies.

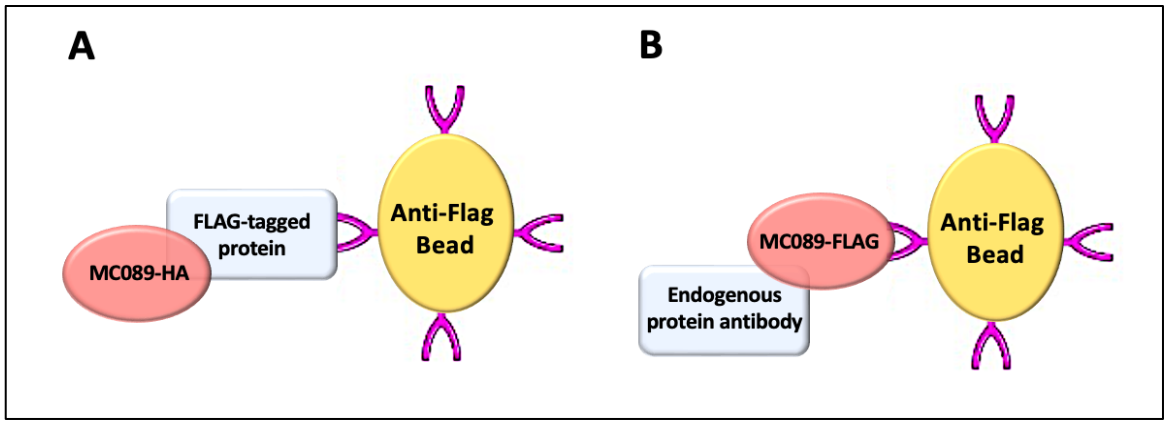

Figure 2.2.3 Schematic of the principle of Immunoprecipitation (IP). Anti-flag agarose beads were used for immunoprecipitation of FLAG-tagged proteins bound to their binding partners. The pulled-down proteins were eluted from the beads by FLAG tag peptide. (A) Anti-flag beads pulled down the overexpressed FLAG-tagged protein bound to HA-tagged MC089. (B) Anti-flag beads pulled down the FLAG-tagged MC089 bound to its target endogenous protein. Servier Medical Art (https://smart.servier.com/) was used in the illustration.

Generation of MC089-expressing stable cell lines. HEK293T cells were seeded at $5x10^5$ cells /ml in six-well plates and transfected 24 hours later with 4 µg of pMEP4-MC89-FLAG via GeneJuice reagent. The next day, hygromycin B gold (InvivoGen # ant-hg) (200 ug/ml) was added for the selection of transfected cells. The growth of selective cells was maintained with 100 µg/ml hygromycin B. Transfected cells were induced for 24 hours with 1 µM of $CdCl_2$ to express MC089.

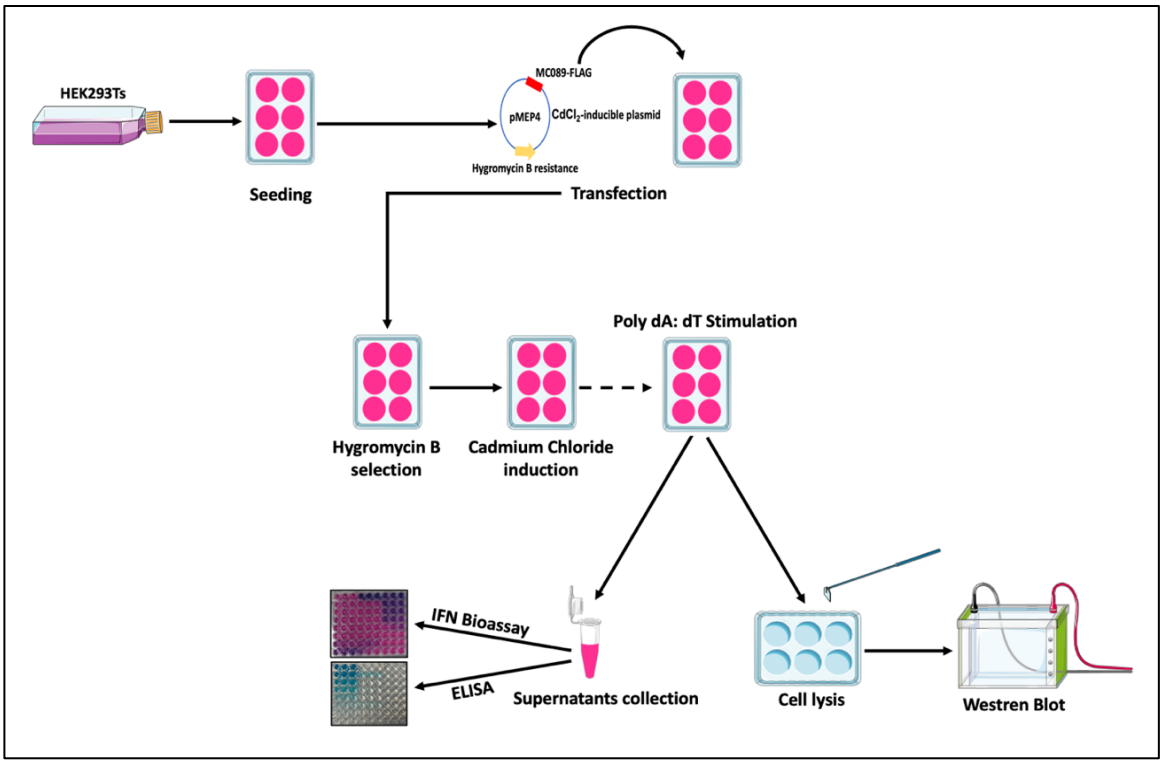

Figure 2.2.4 Schematic overview of the generation of pMEP4-MC089-expressing stable cells. HEK293T cells were seeded in 6-well plates and transfected 24 hours later with a pMEP4 vector containing the MC089 gene. The following day, the transfected cells were selected with hygromycin B antibiotic. Hygromycin-resistant cells were induced with cadmium chloride to express MC089. After 24 hours, the cells can be stimulated with DNA for 16 hours. Supernatants were collected for IFN bioassay and ELISA. Cell lysates were harvested, and western blot was used to analyze the expression of MC089 and to detect phosphorylation events. Servier Medical Art (https://smart.servier.com/) was used in the illustration.

ELISA. The supernatants from $CdCl_2$-induced MEP4-MC089 HEK293T cells were assayed for IP-10/CXCL10 with an ELISA kit (R&D Systems # DY266-05) according to the manufacturer's protocol. Plates were displayed with a Thermo Scientific Multiskan FC microplate photometer at 450 nm.

IFN bioassay. HEK-blue IFN-α/β cells (InvivoGen # hkb-ifnab) were selected with 30 μg/ml blasticidin (InvivoGen # ant-bl), 100 μg/ml zeocin (InvivoGen # ant-zn) and 100 μg /ml normocin (InvivoGen # ant-nr). A two-fold serial dilution of recombinant human IFNβ standard (R&D Systems # 8499-IF-010/CF) was prepared using DMEM with 10% FBS, 1% penicillin and normocin (100 μg/ml). Supernatants were collected from $CdCl_2$-induced MEP4-MC089 HEK293T cells and assayed for IFN secretion. Using flat-bottom 96-well culture plates, 80 μl of each standard and sample was added in triplicate with 120 μl/well of HEK-blue cells at $5x10^4$/well. After 24 hours, 20 μl of induced HEK-blue supernatants was mixed with 180 μl QUANTI-blue (InvivoGen # rep-qb) in new flat-bottom 96-well culture plates. The plates were sealed with tin foil and incubated at 37 ℃ / 5% CO_2 for 15 minutes or until a blue-coloured reaction was observed. SEAP levels were read at 620 nm using a Thermo Scientific Multiskan FC microplate photometer.

Confocal Microscopy. HEK293T cells were seeded at $8x10^4$ cells/well on glass chamber slides (Thermo Scientific # 154534) and transfected 24 hours later using GeneJuice. MitoTracker deep red FM (Cell Signaling Technology # 8778) was prepared with DMSO according to manufacturer's specifications and added to the growth media to a final concentration of 200 nM for 30 minutes. Cells were then washed once with PBS (1x) and incubated with paraformaldehyde (PFA) diluted in PBS (Thermo Scientific # J19943K2) for 15 minutes. Following a triplicate wash with PBS, cells were blocked and permeabilized with 2% (wt/vol) BSA, 0.05% (vol/vol) tween 20 and 0.3% (vol/vol) X-100 Triton diluted in PBS for one hour. Cells were next incubated overnight in blocking buffer with the indicated antibodies: Alexa Fluor 488 FLAG tag antibody (1:1500), Alexa Fluor 647 HA tag antibody (1:500), anti-MAVS antibody (1:2000) and anti-TBKBP1 antibody (1:2000). The slides were washed with PBS three times and mounted with ProLong Gold Antifade

reagent with DAPI (Invitrogen, P36931). Images were obtained using a Lecia SP8 confocal microscope with LAS X Life Science software.

Statistical Analysis. GraphPad PRISM 8 was used for statistical analysis and generation of graphs. Statistical significance was measured using unpaired student's T-tests and presented as * $P<0.05$, ** $P<0.01$, *** $P<0.001$, **** $P<0.001$.

Chapter 3 Investigation of MC089 as an Inhibitor of Innate Signaling Pathways

A library of MCV open reading frames (ORFs) was screened by the host laboratory for the ability to inhibit innate antiviral signaling pathways using a high throughput luciferase assay-based screening system and identified MC089 as an inhibitor of ISRE reporter activation for further investigation prior to the initiation of this PhD (data not shown).

MC089 is a 114-amino-acid protein (predicted 13 kDa) encoded by the MC089L ORF located on the left-hand terminus of the MCV genome (450). It shows homology with the Fowlpox virus protein FPV145 sharing approximately 28% sequence identity (485) and a 56% similarity to the hypothetical protein EMCLV086L from the recently sequenced Equine molluscum contagiosum-like virus genome (454). MC020, a 139-amino acid MCV protein with a predicted size of 14 kDa and no inhibitory activity on any innate or control signaling pathways tested, was employed previously as a negative control (470). Thus, MC020 was also used as a negative control MCV protein in these experiments. Equivalent expression of MC089 and MC020 was detected by immunoblotting (**Fig.3.1A**). Confocal analysis showed that MC089 displays distinctive punctate distribution in the cytoplasm of expressing cells (**Fig.3.1B**). In this chapter, mapping the inhibitory effect of MC089 on major innate signaling pathways using luciferase reporter assays will be described.

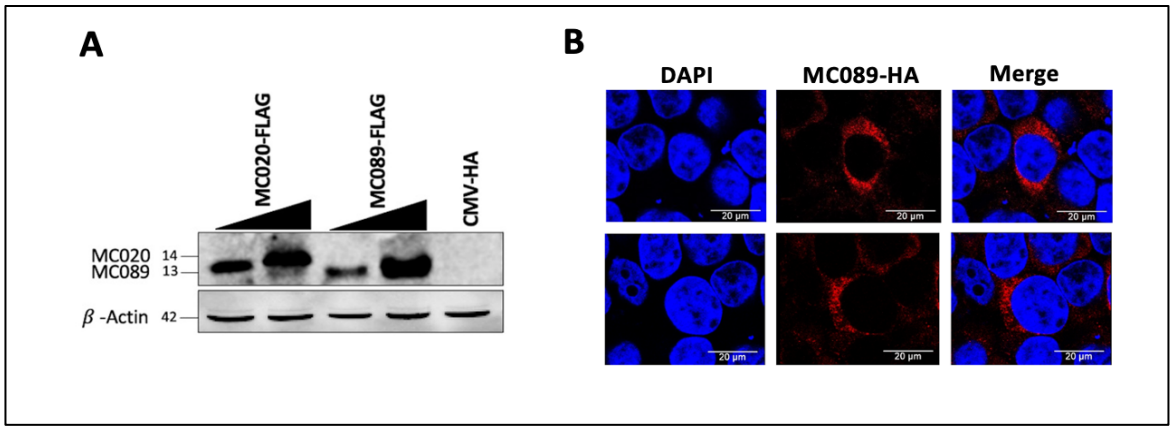

Figure 3.1 MC089 expression in HEK293T cells. (A) MC089 and MC020 western blot expression. HEK293T cells were seeded at $5x10^5$ cells/well in six-well plates and transfected 24 hours later with 1.5 µg or 3 µg (equivalent to amounts used in luciferase assay) empty vector (CMV-HA) or pCEP4 vectors expressing MC089-FLAG or MC020-FLAG. Cell lysates were harvested and western blotted with anti-FLAG or anti-β-actin antibodies. (B) Confocal localization of MC089 in HEK293T cells. Cells were transfected with 500 ng of pCEP4-MC089-HA expression vector, fixed 24 hours later and stained with HA tag antibody (red) and DAPI (blue).

3.1 MC089 is an inhibitor of IRF-dependent gene induction by nucleic acid sensing pathways

We employed a luciferase assay-based screening system where pathway activation is driven at defined points with PRR-agonists or overexpressed key proteins of associated innate signaling pathways to measure the effect of MC089 on ISRE luciferase and IFNβ promoter luciferase. Whilst the ISRE luciferase reporter measures IRF (primarily IRF3) activity in primary sensing pathways (58), both NF-κB and IRFs regulate the activation of the natural IFNβ promoter reporter (54). However, it is important to note that IRFs have a more dominant role in regulating the IFNβ promoter due to potent ISRE sites in two promoter regions (PRDI and PRDIII) (65, 246, 247, 486, 487) (**Fig.1.1.1**). In probing the

effect of MC089 on these pathways, we used the vaccinia virus IRF activation inhibitor C6 (VVC6) (352) for comparison with inhibitory activity of MC089. The cGAS-STING DNA sensing pathway can be reconstituted in cGAS and STING co-transfected HEK293T cells where both proteins are not normally expressed (131, 488). Analogous to VVC6, MC089 expression potently inhibited cGAS-STING-induced IRF and IFNβ promoter activation system (**Fig.3.2C & Fig.3.3B**). Interestingly, MC089 was substantially more potent in doing so with lower levels of expression than VVC6 (**Fig.3.2B**).

We next looked into the effect of MC089 on dsRNA sensing TLR3-driven pathway, by overexpressing a constitutively active chimeric construct of the CD4 signaling domain and TLR3, or by overexpressing TLR3's primary adapter TRIF (489). We found CD4-TLR3-driven ISRE activation to be inhibited by MC089 expression displaying approximately 50% reduction in activation with the highest plasmid transfection (50ng) of MC089 and VVC6 (**Fig.3.2D**). Similarly both MC089 and VVC6 expression inhibited ISRE activation and that of the IFNβ promoter (**Fig.3.2E & Fig.3.3C**).

The RIG-I pathway has been shown to indirectly recognize dsDNA in HEK293T cells through the transcription of AT-rich dsDNA into 5′- triphosphate RNA ligand of RIG-I by the enzyme RNA Pol III (490) (**Figure 1.1.7)**. Thus, stimulation by synthetic dsDNA ligand, Poly(dA:dT), and overexpression of the fundamental regulator of RIG-I, MAVS, were each used to drive RIG-I-pathway activation. Both MC089 and VVC6 potently inhibited activation of ISRE and IFNβ promoter in a dose-dependent manner recording the highest score of significance among the examined upstream signaling driving elements of ISRE activation (**Fig.3.2F-G & Fig.3.4D-E**).

MC089 specificity to IRF inhibition was confirmed by the absence of an inhibitory effect on the Elk1 mitogenic signaling pathway driven by RasV and tracked using an Elk-1-GAL4 fusion promoter luciferase construct (**Fig.3.4F**). Together, these data suggested that MC089, like VVC6, is an inhibitor of IRF activation and targets at a downstream point common to multiple innate virus sensing pathways.

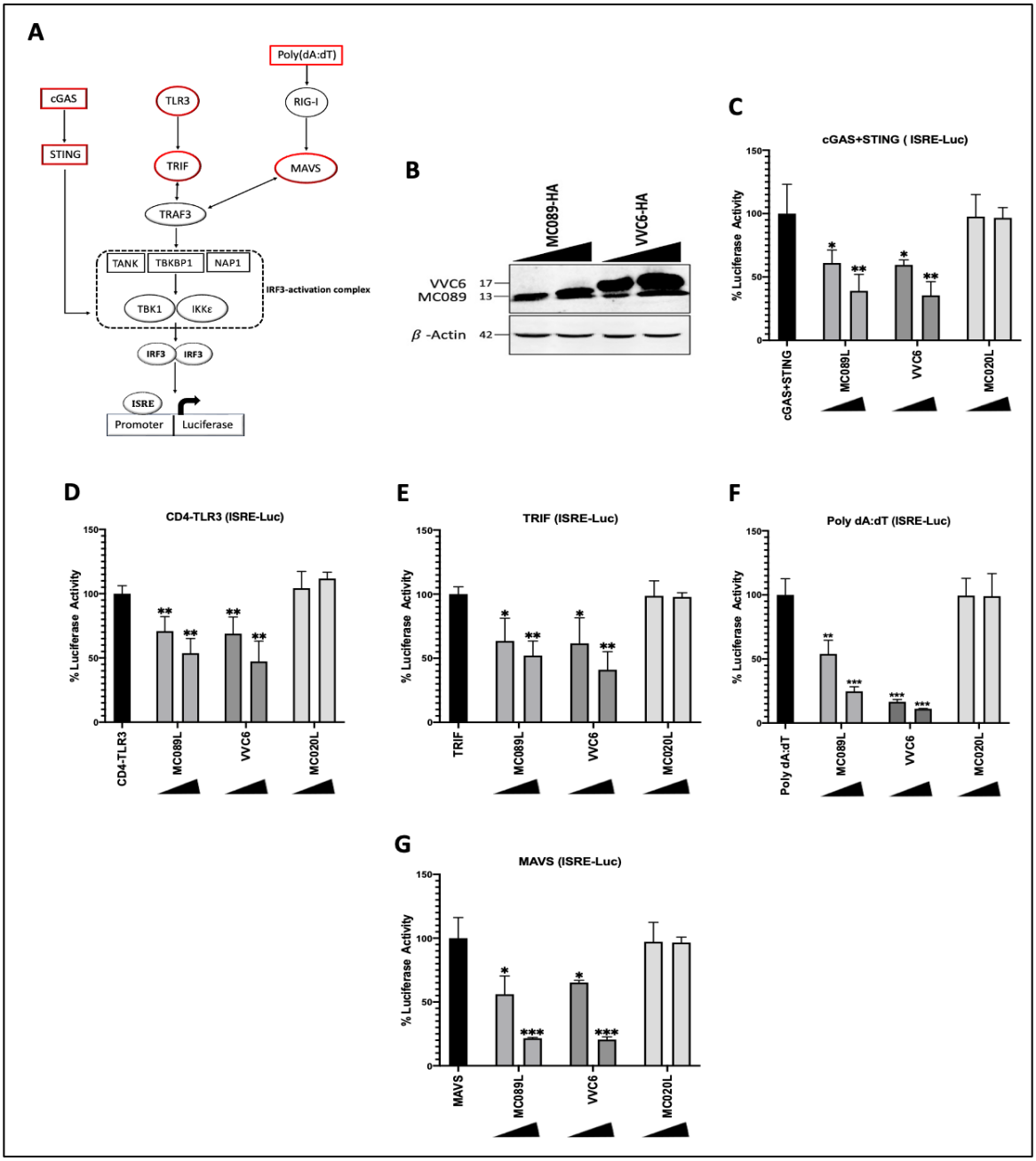

Figure 3.2 MC089 inhibits ISRE activation by nucleic acid sensing pathways. (A) Schematic of the main antiviral IRF3 pathways. The targeted signaling elements are highlighted in red.

(B) MC089 and VVC6 western blot expression. HEK293T cells were seeded at $5x10^5$ cells/well in six-well plates and transfected 24 hours later with 1.5 µg or 3 µg (equivalent to amounts used in luciferase assay) HA-tagged pCEP4 vectors expressing MC089 or VVC6. Cell lysates were harvested and western blotted with anti-HA antibody. (C-G) HEK293T cells were seeded at $2x10^5$ cells /ml and transfected 24 hours later with 80 ng of ISRE luciferase reporter. To normalize firefly luciferase, 40 ng of pGL3-*Renilla* control was utilized. Cells were transfected with two doses of pCEP4 constructs expressing MC089, VVC6 or MC020: 25 ng and 50 ng. Activators of the pathways were employed accordingly: cGAS (25 ng) and STING (25 ng), 50 ng of CD4-TLR3, 10 ng of TRIF, Poly(dA:dT) (1 µg/ml) and MAVS (10 ng). The total amount of DNA was adjusted to a final volume of 220 ng using the empty vector control (pCMV-HA). Cell lysates were harvested and assayed for luciferase activity. Schematics are representative of three or more individual experiments. Data were normalized to the empty vector and presented by percentage activity compared to positive control. Bars indicate mean ± the standard deviation. Statistical significance is denoted as * $P<0.05$, ** $P<0.01$ and *** $P<0.001$.

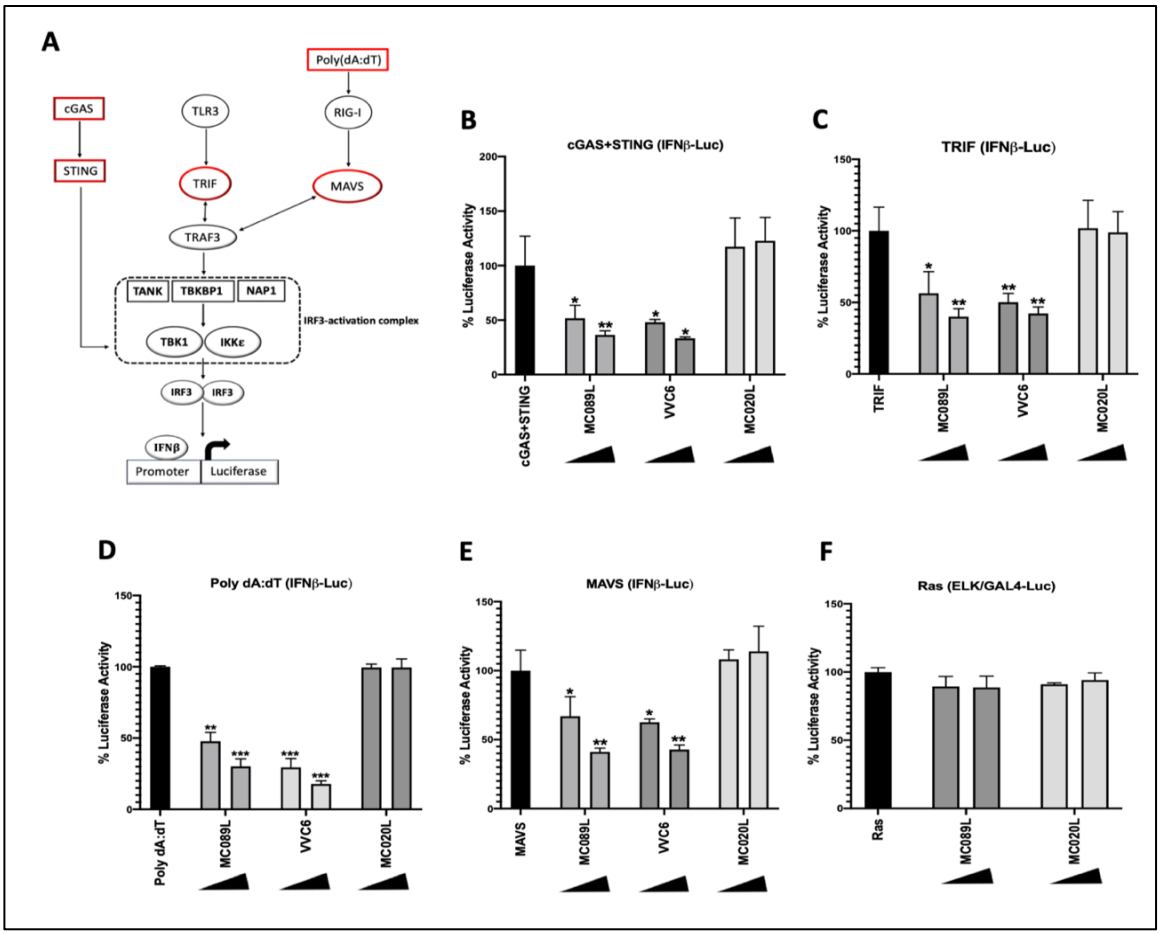

Figure 3.3 MC089 inhibits IFNβ promoter activation by nucleic acid sensing pathways. (A) Schematic of the main antiviral IRF3 pathways. The targeted signaling elements are highlighted in red. (B-F) HEK293T cells were seeded at $2x10^5$ cells /ml and transfected 24 hours later with 80 ng of IFNβ or Elk1-Gal4 luciferase reporter. To normalize firefly luciferase, 40 ng of pGL3-*Renilla* control was utilized. Cells were transfected with two doses of pCEP4 constructs expressing MC089, VVC6 or MC020: 25 ng and 50 ng. Activators of the pathways were employed accordingly: cGAS (25 ng) and STING (25 ng), 10 ng of TRIF, Poly(dA:dT) (1 µg/ml), MAVS (10 ng) and Ras (50 ng). The total amount of DNA was adjusted to a final volume of 220 ng using the empty vector control (pCMV-HA). Cell lysates were harvested and assayed for luciferase activity. Schematics are representative of three or more individual experiments. Data were normalized to the empty vector and presented by percentage activity compared to positive control. Bars indicate

mean ± the standard deviation. Statistical significance is denoted as * P<0.05,** P<0.01 and *** P<0.001.

3.2 MC089 does not affect NF-κB activation

To determine if MC089 also affects activation of the other major antiviral signaling transcription factor, NF-κB, we repeated the luciferase mapping experiments using NF-κB luciferase reporter to monitor NF-κB activity. Unlike cGAS-STING-dependent IRF activation, MC089 had no effect on the pathway activating NF-κB luciferase showing a similar pattern to the negative control MC020 (**Fig.3.4B**). This observation was consistent with TLR3 and RIG-I-driven NF-κB activation where MC089 had no inhibitory effect (**Fig.3.4C-F**).

We also looked at MC089 inhibitory effect on NF-κB activity upon stimulation with overexpressed TRAF3, a mediator protein used by both TRIF and MAVS, and found a comparable luciferase activation with the controls (**Fig.3.4G**). The MC089 lack of inhibition of on NF-κB activation was confirmed by the absence of an effect upon activating the system downstream with overexpressed IKKβ construct (**Fig.3.4H**). Therefore, we concluded that MC089, similar to VVC6, specifically targets IRF activation for inhibition.

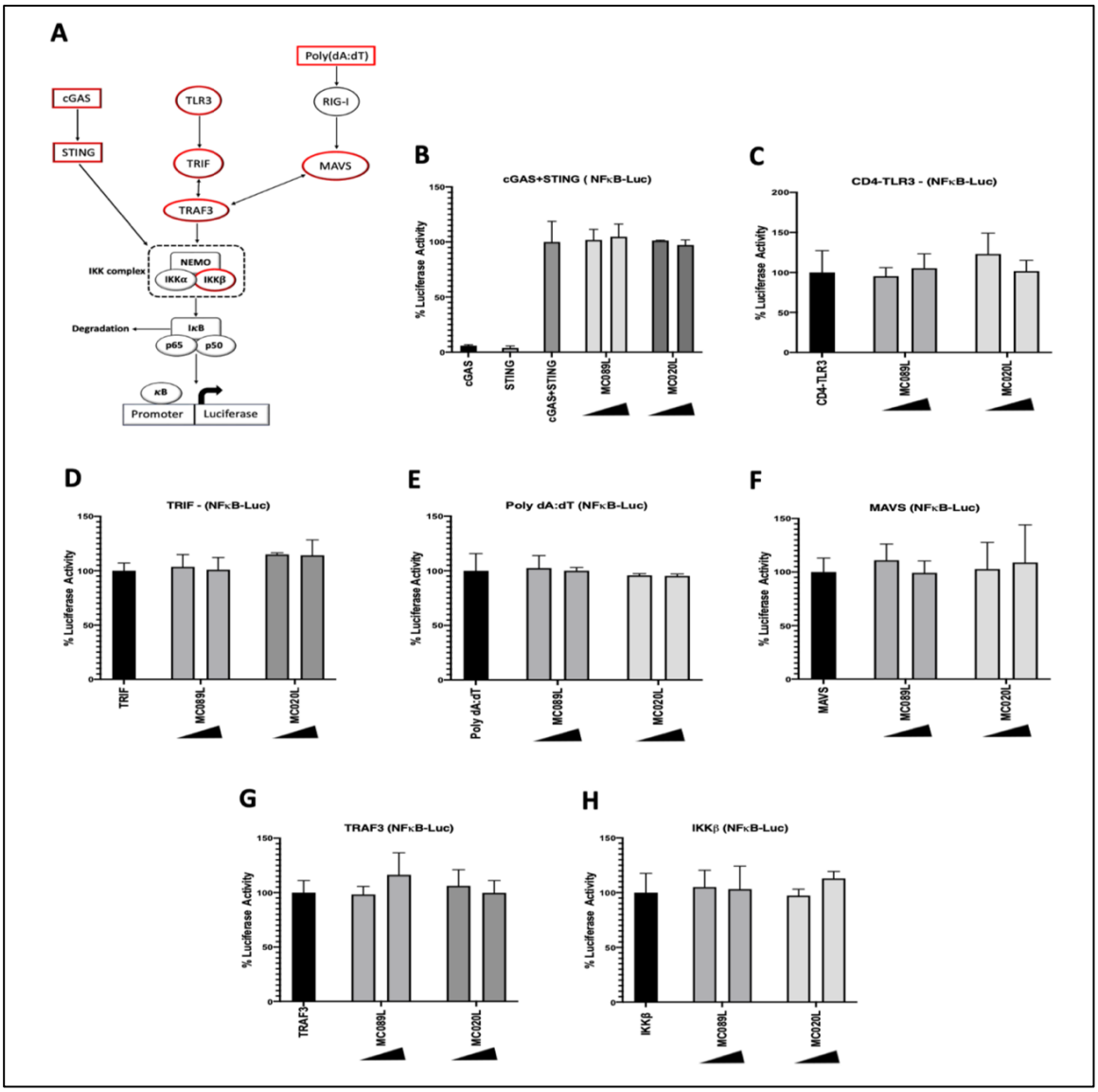

Figure 3.4 MC089 does not affect NF-*κ*B activation. (A) Schematic of the main antiviral NF-*κ*B pathways. The targeted signaling elements are highlighted in red. (B-H) HEK293T cells were seeded at $2x10^5$ cells /ml and transfected 24 hours later with 80 ng of NF-*κ*B luciferase reporter. To normalize firefly luciferase, 40 ng of pGL3-*Renilla* control was utilized. Cells were transfected with two doses of pCEP4 constructs expressing MC089 or MC020: 25 ng and 50 ng. Activators of the pathways were employed accordingly: cGAS (25 ng) and STING (25 ng), 50 ng of CD4-TLR3, 10 ng of TRIF, poly (dA:dT) (1 µg/ml), MAVS (10 ng), 50 ng of TRAF3 and IKKβ. The total amount of DNA was adjusted to a final volume of 220 ng using the empty vector control (pCMV-HA). Cell lysates were harvested and

assayed for luciferase activity. Schematics are representative of three or more individual experiments. Data were normalized to the empty vector and presented by percentage activity compared to positive control. Bars indicate mean ± the standard deviation.

3.3 MC089 potently inhibits IRF-dependent gene activation driven by IKKε and TBK1

To further clarify the point of inhibition of MC089 on IRF-activating pathways, we next examined the effect of MC089 on signaling by the direct activators of IRFs, TBK1 and IKKε. As VVC6 is known to inhibit IRF3 activation by binding to the scaffold proteins TANK, TBKBP1 and NAP1, it was used again as an inhibitory reference in these experiments (352). Comparable to VVC6, MC089 inhibited both IKKε-and TBK1-dependent ISRE and IFNβ promoter activation (**Fig.3.5B-E**). Interestingly, MC089 was substantially more potent than VVC6 at inhibiting IKKε-induced ISRE activation (**Fig.3.5B**). We also attempted to drive ISRE luciferase activity by the scaffold proteins of the IRF3-activation complex but did not observe an activation of the system using these proteins(**Fig.3.5F-G**). This was not unexpected as the host laboratory has previously observed that overexpression of some signaling components does not function to drive activation of the system.

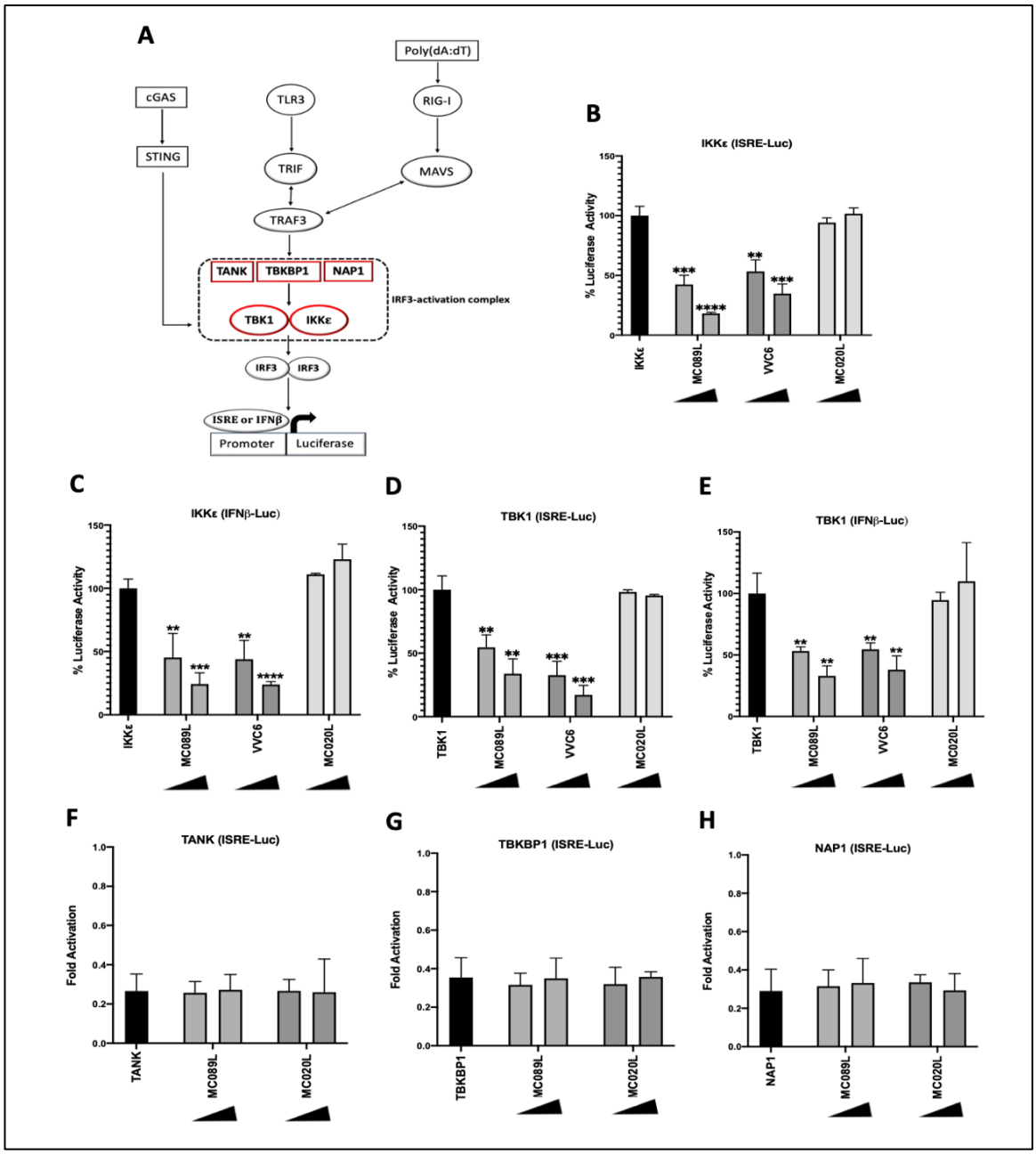

Figure 3.5 MC089 potently inhibits IRF-dependent gene activation driven by IKKε and TBK1. (A) Schematic of the main antiviral IRF3 pathways. The targeted signaling elements are highlighted in red. (B-H) HEK293T cells were seeded at $2x10^5$ cells /ml and transfected 24 hours later with 80 ng of ISRE or IFNβ luciferase reporter. To normalize firefly luciferase, 40 ng of pGL3-*Renilla* control was utilized. Cells were transfected with two doses of pCEP4 constructs expressing MC089, VVC6 or MC020: 25 ng and 50 ng. Activators of the pathways were added accordingly: TBK1 (50 ng), IKKε (50 ng), TANK (50 ng), TBKBP1 (50 ng) or NAP1 (50 ng). The total amount of DNA was adjusted to a final

volume of 220 ng with the empty vector control (pCMV-HA). Cell lysates were harvested and assayed for luciferase activity. Schematics are representative of three or more individual experiments. (B-E) Data were normalized to the empty vector and presented by percentage activity compared to positive control. Bars indicate mean ± the standard deviation. Statistical significance is denoted as ** P<0.01, *** P<0.001 and **** P<0.0001. (F-H) Data were normalized to the empty vector and presented by fold activation. Bars indicate mean ± the standard deviation.

3.4 Direct activation of ISRE by IRFs bypasses MC089 inhibitory effect

We next investigated the effect of MC089 on direct activation of ISRE by overexpression of IRF3. Consistent with inhibition at a point upstream of IRF3, overexpression of this transcription factor bypassed ISRE reporter inhibition by MC089 (**Fig.3.6B**). Previous work on the MCV inhibitor MC132, which targets the NF-κB p65 subunit for degradation, p65 expression was titrated down and determined that while MC132 was unable to inhibit at high levels of p65 expression, its inhibitory effect could be observed at lower levels of expression (472). In contrast to MC132 targeting of p65, MC089 was observed not to suppress IRF3-activated ISRE even at low levels of expression (**Fig.3.6C)** suggesting that the inhibition was not occurring at the level of IRF3, but rather at the level of upstream activating complexes. MC089 also had no effect on direct activation of IRSE by overexpression of other antiviral IRFs, IRF7 and IRF5 (**Fig.3.6D-E**).

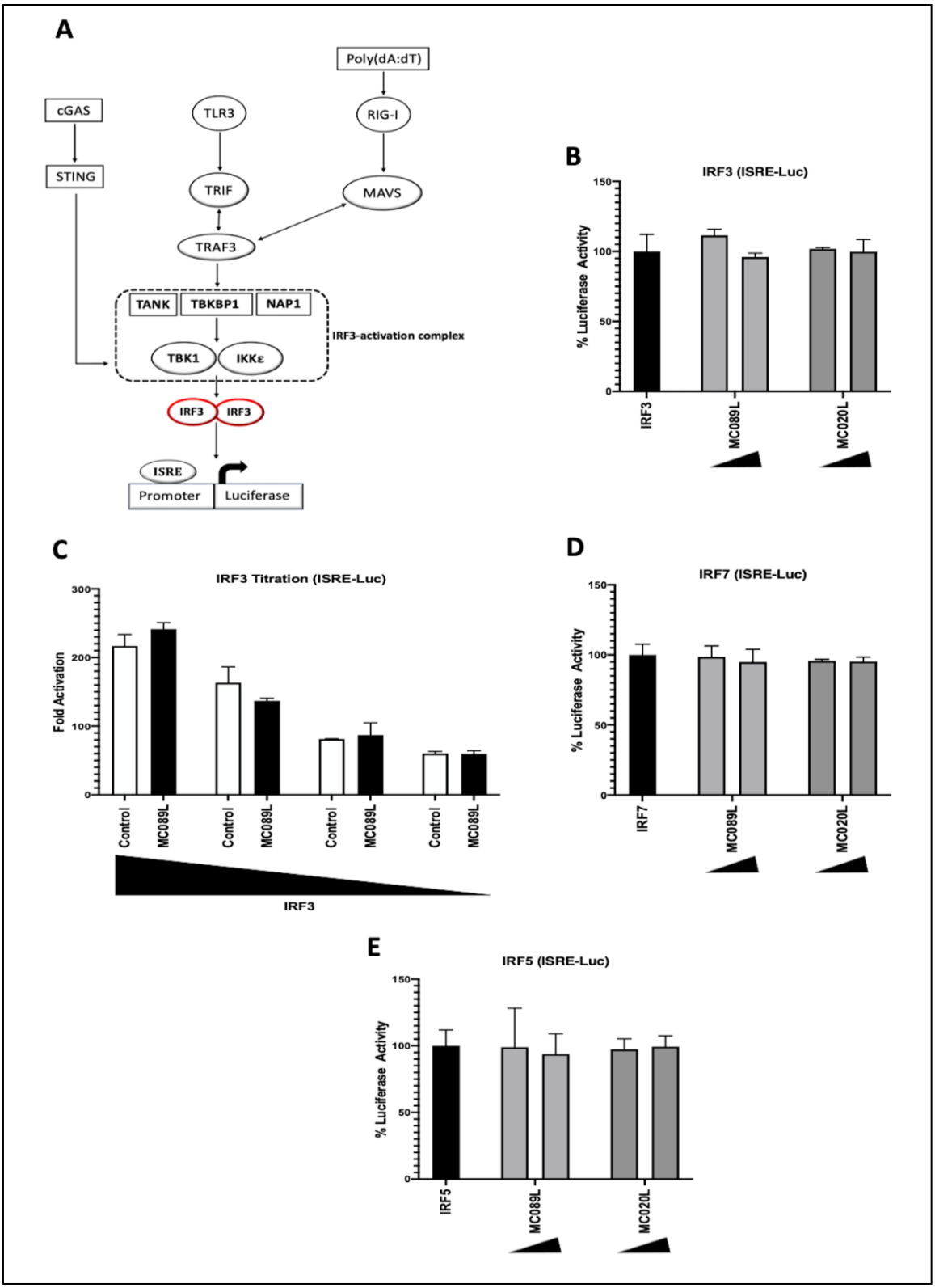

Figure 3.6 Direct activation of ISRE by IRFs bypasses MC089 inhibitory effect. (A) Schematic of the main antiviral IRF3 pathways. The targeted signaling elements are highlighted in red. (B, D-E) HEK293T cells were seeded at $2x10^5$ cells/ ml and transfected 24 hours later with 80 ng of ISRE luciferase reporter. To normalize firefly luciferase, 40 ng of pGL3-*Renilla*

control was used. Cells were transfected with two doses of pCEP4 constructs expressing MC089 or MC020: 25 ng and 50 ng. Activators of the pathways were added accordingly: IRF3 (50 ng), IRF7 (50 ng) or IRF5 (50 ng). The total amount of DNA was adjusted to a final volume of 220 ng with the empty vector control (pCMV-HA). Cell lysates were harvested and assayed for luciferase activity. Schematics are representative of three or more individual experiments. Bars indicate mean ± the standard deviation. (C) Similarly, HEK293T cells were seeded at $2x10^5$ cells/ml and transfected 24 hours later with 80 ng of ISRE luciferase reporter and 40 ng of pGL3-*Renilla* control. IRF3 doses used were 25 ng, 10 ng, 5 ng and 3 ng, respectively. The total amount of DNA was adjusted to a final volume of 220 ng using the empty vector control (pCMV-HA). Data are presented by fold activation calculated by normalizing to the empty vector and are representative of triplicate experiments. Bars indicate mean ± the standard deviation.

3.5 Discussion

MCV is the only known extant human-specific poxvirus that appears to have evolved for human infection. It causes benign skin lesions typically absent of inflammation with a long duration to clearance (457). The human-specific nature of MCV, duration of infection and mild presentation of its lesions suggest that MCV possesses highly effective innate immune inhibitors like all other well-characterized poxviruses. Unfortunately, attempts to culture MCV in vitro and infect cells in culture have not been successful which restricts the investigation of host-pathogen interactions (450, 491). Nevertheless, several novel MCV-derived inhibitors have been discovered through the characterization of MCV ORFs in isolation where most of them target NF-κB activation (**Section 1.4**). Because IRF activation is a critical component of antiviral immunity, it is predicted that MCV encodes multiple inhibitors that target this system as found in other poxviruses (235, 352). Until

recently, only two MCV-derived inhibitors, MC159 and MC160, have been discovered to target IRF activation at the level of IRF3 kinases. Whilst MC159 interacts with TBK1 and IKKε for inhibition of IRF3/IRF7 activity, the mechanism by which MC160 impedes the same system is currently unknown (236). A previous screening of MCV ORFs by the host laboratory identified MC089 as a possible inhibitor of IRF activation through inhibition of ISRE luciferase reporter activation. In this chapter, we investigated MC089 inhibitory effect on essential antiviral signaling pathways using luciferase assay-based screening system.

The cellular model of MC089 in this investigation was based on the commonly used epithelial-like HEK293T cells. These cells are highly effective for transient and stable transfection mediated by the insertion of the oncogenic DNA simian virus 40 (SV40) T antigen that allows for a high yield expression of target proteins within vectors carrying the SV40T promoter including the pCEP4 vector (492)(**Fig.2.2.1)**. Because many of the presented experiments depended on protein overexpression and because HEK293T cells have been demonstrated in multiple viral studies to trigger antiviral responses upon stimulation (131, 488, 493, 494), HEK293T cells were chosen for these in vitro studies.

We mapped MC089 inhibitory effect to be specific to IRF activation through inhibition of IRF-dependent gene induction and the absent of effect on NF-κB activation. Therefore, since MC159 and MC160 also inhibit NF-κB activation (471, 473), MC089 is the first MCV inhibitor to specifically target IRF-activating pathways. Because MC089 inhibited IRF activation by both DNA and RNA sensing pathways, we expected MC089 to target at a downstream point common to multiple innate virus sensing pathways supported by the

potent inhibition of IRF-dependent gene activation driven by IKKε and TBK1 and the absent of effect on direct ISRE activation driven by IRF transcription factors.

Activating ISRE luciferase by the scaffold proteins of IRF3 kinases was limited by the luciferase system at which the overexpression of such signaling elements does not work to drive the luciferase promoter. However, it is essential not to exclude TANK, TBKBP1 and NAP1 association with MC089 due to their importance in IRF3-activation complex **(Section 1.1.5.3)**, and subject them, to further investigate their potential targeting assessment, with other types of experiments.

MC089 showed a similar pattern of inhibition to another specific inhibitor of IRF activation, the VACV C6 protein which interacts with the scaffold proteins TANK, TBKBP1 and NAP1 to suppress IRF3 activity (352). This also indicates that MC089 might follow a similar mode of targeting at the level of the IRF3-activation complex. However, MC089's ability to inhibit the activation of the system at lower levels of expression suggested a much potent inhibitory mechanism where multiple key proteins of IRF3 pathways are involved. Additionally, MC089 was significantly more potent than VVC6 at inhibiting IKKε-induced ISRE activation implying a possible direct association with the kinase comparing with VVC6 which does not directly interact with either IKKε or TBK1.

3.6 Conclusion

Luciferase pathways mapping of MC089 effect revealed that MC089 is a specific novel inhibitor of IRF-dependent gene induction by nucleic acid sensing pathways and that this inhibitory effect bypasses the direct activation of ISRE by IRF3. Because the IRF3-activation complex, composed of the IRF3 kinases IKKε and TBK1 and the scaffold proteins TANK, TBKBP1 and NAP1, is a key convergence point downstream of IRF3 activation, we expect MC089 to target the system at the level of this complex.

Chapter 4 Investigation of MC089 targeting of MAVS and IRF3-activation complex components

The luciferase pathways mapping of the MC089 inhibitory effect on IRF activation indicated that MC089 targets a common downstream point of IRF main pathways. Since direct activation of the IRF-dependent gene by the transcription factors bypassed MC089 inhibition, targeting of IRF3-activation complexes seemed likely. In this chapter, the precise point of MC089 inhibition of IRF-activating pathways will be investigated.

4.1 MC089 associates with mitochondria

During the initial investigation of MCV inhibitors of human antiviral immunity prior to the commencement of this research, unbiased affinity purification and mass spectrometry (AP-MS) was performed on MEP4-MC089-expressing HEK293T lysates to identify co-purifying proteins. AP-MS analysis of MC089 co-purifying proteins revealed enrichment of mitochondrial proteins including multiple mitochondrial ATP synthase subunits (ATP5J, ATP5O, ATP5H ATP5B ATP5F1 ATP5A1 and ATP5A2) (495, 496) and voltage-dependent anion channel 2 (VDAC2), a key protein of the mitochondrial outer membrane (497) **(Fig.4.1)** (collaboration with Andreas Pichlmair, Technical University of Munich, Germany). This suggested that MC089 associates with mitochondria, which also pointed towards a possible link between MC089 and MAVS, since the latter is a protein known to associate primarily with mitochondria and partially with endoplasmic reticulum (ER) and peroxisomes (498-501).

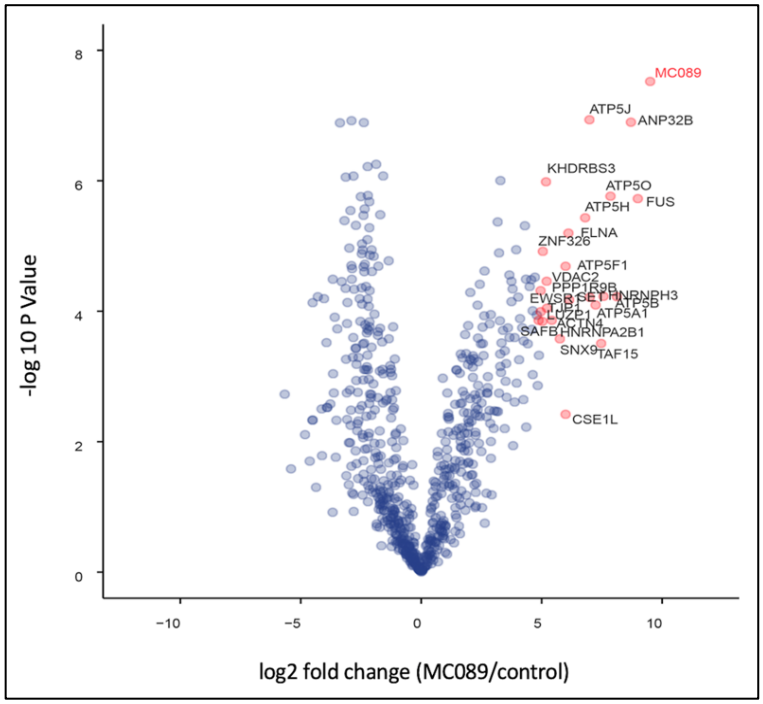

Figure 4.1 Unbiased AP-MS volcano plot of MC089-interacting proteins. Affinity purification and mass spectrometry (AP-MS) was performed on MEP4-MC089-expressing HEK293T lysates. This volcano plot displays proteins (highlighted in black) co-purifying with immunoprecipitated MC089 (highlighted in red). These data are included to provide a perspective of the course of the MC089 investigation and were provided by Prof. Andreas Pichlmair in collaboration with Prof. Gareth Brady.

To confirm the mitochondrial association of MC089, we first optimized the working concentration of the MitoTracker dye in HEK293T cells to maintain mitochondrial morphology while avoiding mitochondrial artifacts and toxicity. We prepared three different dilutions of MitoTracker Deep Red FM dye with DMSO: 100 nM, 200 nM and 500 nM and found the working concentration of 200 nM to be optimal to track mitochondria in HEK293T cells (**Fig.4.2**). We next stained mitochondria with MitoTracker dye in MC089 and MAVS expressing cells and examined cells by confocal microscopy. We first confirmed that both overexpressed MAVS-FLAG and endogenous MAVS partly associate with mitochondria in HEK293Ts (**Fig. 4.3A**).

We then observed that MC089 displays a similar pattern of partial association with mitochondria (**Fig.4.3B**).

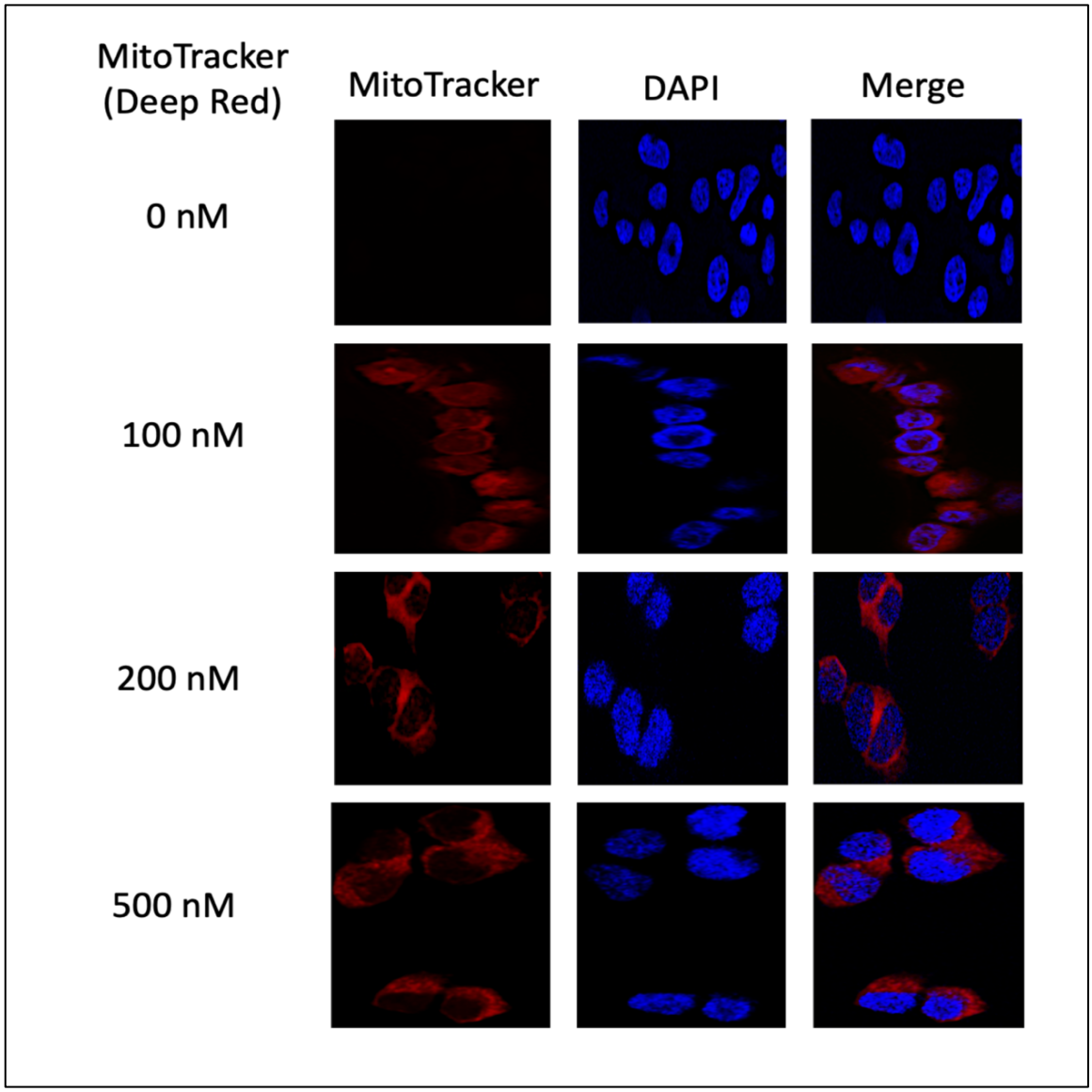

Figure 4.2 Optimization of the MitoTracker working concentration in HEK293T cells. HEK293T cells were seeded at $8x10^4$ cells/well on glass chamber slides and 24 hours later, MitoTracker deep red FM diluted in DMSO was added to the growth media at the indicated concentrations for 30 minutes. Cells were then fixed and stained with DAPI (blue).

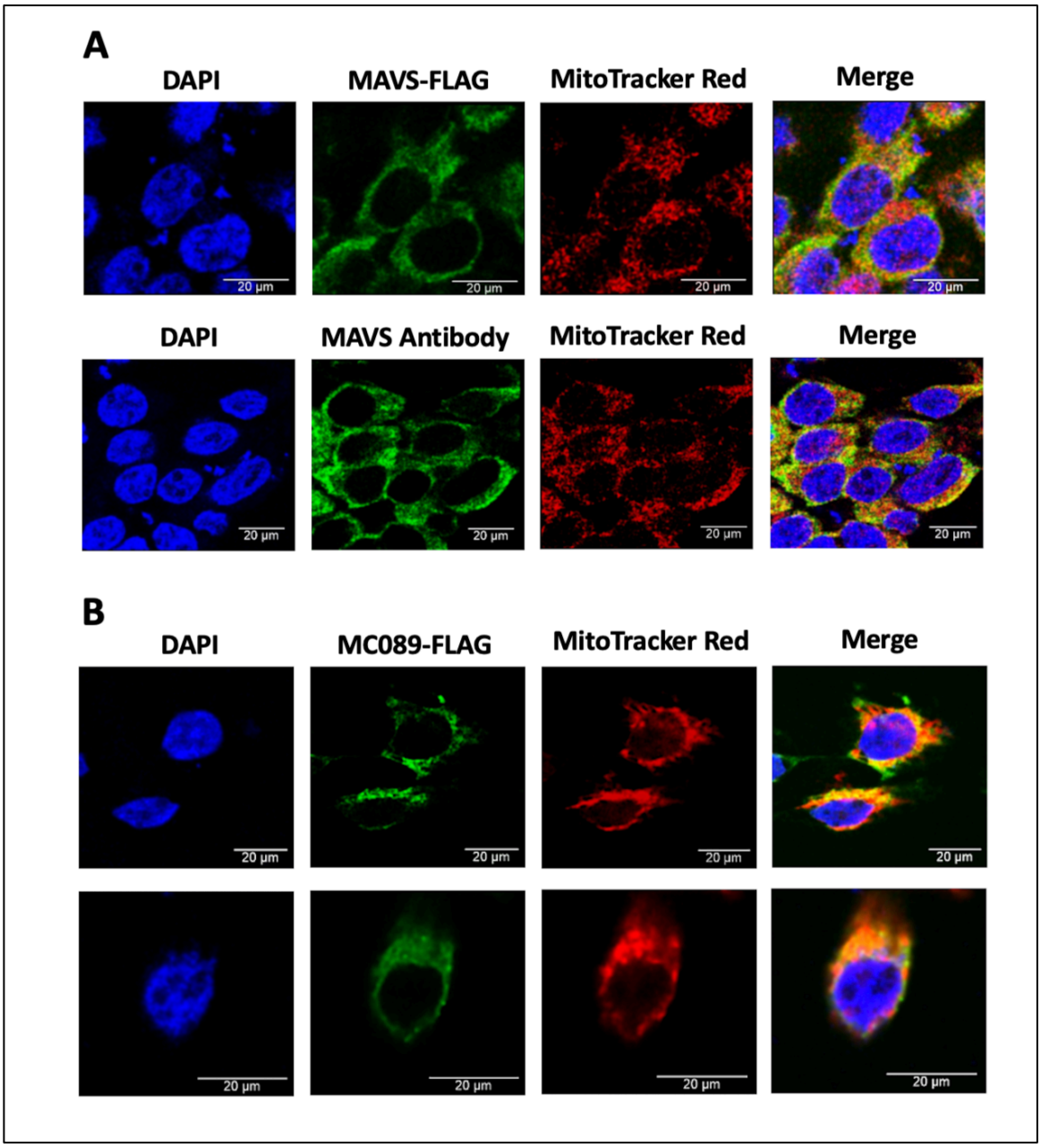

Figure 4.3 MAVS and MC089 associate with mitochondria. Mitochondrial confocal localization of MAVS and MC089. HEK293T cells were seeded at $8x10^4$ cells/well on glass chamber slides and transfected 24 hours later with a total of 500 ng of MAVS-FLAG (A, upper panel) or pCEP4-MC089-FLAG (B). After 24 hours, MitoTracker deep red FM diluted in DMSO was added to the growth media at 200 nM for 30 minutes. Cells were fixed and stained with DAPI (blue), MAVS antibody (green) (A, lower panel) or FLAG tag antibody (green). Results are representative of triplicate experiments.

4.2 MC089 selectively associates with MAVS, IKKε, TBKBP1 and NAP1

We next investigated the possible association of MC089 with known constituent proteins of the IRF3 activating complexes, and with MAVS. The NF-κB-regulating kinase IKKβ was used as a negative control for MC089 in co-immunoprecipitation experiments due to its lack of involvement in IRF activation and similarity to IRF-activating members of the IKK family. Although no association was detected with TBK1 or IKKβ, a strong association was detected with IKKε and MAVS (**Fig. 4.4).**

We next probed the association of MC089 with the IRF-activating complex adapter proteins TBKBP1, TANK and NAP1. These adapters provide a platform for the assembly of IRF-activating kinases for their subsequent phosphorylation of IRF3 (332-335). While we detected no association with TANK, MC089 interacted with both TBKBP1 and NAP1 (**Fig.4.5**). Furthermore, the interaction of MC089 with endogenous MAVS and TBKBP1 was confirmed in HEK293T cells using cognate antibodies for their proteins (**Fig. 4.7A**).

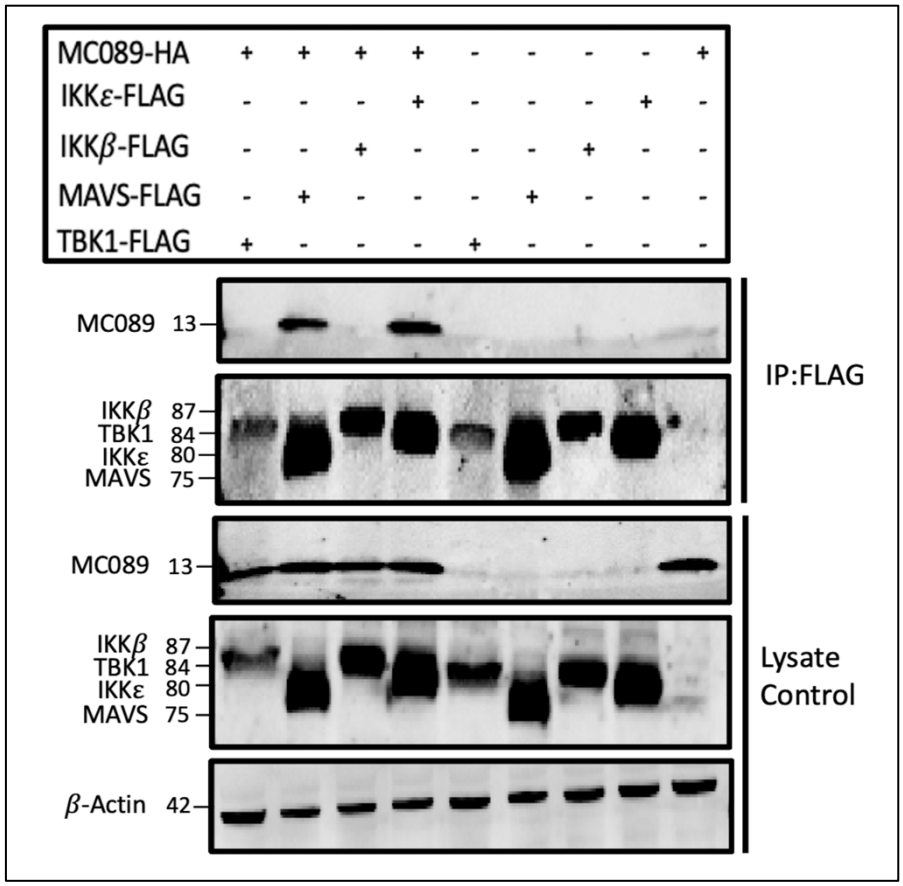

Figure 4.4 MC089 interacts with IKKε and MAVS. HEK293T cells were seeded at $3x10^6$ cells/ culture dish and transiently transfected 24 hours later with a total of 8 μg of pCEP4-MC089-HA and the indicated signaling pathway component FLAG-tagged plasmids. After 24 hours, cell lysates were immunoprecipitated using anti-FLAG M2 affinity gel beads, eluted with FLAG tag peptide, and probed with the appropriate antibodies: anti-HA (first and third panels), anti-FLAG (second and fourth panels) and anti-β-actin (fifth panel). Blots are representative of triplicate experiments.

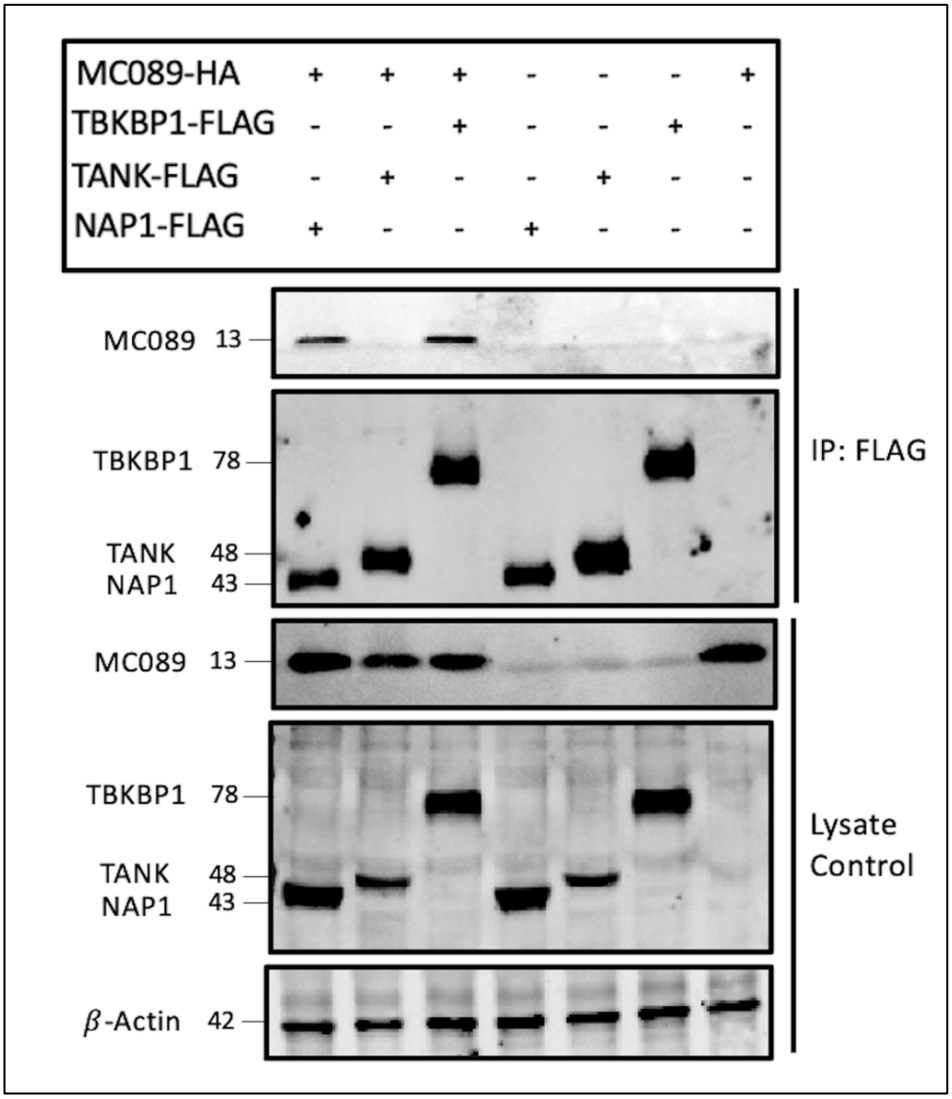

Figure 4.5 MC089 interacts with TBKBP1 and NAP1. HEK293T cells were seeded at $3x10^6$ cells/ culture dish and transiently transfected 24 hours later with a total of 8 μg of pCEP4-MC089-HA and the indicated signaling pathway component FLAG-tagged plasmids. After 24 hours, cell lysates were immunoprecipitated using anti-FLAG M2 affinity gel beads, eluted with FLAG tag peptide, and probed with the appropriate antibodies: anti-HA (first and third panels), anti-FLAG (second and fourth panels) and anti-β-actin (fifth panel). Blots are representative of triplicate experiments.

We also probed for co-localization of IRF3-activating complex proteins and MC089 by confocal microscopy to examine if MC089 and its immunoprecipitated proteins relatively express in close proximity within the cell for a possible interaction to occur. Consistent with co-immunoprecipitation data, strong co-localization was observed for MC089 with IKKε, NAP1, TBKBP1 with partial co-localization with MAVS (**Fig.4.6 and Fig.4.7**). Also consistent with co-immunoprecipitation data, no significant co-localization was detected between MC089 and TANK, and between MC089 and TBK1 to which MC089 showed atypical nuclear localization. Additionally, as for co-immunoprecipitation experiments, we confirmed the co-localization of MC089 with endogenous MAVS (predicted 75 kDa and 52 kDa) and TBKBP1(predicted 78 kDa) in HEK293T cells (**Fig.4.8**). The two bands pattern of endogenous MAVS protein is common and has been reported before in multiple cell lines where the 75 kDa band indicated to be full-length MAVS and the 52 kDa band suggested to be processing products of the protein (499).

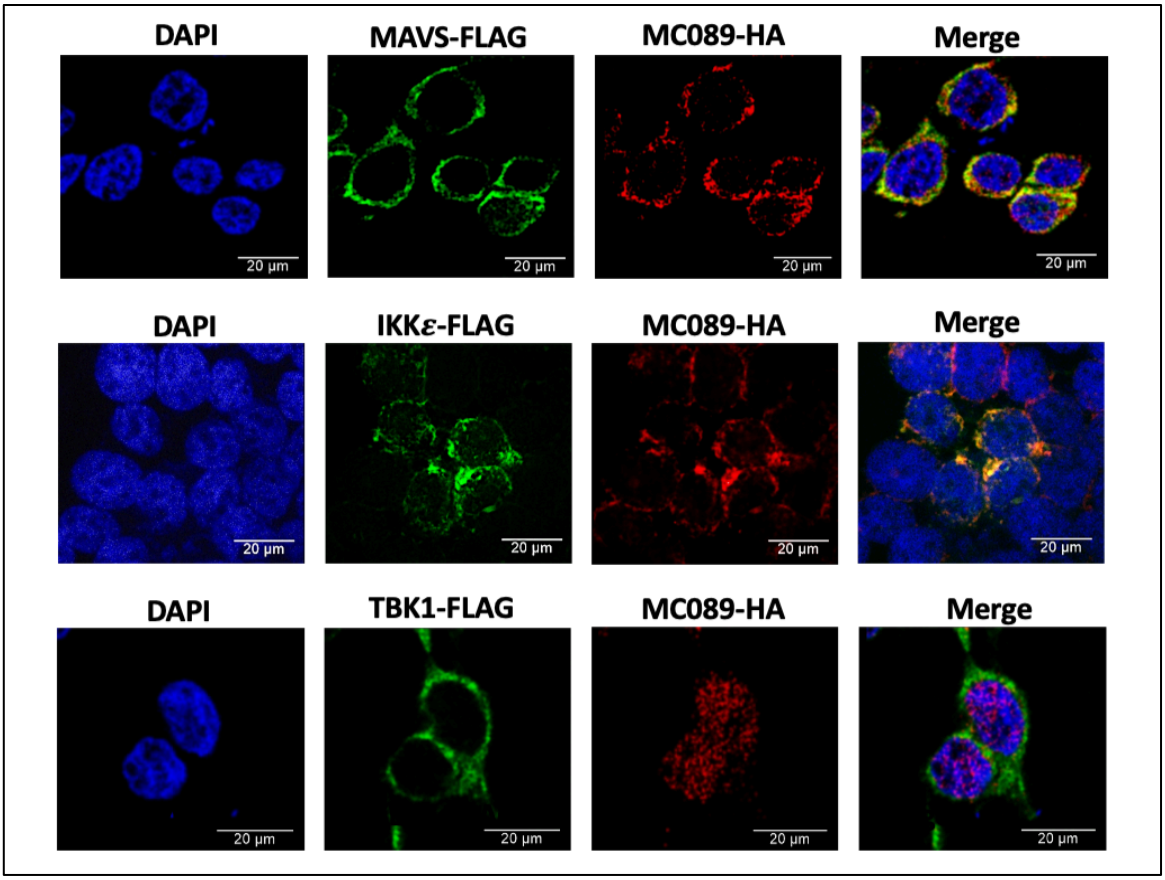

Figure 4.6 MC089 colocalizes with MAVS and IKKε. HEK293T cells were seeded at 8 x10^4 cells/ well on glass chamber slides and transiently transfected 24 hours later with a total of 500 ng of pCEP4-MC089-HA and the indicated signaling pathway component FLAG-tagged plasmids. Cells were fixed 24 hours later and stained with HA tag antibody (red), FLAG tag antibody (green) and DAPI (blue). Results are representative of triplicate experiments.

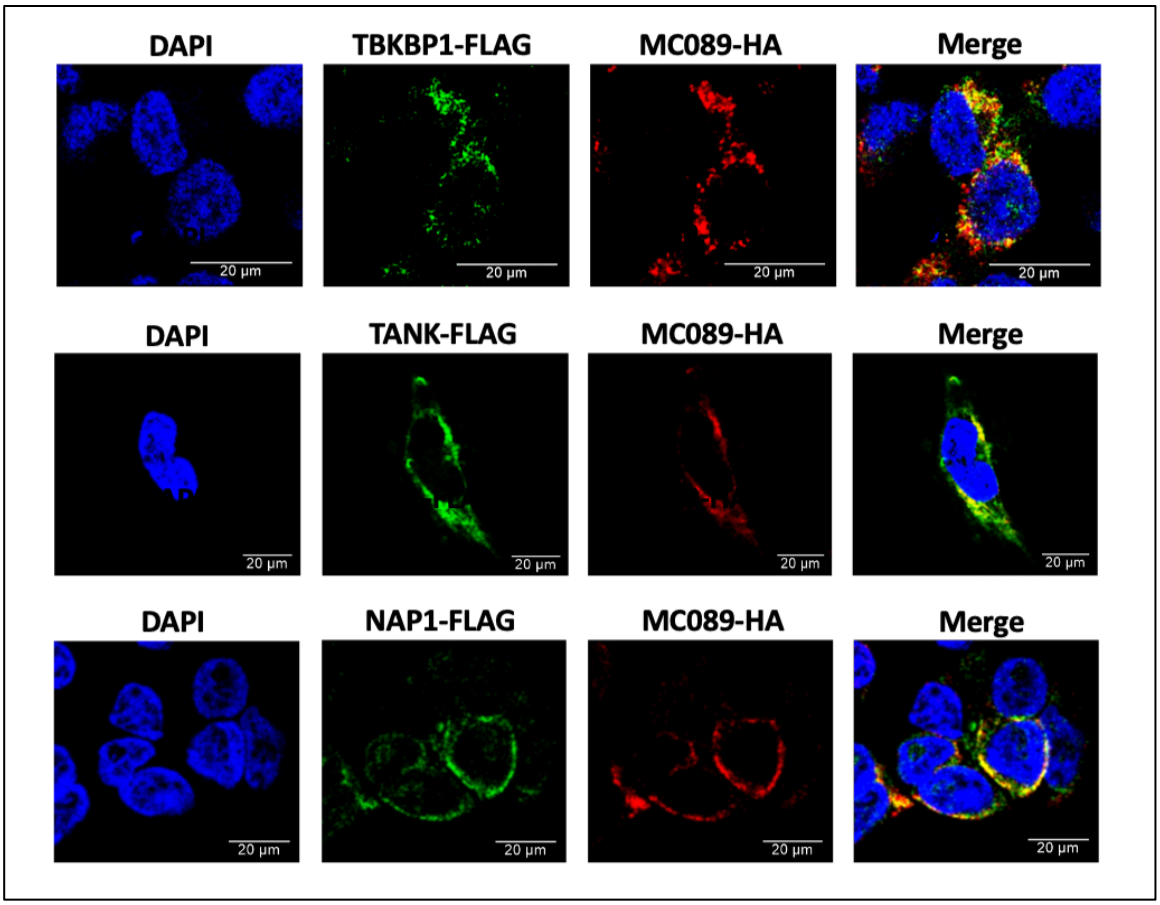

Figure 4.7 MC089 colocalizes with TBKBP1 and NAP1. HEK293T cells were seeded at $8x10^4$ cells/ well on glass chamber slides and transiently transfected 24 hours later with a total of 500 ng of pCEP4-MC089-HA and the indicated signaling pathway component FLAG-tagged plasmids. Cells were fixed 24 hours later and stained with HA tag antibody (red), FLAG tag antibody (green) and DAPI (blue). Results are representative of triplicate experiments.

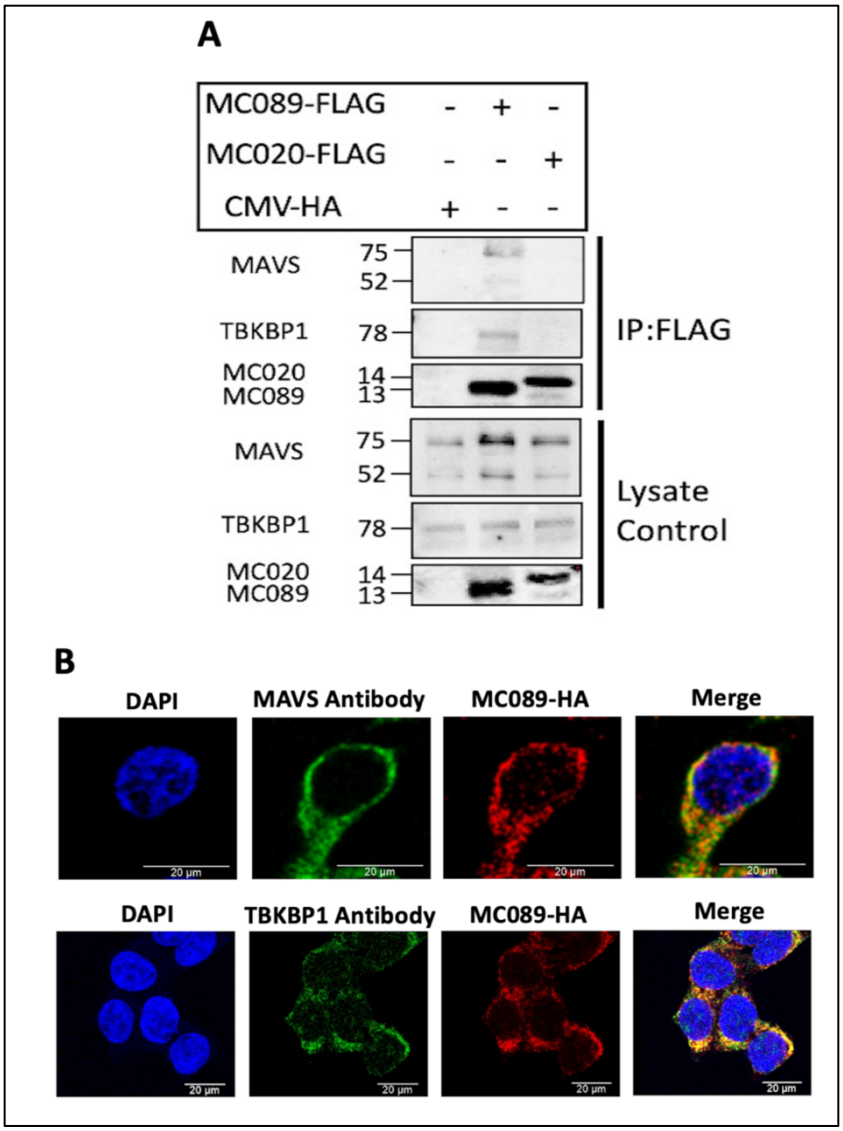

Figure 4.8 MC089 associates with endogenous MAVS and TBKBP1. (A) HEK293T cells were seeded at $3x10^6$ cells/ culture dish and transiently transfected 24 hours later with a total of 8 μg of empty vector (pCMV-HA) or pCEP4-FLAG vectors expressing the indicated MCV ORFs. After 24 hours, cell lysates were immunoprecipitated using anti-FLAG M2 affinity gel beads, eluted with FLAG tag peptide, and probed with the indicated antibodies: anti-MAVS (first and fourth panels), anti-TBKBP1 (second and fifth panels) and anti-FLAG (third and sixth panels). (B) HEK293T cells were seeded at $8x10^4$ cells/ well on glass chamber slides and transiently transfected 24 hours later with a total of 500 ng of pCEP4-MC089-HA. Cells were fixed 24 hours later and stained with HA tag antibody (red), DAPI

(blue), MAVS antibody (green) or TBKBP1 antibody (green). Results are representative of triplicate experiments.

4.3 Discussion

In this chapter, we investigated potential proteins being targeted by MC089 that might explain its pattern of inhibition of IRF3-dependant gene expression. Luciferase pathway screening indicated a point of inhibition at the level of IRF3-activation complex proteins. MS analysis of MC089 co-purifying proteins also indicated mitochondrial association and subsequently found that MC089 co-localizes with mitochondria showing a similar pattern of localization to MAVS and suggesting MAVS may be a potential target for MC089 in the RIG-I-dependent IRF3 activation.

Targeted co-immunoprecipitation experiments showed that MC089 specifically interacts with the IRF-activating complex components IKKε, TBKBP1, NAP1 and MAVS, the latter at least partly in association with mitochondria. These proteins likely were not co-purified with MC089 in AP-MS due to low abundance in HEK293T cells where more highly expressed proteins are captured, such as mitochondrial proteins. The specificity of MC089 binding only the IKKε kinase is distinct from MC159 interaction with both TBK1 and IKKε (471). Additionally, the specific association with TBKBP1 and NAP1, but not TANK, differs from VACV C6 binding all three scaffold proteins without direct interaction with either of the IRF3 kinases (352). This makes MC089's mechanism of inhibition of IRF3-activating pathways unique for poxviral inhibitors of this type and the first MCV IRF activation inhibitor to specifically target this system and not NF-κB activation.

The inhibition of both the cGAS-STING DNA sensing pathway and the TLR/RLR RNA sensing pathways may be explained by MC089 targeting of IKKε as well as TBKBP1 and NAP1. However, MC089 also displays specific targeting of the RLR pathway by direct association with MAVS at the level of mitochondria as indicated by MC089 co-purifying mitochondrial proteins and co-localization with both MAVS and mitochondria in HEK293T cells. It is also worth noting that there is considerable crosstalk between STING and RLR pathways suggesting that MAVS interaction might also contribute to MC089 inhibition of cGAS-STING-mediated IRF3 activation. For example, the ssRNA genome of Japanese encephalitis virus (JEV) is recognized by RIG-I, which then recruits STING to initiate a downstream cascade leading to the antiviral response in neurons (502). In several studies, STING appeared to interact with RIG-I and MAVS, in a complex that was stabilized upon virus infection (502-504). Indeed, a role for STING in RNA sensing pathways is further indicated by the fact that many RNA viruses have evolved STING inhibitory strategies like hepatitis C virus, influenza A virus and Dengue virus (505-508). Additionally, in HeLa or HepG2 cells, TBK-1 phosphorylation after DNA transfection or DNA virus infection required MAVS-TBK1 interaction and MAVS knockdown in these cells markedly reduced phospho-TBK1 and IFN-β levels induced by cytoplasmic DNA (509).

Despite the lack of interaction of MC089 with TBK1, inhibition of TBK1-driven IRF activation could be explained by its targeting of TBKBP1 and NAP1. These scaffold proteins along with TANK are essential for the dimerization and auto-phosphorylation of IRF3 kinases recruiting them at a specific cellular site (329, 335). Although, the exact mechanism by which IRF3 kinases interact with their scaffold proteins is still not fully understood (510), all three scaffold proteins target the same binding site at the kinases,

suggesting a competitive mode of binding and signal transduction specificity (102). Viruses evolving specific inhibitors, including VVC6, of the three scaffold proteins reflects their importance on IRF3 regulation. MC089 interaction with TBKBP1 and NAP1, but not TANK, could give new insights into the roles and subcellular localization of these scaffold proteins. TANK has been discovered to migrate from its perinuclear localization to autophagy-related vesicles upon DNA stimulation (335), while NAP1 and TBKBP1 have been reported to have punctate subcellular localization and they have been also partially detected at the Golgi compartments (335, 353). As MC089 also displays punctate distribution and partial association with mitochondria, this along with its interaction with MAVS may indicate a mitochondrial functional specificity for TBKBP1 and NAP1. It might also suggest that MC089 uses TBKBP1-NAP1 to recruit IKKε to MAVS in the mitochondria.

Additionally, MC089 targeting of both MAVS and IKKε may give insights into their association with virus infection. MAVS has been found to bind IKKε through its C-terminal region (300-540 amino acid residues), resulting in the recruitment of IKKε and the subsequent phosphorylation of IRF3 and that LGP2 (**Section 1.1.2**) competes with IKKε to interact with MAVS at the same region to inhibit antiviral RLR pathways (114). Interestingly, IKKε has been previously reported to colocalize strongly with MAVS on mitochondria upon RNA virus infection, which was disrupted by the hepatitis C virus protein NS3-4A (511). This was not observed with TBK1 in virus infection indicating that it rather has an indirect association with MAVS mediated by other adaptor proteins, such as STING or tumour necrosis factor receptor-associated factor 3 (TRAF3) (503, 504, 511, 512). A follow-up study revealed that upon virus infection, MAVS is subjected to K63-linked ubiquitination of the 500-residue site (K500) leading to the mitochondrial

recruitment of IKKε where it interacts with MAVS through its C-terminus causing its phosphorylation. This has been found to reduce the expression of IFN-stimulated genes (ISGs), IFN-β and, surprisingly, IL-6, which suggests negative regulation of the NF-κB pathway (512). Nevertheless, MC089 could use the same approach to direct IKKε to MAVS on the mitochondria, either through direct interaction or via TBKBP1-NAP1, resulting in MAVS phosphorylation and suppression of IRF3 activation. If so, it would indicate that IKKε is both a positive and a negative regulator of MAVS-dependent IRF3 activation.

In the Senkevich et al analysis of the MCV-I genome, MC089 was predicted to have a signal peptide expressed during the late phase of the MCV replication cycle (450). Thus, MC089 could act as a signal peptide that causes subcellular translocation of its target proteins to suppress IRF activation, such as migration of IKKε to MAVS. Overall, late-phase viral immunomodulators have been linked to mitochondria including the major protein component of poxviral LBs F17 (**Section 1.3.1**), the human cytomegalovirus (HCMV) US9 membrane glycoprotein which stimulates MAVS leakage from the mitochondria for inhibition of the RIG-I pathway, the herpes simplex virus (HSV) viral protein UL7 that localizes to mitochondria and associates with the virus proliferation and pathogenicity and the mitochondrial redox LB VACV proteins G4L, A2.5L, A19L, A45R and O2L (411, 432, 433, 513-515). MC089 predicted late expression during infection, unlike the currently discovered early-expressed MCV inhibitors, could provide more insights into the involvement of mitochondria and MC089 target proteins during the late stage of viral infection which could be revealed by further elaboration of the exact inhibitory mechanism of MC089. However, MC089's functional complexity of targeting multiple signaling proteins complicates the investigation.

4.4 Conclusion

This chapter reveals that MC089 targets IRF-dependent gene activation for inhibition by directly interacting with IKKε, IKKε scaffold proteins TBKBP1 and NAP1, and the major regulator of RIG-I pathway MAVS, in association with mitochondria. The precise mechanism by which MC089 binds with its target proteins is still unclear and of interest for further investigation.

Chapter 5 Investigation of MC089 Functionality

Having identified MC089 as a novel MCV inhibitor of IRF activation by association with IKKε, NAP1, TBKBP1 and MAVS at the level of mitochondria, we next sought to further understand its effects on key events of IRF3 activation and its downstream consequences on IRF3-dependant gene expression. In this chapter, we will investigate the functional regions of MC089 required for its inhibitory effect and the outcomes of MC089 targeting the IRF3-activation complex. To examine MC089 effects on phosphorylation events and TI-IFN production, we made stable MC089-expressing HEK293T cells by transfecting the cells with pMEP4-MC089-FLAG vector which upon the addition of metallic salts, such as cadmium chloride, activates the hMTII promoter to express MC089 (**Fig.2.2.1**). We confirmed the expression of MC089 in these cells using western blot and found 1 μM of $CdCl_2$ to be an optimal concentration (**Fig.5.1**).

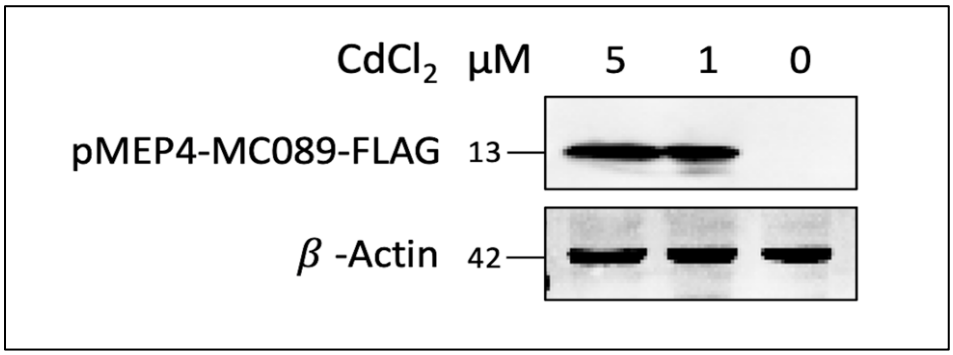

Figure 5.1 pMEP4-MC089 expression in HEK293T cells. HEK293T cells were stably transfected with MEP4-MC089-FLAG vector and treated with $CdCl_2$ at the indicated concentrations to induce MCV protein expression. Cell lysates were harvested for western blot and probed with anti-Flag antibody.

5.1 Full-length MC089 is required for the inhibition of IRF-dependent gene activation

To identify the functional regions of MC089 required for the inhibition of IRF activation, previous work in the host laboratory generated truncations of MC089: M1 (1-57 amino acid residues), M2 (58-114 amino acid residues) and M3 (27-87 amino acid residues). This approach was used in other MCV studies to identify the regions of MC132 and MC005 required for inhibition of NF-κB activation (469, 472). Since MC089 was established to be a potent inhibitor of IKKε- driven ISRE luciferase activation, we employed this system to investigate the inhibitory effect of MC089 truncations. Whilst full-length MC089 was capable of potently inhibiting ISRE activation induced by IKKε, all three MC089 truncations had no effect on the system showing a similar pattern to the control (**Fig.5.2**). This indicated that MC089 requires the full protein for its inhibitory activity.

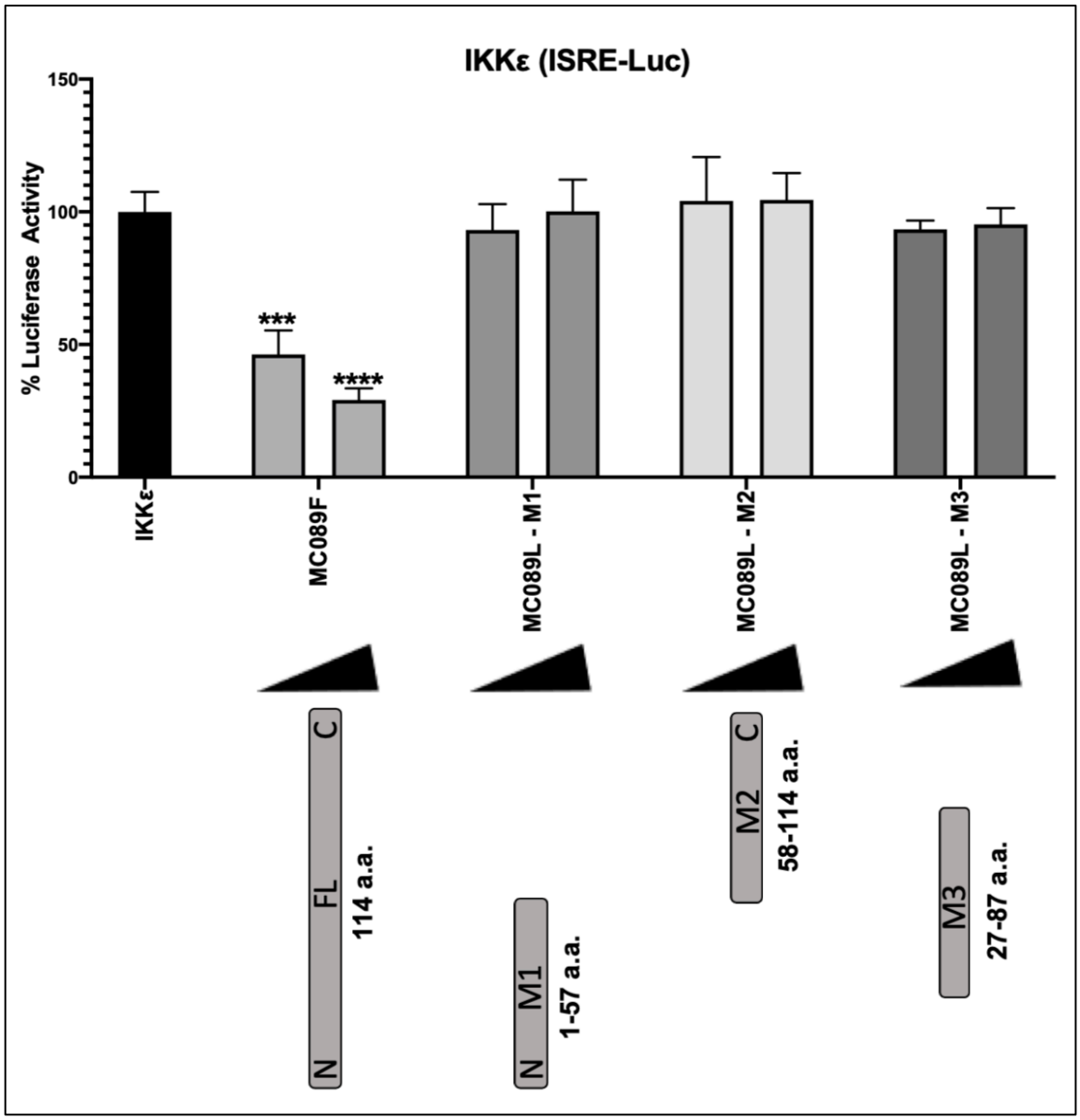

Figure 5.2 Full-length MC089 is required for the inhibition of IRF-dependent gene activation. HEK293T cells were seeded at $2x10^5$ cells /ml and transfected 24 hours later with 80 ng of ISRE luciferase reporter. To normalize firefly luciferase, 40 ng of pGL3-*Renilla* control was utilized. Cells were transfected with two doses of pCEP4-MC089-FLAG or truncations: 25 ng (low dose) and 50 ng (high dose). IKKε (50 ng) was added to drive the pathway. The total amount of DNA was adjusted to a final volume of 220 ng with the empty vector control (pCMV-HA). Cell lysates were harvested and assayed for luciferase activity. The schematic is representative of triplicate experiments. Data were normalized to the empty vector and presented by percentage activity compared to positive control. Bars

indicate mean ± the standard deviation. Statistical significance is denoted as *** P<0.001 and **** P<0.0001.

5.2 MC089 specifically inhibits IRF3 phosphorylation at serine 396

An essential modification step in IRF3 activation is phosphorylation (**Section 1.1.5**), thus, we aimed to determine if MC089 inhibition of IRF activation blocks this event. To do this we probed Poly(dA-dT)-activated phosphorylation of two key sites on IRF3, serine 386 and serine 396, known to be critical for IRF3 activation and transactivation (261). Interestingly, while MC089 inhibited Poly(dA-dT)-induced phosphorylation of IRF3 serine 396, it did not affect serine 386 phosphorylation. The interaction between MC089 and IKKε also raised the possibility that it may block IKKε phosphorylation. To investigate this, we probed the phosphorylation of IKKε at the serine residue 172 and found that MC089 had no effect. This suggested that MC089 prevents pIRF3 Ser396 independently from IKKε Ser 172 (**Fig.5.3**).

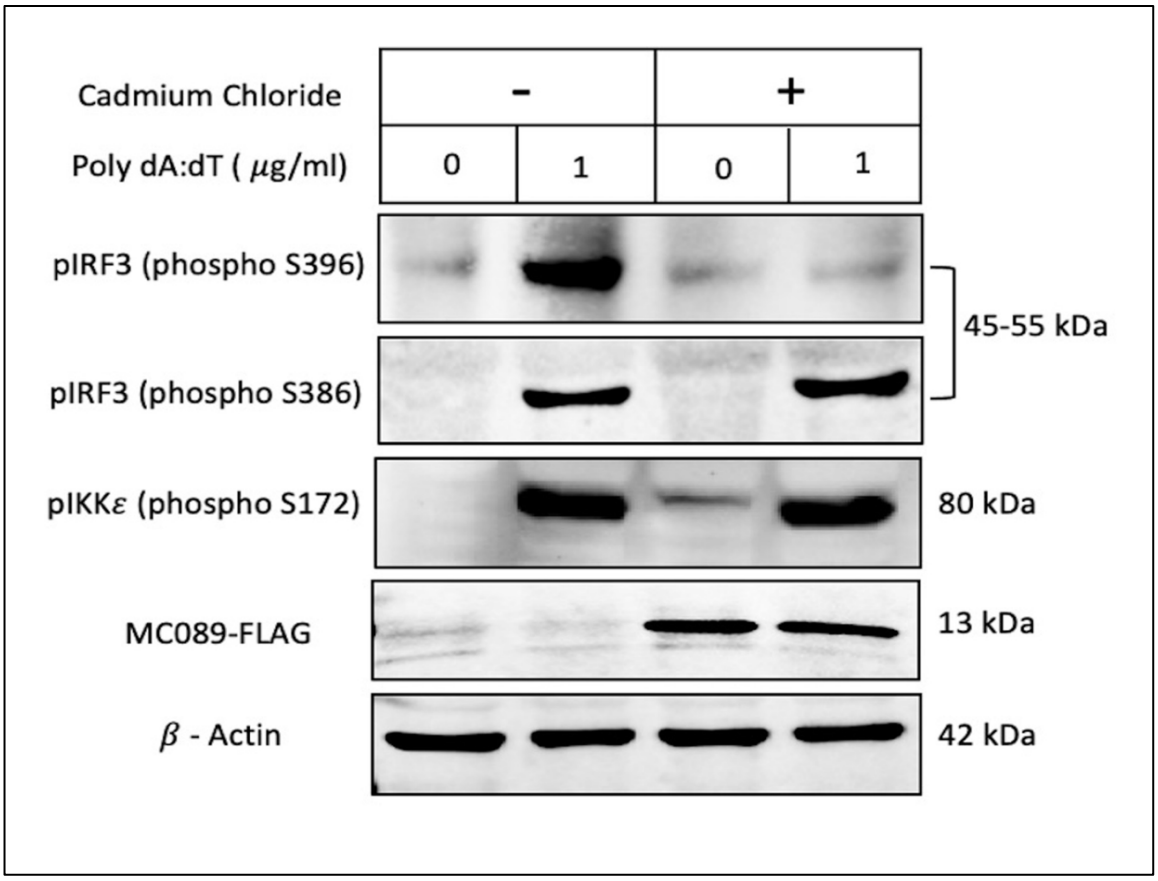

Figure 5.3 MC089 inhibits IRF3 phosphorylation at Ser396. HEK293T cells were stably transfected with MEP4-MC089-FLAG vector and treated with 1 μM of $CdCl_2$ to induce MCV protein expression. After 24 hours, cells were stimulated with 1 μg/ml of Poly(dA:dT) for 16 hours to induce protein phosphorylation. Cell lysates were harvested for western blot and probed with the indicated antibodies. Blots are representative of triplicate experiments.

5.3 MC089 suppresses IRF3-dependent TI-IFN and IP-10 production

We next examined if MC089 suppression of IRF3 activation blocks the expression of one of the most important IRF3-induced cytokines, TI-IFNs. To do so, we harvested supernatants from MEP-MC089-FLAG stable HEK293T cells $CdCl_2$-induced to express MC089-FLAG. We then assessed the effect of MC089 on Poly(dA-dT)-activated IRF3-dependant gene expression, specifically IP-10 and TI-IFNs. Like IFNβ, IP-10 is known to

be a strong ISRE- and IRF-regulated gene (326, 516, 517). We measured IFN-α/β levels in MC089-expressing HEK293T cell supernatants after Poly((dA:dT)) stimulation using HEK-blue IFN-α/β bioassay reporter cells which possess a secreted embryonic alkaline phosphatase (SEAP) reporter under the control of the IFN-stimulated gene 54 (ISG54) promoter. We observed that MC089 expression inhibited both Poly((dA:dT))-induced IP-10 and IFNα/β production (**Fig.5.4 B and C**).

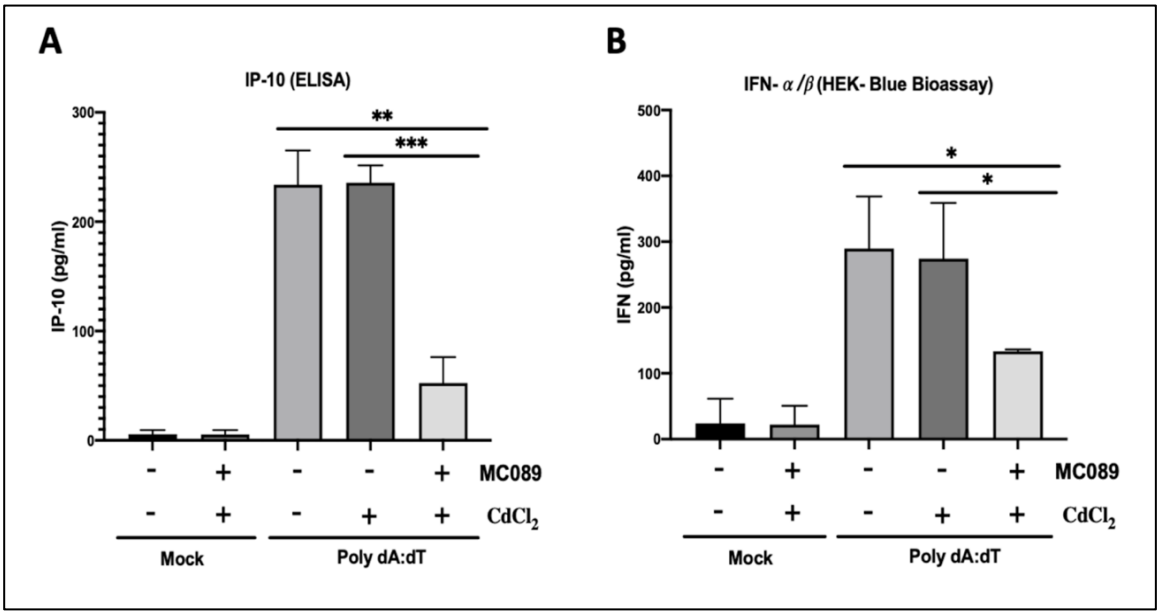

Figure 5.4 MC089 suppresses TI-IFN and IP-10 secretion. MEP4-MC089-expressing HEK293T supernatants were harvested and assayed for (A) IP-10 ELISA and (B) IFN-α/β detection. Cells were stimulated 1 μg/ml of Poly(dA:dT) for 16 hours, with mock-transfected cells (mock) serving as a negative control for cytokine secretion. Concentrations were calculated from standard curves generated from measured optical density. Data are representative of triplicate experiments. Bars indicate mean ± the standard deviation. Statistical significance is denoted as * $P<0.05$, ** $P<0.01$ and *** $P<0.001$.

5.4 Discussion

In this chapter, we aimed to identify the functional amino acid residues that are essential for the inhibitory activity of MC089. Defining the functional regions and residues can assist in the analysis of molecular interactions with cellular targets (469). One way to approach this is by generating truncation mutants of MC089 which were previously constructed in the host laboratory, where the sequence was subcloned as truncated distinct regions from the N-terminus to the C-terminus. MC089 is a small protein of only 114 amino acid residues, thus, it was truncated equally into three parts: 1-57 amino acids, 27-87 amino acids and 58-114 amino acids, and the mutants were compared to wild-type MC089 (full-length) for their inhibitory activity on IKKε-driven ISRE activation, one of the IRF3 systems potently inhibited by MC089. Whilst wild-type MC089 inhibited the pathway in a dose-dependent manner, all truncations lost inhibitory activity indicating the requirement of full-length MC089 for IRF pathway inhibition. The same principle can be used for future investigation where truncated IKKε, TBKBP1, NAP1 and MAVS can be examined for their immunoprecipitation and co-localization with MC089.

Although the precise mechanism by which MC089 interacts with its target proteins is unclear, we found MC089 to inhibit IRF3 phosphorylation at serine 396 without affecting the phosphorylation of serine 386. Such specific targeting could indicate differences in the functional specificity of these two sites. Even though both Ser386 and Ser396 are considered critical for IRF3 dimerization and phosphorylation, the exact role of each site is still debated. It has been reported that IRF3 Ser396 causes IRF3 oligomerization leading to a strong interaction with the coactivator CREB-binding protein (CBP)/p300, while pIRF3 Ser386 does not associate strongly with (CBP)/p300 but rather strengthens pIRF3

Ser396 binding to the coactivator (261). In contrast, a study using phosphorylation mutants of the two sites demonstrated that, whilst both sites are important for IRF3 dimerization, Ser386 plays a stronger role in IRF3 activation (301).

The identity of the kinase could play a role in site-specific IRF3 phosphorylation. Even though TBK1 phosphorylates IRF3 Ser396 (296, 320, 518, 519), MC089 specifically targeting IKKε and pIRF3 Ser396 may indicate that this kinase can phosphorylate this site too, potentially in the context of MAVS-associated activation. In fact, several viral inhibitors target IKKε and MAVS resulting in inhibition of pIRF3 Ser396. For example, Epstein-Barr Virus (EBV) protein BFRF1 binds IKKε and inhibits pIRF3 Ser396 and SeV-induced IFNβ expression (520). Middle East respiratory syndrome coronavirus (MERS-CoV) accessory protein ORF8b inhibits pIRF3 Ser396 and IFNβ production via inhibition of the heat shock protein 70 (Hsp70) required for IKKε activation (521). Additionally, Rotavirus non-structural protein 1 (RNP1) that degrades MAVS through direct interaction, inhibits pIRF3 Ser396 and IFNβ promoter activation (522). IKKε and MAVS-linked pIRF3 Ser396 have been also demonstrated through the scaffold protein FAS-Associated Factor 1 (FAF1) which acts as a negative regulator of MAVS by blocking its ubiquitination through the ligase TRIM31. Upon virus infection, IKKε causes FAF1 degradation by direct phosphorylation at serine 556 resulting in its release from MAVS. Interestingly, mutations of Ser556 prevent IKKε-dependent FAF1 degradation which blocks efficient TBK1 and IRF3 Ser396 phosphorylation (523). MC089 may use a similar inhibitory mechanism by mimicking FAF1 to negatively regulate MAVS or MC089 interaction with IKKε can prevent the kinase from degrading FAF1. Either way, the ability of MC089 to significantly impede TI-IFN induction could make the viral inhibitor a potential therapeutic for TI-interferonopathies and IRF3-related diseases and disorders (**Section 1.1.5.5**).

5.5 Conclusion

This chapter showed that MC089 requires its full-length sequence for its inhibitory activity, and it specifically inhibits IRF3 activation at the phosphorylation site Ser396 without affecting the phosphorylation at Ser386. MC089 inhibition of IRF3 activation suppresses the production of TI-IFNs and IP-10.

Chapter 6 Conclusions and Future Work

In this thesis, the MCV-derived protein MC089 was described as a novel inhibitor of IRF3 activation from both DNA and RNA sensing pathways. MC089 selectively interacts with the IRF3 kinase IKKε and its scaffold proteins TBKBP1 and NAP1. It was also revealed that MC089 associates with MAVS on mitochondria. Additionally, MC089 specifically inhibits IRF3 phosphorylation at Ser396 which is essential for its activation, dimerization and binding to coactivators, thus, suppressing the induction of TI-IFNs. This may give novel insights into the regulation of antiviral IRF3 pathways regarding the involvement of IKKε in the activation of IRF3, the assembly of the IRF3-activation complex through TBKBP1 and NAP1, the antiviral role of MAVS in association with IKKε on the mitochondria and the functional specificity of IRF3 phosphorylation at Ser396. Introducing MC089 as a mitochondrial protein may also provide a better understanding of the mitochondrial roles in antiviral immunity against poxviruses. A model of MC089-mediated inhibition of IRF3 activation is outlined (**Fig.6.1**).

Further investigation of the precise inhibitory mechanism used by MC089 may offer novel insights into the regulation of IRF3 sensing pathways, in particular, the roles of the constituents of its activation complexes may offer a basis for potential therapeutics targeting selective routes to IRF3 activation in diseases and disorders. Truncation mutants of targeted IRF3-activating components and MAVS can be used to determine the functional regions required for MC089 association and IRF3 activation. Additionally, it would be useful to reproduce the inhibitory effect of MC089 in other cell types and demonstrate that MC089 activity is not cell type-specific. A cell line harbouring the natural environment of MCV would be a preferential model for MC089 investigation, such as high sensitivity of

human epidermal keratinocytes (HaCaT cells) that are enriched with multiple types of PRRs.

Since MC089 expression does not intervene with IKKε phosphorylation, we can next examine the effect of MC089 on two essential modification steps of MAVS regulation: ubiquitination and phosphorylation. We know from literature that MAVS ubiquitination at K500 leads to its phosphorylation and inhibition by IKKε (512). Therefore, an induction of MAVS ubiquitination at K500 by MC089 and MC089-triggered phosphorylation of MAVS could be a possible inhibitory mechanism of MC089 which can be investigated using the appropriate antibodies. Additionally, IKKε, TBKPB1 and NAP1 confocal localization to mitochondria could be tracked in MC089-expressing cells. Particularly, IKKε localization to MAVS on mitochondria upon virus infection could be examined before and after MC089 expression to determine if MC089 disrupts IKKε-MAVS interaction like in the case of the hepatitis C virus protein NS3-4A (511). Negative regulators of MAVS could be also investigated for their association with MC089. A protein of interest is FAS-Associated Factor 1 (FAF1) (523), and it could be examined for its immunoprecipitation and co-localization with MC089. If so, MAVS and FAF1 interaction could also be tested in MC089-expressing cells.

Although viruses have been routinely used in the production and delivery of clinically approved therapeutics that include vaccines, viral vector-based gene therapy and virotherapy, using virus-derived immune-modulating tools as therapeutics is still considered an emerging approach in the early stages of development. However, pre-clinical and clinical trials of virus-derived immunomodulators, many of which are poxvirus-based, have shown optimistic data regarding efficacy. Examples of such poxviral

immunomodulators are the serine protease inhibitor I (Serp1) from myxoma virus for the treatment of acute coronary syndrome (Phase I/II), the chemokine modulators 35K from vaccinia virus for the treatment of atherosclerosis and arthritis (murine models), the TNF-binding protein (CrmB) from variola virus for the treatment of collagen-induced arthritis (murine models), the vaccinia virus complement control protein (VCP) to improve sensory-motor deficits related to brain tumor (murine models) and to improve cardiac graft rejection in guinea pig to rat and the MCV protein MC148 (**Section 1.4**) to prolong cardiac transplants and inhibit donor-lymphocyte immunity (murine models) (524-527).

Developing MC089 as a potential therapeutic for the treatment of IRF3-associated autoimmune and autoinflammatory disorders, such as type-I interferonopathies, cancer and metabolic diseases **(Section 1.1.5.5)**, could be promising as MC089 associates with selective IRF3 regulatory proteins. For example, MC089 could be used to target MAVS-dependent IFN production in SLE and diabetic kidney patients (362, 364, 365, 377-379) or to inhibit IKKε-based IFN secretion in patients with cancer, obesity or TI-diabetes (331, 369, 370, 372). Moreover, MC089 could be used as a tool to inhibit donor-TI-IFN immunity and improve post-transplant outcomes, especially since IRF3 and TI-IFNs have been linked to acute rejection in human transplantation (528). Since MC089 has a low molecular weight of around 13 kDa, it could act as a small-peptide drug that can easily penetrate cells and selectively associate with the target protein. MC089 drug delivery can be enhanced to improve drug uptake and overcome immunogenicity by different strategies that could include cell-penetrating peptides (CPPs), which are composed of 5-30 amino acid residues and can safely and efficiently deliver drugs based on endocytosis, lentiviral or plasmid-mediated gene transfer, polymer-based microencapsulation, such as

conjugation of poly(ethylene glycol) (PEG) and nanoencapsulation, for example, liposome-based drug delivery (524, 525, 529-531).

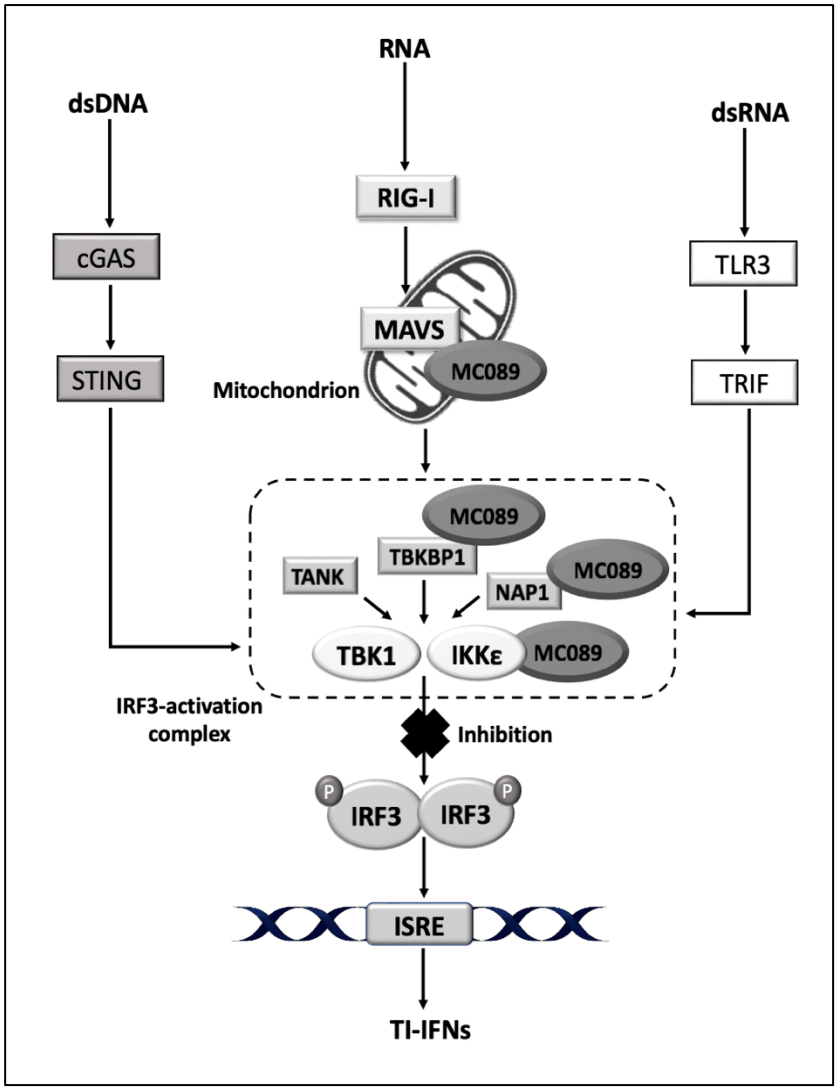

Figure 6.1 Model of MC089-mediated inhibition of IRF3 activation. Upon sensing viral nucleic acids, multiple signaling pathways drive the activation of IRF3 via phosphorylation and ubiquitination of a series of adaptor proteins and kinases. MC089 interacts with the kinase IKKε and its scaffold proteins TBKBP1 and NAP1 at the level of the IRF3-activation complex. It also impedes the RIG-I sensing pathway by localizing to the mitochondria and associating with MAVS. Consequently, MC089 blocks IRF3 activation by inhibiting phosphorylation at serine 396, thus, it prevents the subsequent induction of TI-

IFNs. Servier Medical Art (https://smart.servier.com/) was used in the construction of the illustration.

References

1. Marshall J, Warrington, R, Watson, W, Kim,HL 2018. An introduction to immunology and immunopathology. Allergy Asthma Clin Immunol 14.
2. Dwivedy A, Aich, P. 2011. Importance of innate mucosal immunity and the promises it holds. Int J Gen Med 4:299–311.
3. Bomsel M AA. 2003. Entry of viruses through the epithelial barrier: pathogenic trickery. Nat Rev Mol Cell Biol 4:57-68.
4. Beachboard DC HS. 2016. Innate immune evasion strategies of DNA and RNA viruses. Curr Opin Microbiol 32:113-119.
5. Schleimer RP KA, Kern R, Kuperman D, Avila PC. 2007. Epithelium: at the interface of innate and adaptive immune responses. 120 doi:doi: 10.1016/j.jaci.2007.08.046:1279-84.
6. Bowie AG UL. 2008. Viral evasion and subversion of pattern-recognition receptor signalling. Nat Rev Immunol 8:911-22.
7. Kolli D VT, Casola A. 2013. Host-Viral Interactions: Role of Pattern Recognition Receptors (PRRs) in Human Pneumovirus Infections. Pathogens 2:232–63.
8. Hermesh T MB, Moran TM, López CB. 2010. Antiviral instruction of bone marrow leukocytes during respiratory viral infections. Cell Host Microbe 7:343-53.
9. Ramesh G MA, Philipp MT. 2013. Cytokines and chemokines at the crossroads of neuroinflammation, neurodegeneration, and neuropathic pain. Mediators Inflamm 2013:480739.
10. Nilsson B PB, Eriksson O, Fromell K, Hultström M, Frithiof R, Lipcsey M, Huber-Lang M, Ekdahl KN. 2022. How the Innate Immune System of the Blood Contributes to Systemic Pathology in COVID-19-Induced ARDS and Provides Potential Targets for Treatment. Front Immunol 13:840137.
11. Janeway CJ, Travers, P, Walport, M, Shlomchik , M. 2001. Immunological memory. *In* (ed), Immunobiology: The Immune System in Health and Disease. Garland Science, New York.
12. Libbey JE FR. 2014. Adaptive immune response to viral infections in the central nervous system. Handb Clin Neurol 123:225-47.
13. GR K. 1996. Immune Defenses. *In* S B (ed), Medical Microbiology. University of Texas Medical Branch at Galveston, Galveston (TX).
14. AR N. 2008. Immune Response to Viruses: Antibody-Mediated Immunity. *In* Mahy BWJ, Van Regenmortel, M H.V (ed), Encyclopedia of Virology. Academic Press, doi:doi: 10.1016/B978-012374410-4.00591-4.
15. Amarante-Mendes GP AS, Branco LM, Zanetti LC, Weinlich R, Bortoluci KR. 2018. Pattern Recognition Receptors and the Host Cell Death Molecular Machinery. Front Immunol 9.
16. Thompson MR KJ, Kurt-Jones EA, Fitzgerald KA. 2011. Pattern recognition receptors and the innate immune response to viral infection. Viruses 3:920-40.
17. Ivashkiv L, Donlin, LT. 2014. Regulation of type I interferon responses. Natrue 14:36-49.
18. McNab F, Mayer-Barber, K, Sher, A, Wack, A, O'Garra, A. 2015. Type I interferons in infectious disease. Nature 15:87-103.
19. Li S, Gonga, MJ, Zhaoa, FR, Shaoa, JJ, Xie,YL, Zhang,YG, Chang, HY. 2018. Type I Interferons: Distinct Biological Activities and Current Applications for Viral Infection. Cell Physiol Biochem 51:2377-2396.

20. Cheon H BE, Stark GR. 2014. Interferons and their stimulated genes in the tumor microenvironment. Semin Oncol 41:156-73.
21. Schneider WM CM, Rice CM. 2014. Interferon-stimulated genes: a complex web of host defenses. Annu Rev Immunol 32:513-45.
22. N K-J. 2017. The Role of Interferons in Inflammation and Inflammasome Activation. Front Immunol 8:873.
23. JW S. 2014. Interferon-stimulated genes: roles in viral pathogenesis. Curr Opin Virol 6:40-6.
24. Ventoso I SM, Molina S, Berlanga JJ, Carrasco L, Esteban M. 2006. Translational resistance of late alphavirus mRNA to eIF2alpha phosphorylation: a strategy to overcome the antiviral effect of protein kinase PKR. Genes Dev 20:87-100.
25. Pilla-Moffett D BM, Taylor GA, Coers J. 2016. Interferon-Inducible GTPases in Host Resistance, Inflammation and Disease. J Mol Biol 428:3495-513.
26. Haller O KG. 2002. Interferon-induced mx proteins: dynamin-like GTPases with antiviral activity. Traffic 3:710-7.
27. Sadler AJ WB. 2008. Interferon-inducible antiviral effectors. Nat Rev Immunol 8:559-68.
28. ZhanZhang M LJ, Yan H, Huang J, Wang F, Liu T, Zeng L, Zhou Fg M, Li J, Yan H, Huang J, Wang F, Liu T, Zeng L, Zhou F. 2021. ISGylation in Innate Antiviral Immunity and Pathogen Defense Responses: A Review. Front Cell Dev Biol 9:788410.
29. Baldanta S F-EM, Acín-Perez R, Albert M, Camafeita E, Jorge I, Vázquez J, Enríquez JA, Guerra S. 2017. ISG15 governs mitochondrial function in macrophages following vaccinia virus infection. PLoS Pathog 13:e1006651.
30. Eduardo-Correia B M-RC, García-Sastre A, Guerra S. 2014. SG15 is counteracted by vaccinia virus E3 protein and controls the proinflammatory response against viral infection. J Virol 88:2312-8.
31. Peteranderl C, Herold, S. 2017. The impact of the interferon/TNF- Related Apoptosis-inducing Ligand Signaling Axis on Disease Progression in Respiratory viral infection and Beyond. Frontiers in Immunology 8.
32. Nainu F, Shiratsuchi, A, Nakanishi,Y. 2017. Induction of Apoptosis and Subsequent Phagocytosis of virus-infected Cells As an Antiviral Mechanism. Frontiers in Immunology 8.
33. Chai H GQ, Robertson DL, Hughes J. 2022. Defining the characteristics of interferon-alpha-stimulated human genes: insight from expression data and machine learning. Gigascience 11:giac103.
34. Lee H, Chathuranga, K, Lee, JS. 2019. Intracellular sensing of viral genomes and viral evasion. Experimental & Molecular Medicine 51.
35. ISAACS A LJ. 1957. Virus interference. I. The interferon. Proc R Soc Lond B Biol Sci 147:258-67.
36. MW T. 2014. Interferons. Viruses and Man: A History of Interactions doi:doi: 10.1007/978-3-319-07758-1_7:101–19.
37. F D. 1975. Viral interference and interferon. Ric Clin Lab 5:196-213.
38. S P. 2007. The interferons: 50 years after their discovery, there is much more to learn. J Biol Chem 282:20047-51.
39. NAGANO Y KY, SAWAI Y. 1954. Immunité et interférence dans la vaccine; inhibition de l'infection dermique par le virus inactivé [Immunity and interference in vaccinia; inhibition of skin infection by inactivated virus]. C R Seances Soc Biol Fil 148:750-2.

40. Lee A, Ashkar, AA. 2018. The Dual Nature of Type I and Type II Interferons. Front Immunol 9.
41. Lazear HM SJ, Diamond MS. 2019. Shared and Distinct Functions of Type I and Type III Interferons. Immunity 50:907-923.
42. Donnelly RP KS. 2010. Interferon-lambda: a new addition to an old family. J Interferon Cytokine Res 30:555-64.
43. McNab F M-BK, Sher A, Wack A, O'Garra A. 2015. Type I interferons in infectious disease. Nat Rev Immunol 15:87-103.
44. Manivasagam S KR. 2021. Type III Interferons: Emerging Roles in Autoimmunity. Front Immunol 12:764062.
45. Wells AI CC. 2018. Type III Interferons in Antiviral Defenses at Barrier Surfaces. Trends Immunol 39:848-858.
46. Giroux M SM, Descoteaux A. 2003. IFN-gamma-induced MHC class II expression: transactivation of class II transactivator promoter IV by IFN regulatory factor-1 is regulated by protein kinase C-alpha. J Immunol 171:4187-94.
47. Castro F CA, Gonçalves RM, Serre K, Oliveira MJ. 2018. Interferon-Gamma at the Crossroads of Tumor Immune Surveillance or Evasion. Front Immunol 9:847.
48. Schoenborn JR WC. 2007. Regulation of interferon-gamma during innate and adaptive immune responses. Adv Immunol 96:41-101.
49. Bonjardim C. 2005. Interferons (IFNs) are key cytokines in both innate and adaptive antiviral immune responses--and viruses counteract IFN action. Microbes Infect 7:569-78.
50. Ank N PS. 2009. Type III IFNs: new layers of complexity in innate antiviral immunity. Biofactors 35:82-7.
51. Zhou JH WY, Chang QY, Ma P, Hu Y, Cao X. 2018. Type III Interferons in Viral Infection and Antiviral Immunity. Cell Physiol Biochem 51:173-185.
52. Odendall C KJ. 2015. The unique regulation and functions of type III interferons in antiviral immunity. Curr Opin Virol 12:47-52.
53. Langer JA CE, Kotenko S. 2004. The Class II cytokine receptor (CRF2) family: overview and patterns of receptor-ligand interactions. Cytokine Growth Factor Rev 15:33-48.
54. Iwanaszko M, Kimmel, M. 2015. NF-κB and IRF pathways: cross-regulation on target genes promoter level. BMC Genomics 16.
55. Yu H, Lin L, Zhang Z, Zhang H, Hu H. 2020. Targeting NF-kappaB pathway for the therapy of diseases: mechanism and clinical study. Signal Transduct Target Ther 5:209.
56. Liu T, Zhang L, Joo D, Sun SC. 2017. NF-kappaB signaling in inflammation. Signal Transduct Target Ther 2.
57. Bose S, Kar N, Maitra R, DiDonato JA, Banerjee AK. 2003. Temporal activation of NF-kappaB regulates an interferon-independent innate antiviral response against cytoplasmic RNA viruses. Proc Natl Acad Sci U S A 100:10890-5.
58. Wang J, Basagoudanavar SH, Wang X, Hopewell E, Albrecht R, Garcia-Sastre A, Balachandran S, Beg AA. 2010. NF-kappa B RelA subunit is crucial for early IFN-beta expression and resistance to RNA virus replication. J Immunol 185:1720-9.
59. Honda K, Yanai, H., Negishi, H. et al. 2005. IRF-7 is the master regulator of type-I interferon-dependent immune responses. NATURE 434:772-777.
60. Schwanke H, Stempel M, Brinkmann MM. 2020. Of Keeping and Tipping the Balance: Host Regulation and Viral Modulation of IRF3-Dependent IFNB1 Expression. Viruses 12.

61. Hong Y, Bai M, Qi X, Li C, Liang M, Li D, Cardona CJ, Xing Z. 2019. Suppression of the IFN-alpha and -beta Induction through Sequestering IRF7 into Viral Inclusion Bodies by Nonstructural Protein NSs in Severe Fever with Thrombocytopenia Syndrome Bunyavirus Infection. J Immunol 202:841-856.
62. Honda K, Takaoka A, Taniguchi T. 2006. Type I interferon [corrected] gene induction by the interferon regulatory factor family of transcription factors. Immunity 25:349-60.
63. Chen J YC, Wan C, Li G, Peng L, Peng Y, Fang R. 2021. The Roles of c-Jun N-Terminal Kinase (JNK) in Infectious Diseases. Int J Mol Sci 22:9640.
64. Paul F PS, Uzé G. 2015. IFNA2: The prototypic human alpha interferon. Gene 567:132-7.
65. Honda K, Yanai H, Takaoka A, Taniguchi T. 2005. Regulation of the type I IFN induction: a current view. Int Immunol 17:1367-78.
66. Platanitis E, Decker T. 2018. Regulatory Networks Involving STATs, IRFs, and NFkappaB in Inflammation. Front Immunol 9:2542.
67. Czerkies M, Korwek Z, Prus W, Kochanczyk M, Jaruszewicz-Blonska J, Tudelska K, Blonski S, Kimmel M, Brasier AR, Lipniacki T. 2018. Cell fate in antiviral response arises in the crosstalk of IRF, NF-kappaB and JAK/STAT pathways. Nat Commun 9:493.
68. Ardito F GM, Perrone D, Troiano G, Lo Muzio L. 2017. The crucial role of protein phosphorylation in cell signaling and its use as targeted therapy (Review). Int J Mol Med 40:271-280.
69. Zhang H CX, Tang M, Zhong G, Si Y, Li H, Zhu F, Liao Q, Li L, Zhao J, Feng J, Li S, Wang C, Kaulich M, Wang F, Chen L, Li L, Xia Z, Liang T, Lu H, Feng XH, Zhao B. 2021. A subcellular map of the human kinome. eLife 10:e64943.
70. Pasquier C RA. 2022. Evolutionary Divergence of Phosphorylation to Regulate Interactive Protein Networks in Lower and Higher Species. Int J Mol Sci 23:14429.
71. Davis ME GM. 2015. Ubiquitination in the antiviral immune response. Virology 479-480:52-65.
72. Aalto A M-CG, Kietz C, Tsyganova N, Kreutzer J, Kallio P, Broemer M, Meinander A. 2022. M1-linked ubiquitination facilitates NF-κB activation and survival during sterile inflammation. FEBS J 289:5180-5197.
73. Chow J FK, Kagan JC. 2015. PRRs are watching you: Localization of innate sensing and signaling regulators. Virology 479–480:104-109.
74. Chen Y LJ, Zhao Y, Ma X, Yi H. 2021. Toll-like receptor 3 (TLR3) regulation mechanisms and roles in antiviral innate immune responses. J Zhejiang Univ Sci B 22:609-632.
75. de Marcken M DK, Danielsen AC, Gautron AS, Dominguez-Villar M. 2019. TLR7 and TLR8 activate distinct pathways in monocytes during RNA virus infection. Sci Signal 12.
76. Lund J SA, Akira S, Medzhitov R, Iwasaki A. 2003. Toll-like receptor 9-mediated recognition of Herpes simplex virus-2 by plasmacytoid dendritic cells. J Exp Med 198:513-20.
77. Onomoto K OK, Yoneyama M. 2021. Regulation of RIG-I-like receptor-mediated signaling: interaction between host and viral factors. Cell Mol Immunol 18:539-555.
78. Bai J, Liu, F. 2022. Nuclear cGAS: sequestration and beyond. Protein & Cell 13:90–101.

79. Zhang Z YB, Bao M, Lu N, Kim T, Liu YJ. 2011. The helicase DDX41 senses intracellular DNA mediated by the adaptor STING in dendritic cells. Nat Immunol 12:959-65.
80. Unterholzner L KS, Baran M, Horan KA, Jensen SB, Sharma S, Sirois CM, Jin T, Latz E, Xiao TS, Fitzgerald KA, Paludan SR, Bowie AG. 2010. IFI16 is an innate immune sensor for intracellular DNA. Nat Immunol 11:997-1004.
81. Hornung V AA, Charrel-Dennis M, Bauernfeind F, Horvath G, Caffrey DR, Latz E, Fitzgerald KA. 2009. AIM2 recognizes cytosolic dsDNA and forms a caspase-1-activating inflammasome with ASC. Nature 458:514-8.
82. Takaoka A WZ, Choi MK, Yanai H, Negishi H, Ban T, Lu Y, Miyagishi M, Kodama T, Honda K, Ohba Y, Taniguchi T. 2007. DAI (DLM-1/ZBP1) is a cytosolic DNA sensor and an activator of innate immune response. Nature 448:501-5.
83. Kaiser WJ UJ, Mocarski ESKaiser WJ, Upton JW, Mocarski ES. 2008. Receptor-interacting protein homotypic interaction motif-dependent control of NF-kappa B activation via the DNA-dependent activator of IFN regulatory factors. J Immunol 181:6427-34.
84. Zhang T YC, Boyd DF, Quarato G, Ingram JP, Shubina M, Ragan KB, Ishizuka T, Crawford JC, Tummers B, Rodriguez DA, Xue J, Peri S, Kaiser WJ, López CB, Xu Y, Upton JW, Thomas PG, Green DR, Balachandran S. 2020. Influenza Virus Z-RNAs Induce ZBP1-Mediated Necroptosis. Cell 180:1115-1129.e13.
85. Nüsslein-Volhard C. 2022. The Toll gene in Drosophila pattern formation. Trends Genet 38:231-245.
86. Lester SN LK. 2014. Toll-like receptors in antiviral innate immunity. J Mol Biol 426:1246-64.
87. Zheng W XQ, Zhang Y, E X, Gao W, Zhang M, Zhai W, Rajkumar RS, Liu Z. 2020. Toll-like receptor-mediated innate immunity against herpesviridae infection: a current perspective on viral infection signaling pathways. Virol J 17:192.
88. Sartorius R TM, Manco R, D'Apice L, De Berardinis P. 2021. Exploiting viral sensing mediated by Toll-like receptors to design innovative vaccines. NPJ Vaccines. NPJ Vaccines 6:127.
89. Carty M BA. 2010. Recent insights into the role of Toll-like receptors in viral infection. Clin Exp Immunol 161:397-406.
90. Ohto U ST, Tanji H, Ishida H, Krayukhina E, Uchiyama S, Miyake K, Shimizu T. 2015. Structural basis of CpG and inhibitory DNA recognition by Toll-like receptor 9. Nature 520:702-5.
91. Sameer AS NS. 2021. Toll-Like Receptors (TLRs): Structure, Functions, Signaling, and Role of Their Polymorphisms in Colorectal Cancer Susceptibility. Biomed Res Int doi:doi: 10.1155/2021/1157023.
92. Kornilov FD SA, Lin C, Volynsky PE, Kot EF, Kayushin AL, Lushpa VA, Goncharuk MV, Arseniev AS, Goncharuk SA, Wang X, Mineev KS. 2023. The architecture of transmembrane and cytoplasmic juxtamembrane regions of Toll-like receptors. Nat Commun 14:1503.
93. Bell JK MG, Leifer CA, Mazzoni A, Davies DR, Segal DM. 2003. Leucine-rich repeats and pathogen recognition in Toll-like receptors. Trends Immunol 24:528-33.
94. Matsushima N TT, Enkhbayar P, Mikami T, Taga M, Yamada K, Kuroki Y. 2007. Comparative sequence analysis of leucine-rich repeats (LRRs) within vertebrate toll-like receptors. BMC Genomics. BMC Genomics 8:124.

95. Botos I SD, Davies DR. 2011. The structural biology of Toll-like receptors. . Structure 19:447-59.
96. Loiarro M RV, Sette C. 2010. Targeting TLR/IL-1R signalling in human diseases. Mediators Inflamm doi:doi: 10.1155/2010/674363.
97. CA D. 2018. Overview of the IL-1 family in innate inflammation and acquired immunity. Immunol Rev 281:8-27.
98. Samavati L RR, Du W, Hüttemann M, Fite A, Franchi L. 2009. STAT3 tyrosine phosphorylation is critical for interleukin 1 beta and interleukin-6 production in response to lipopolysaccharide and live bacteria. Mol Immunol 46:1867-77.
99. Piras V SK. 2014. Beyond MyD88 and TRIF Pathways in Toll-Like Receptor Signaling. Front Immunol 5.
100. Yoneyama M KM, Natsukawa T, Shinobu N, Imaizumi T, Miyagishi M, Taira K, Akira S, Fujita T. 2004. The RNA helicase RIG-I has an essential function in double-stranded RNA-induced innate antiviral responses. Nat Immunol 5:730-7.
101. Jiang Y, Zhang, H,Wang, J,Chen, J,Guo, Z,Liu,Y,Hua, H. 2023. Exploiting RIG-I-like receptor pathway for cancer immunotherapy. J Hematol Oncol 16.
102. Ho V YH, Chevrier M, Narang V, Lum J, Toh YX, Lee B, Chen J, Tan EY, Luo D, Fink K. 2019. RIG-I Activation by a Designer Short RNA Ligand Protects Human Immune Cells against Dengue Virus Infection without Causing Cytotoxicity. J Virol 93.
103. Weber M WF. 2014. RIG-I-like receptors and negative-strand RNA viruses: RLRly bird catches some worms. Cytokine Growth Factor Rev 25:621-8.
104. Brisse M, Ly H. 2019. Comparative Structure and Function Analysis of the RIG-I-Like Receptors: RIG-I and MDA5. Front Immunol 10:1586.
105. Rehwinkel J, Gack, MU 2020. RIG-I-like receptors: their regulation and roles in RNA sensing. Nat Rev Immunol 20:537–551.
106. Louber J, Brunel, J, Uchikawa, E, Cusack, S, Gerlier, D 2015. Kinetic discrimination of self/non-self RNA by the ATPase activity of RIG-I and MDA5. BMC Biology 13.
107. Kasumba DM GN. 2019. Therapeutic Targeting of RIG-I and MDA5 Might Not Lead to the Same Rome. Trends Pharmacol Sci 40:116-127.
108. Wu B, Hur , S. 2015. How RIG-I like receptors activate MAVS. Curr Opin Virol 12:91-8.
109. Yu Q, Qu, K, Modis, Y 2018. Cryo-EM Structures of MDA5-dsRNA Filaments at Different Stages of ATP Hydrolysis. Mol Cell 72:999-1012.e6.
110. Wang W, Pyle , AM. 2022. The RIG-I receptor adopts two different conformations for distinguishing host from viral RNA ligands. Mol Cell 82:4131-4144.e6.
111. Runge S SK, Lässig C, Hembach K, Baum A, García-Sastre A, Söding J, Conzelmann KK, Hopfner KP. 2014. In vivo ligands of MDA5 and RIG-I in measles virus-infected cells. PLoS Pathog 10:e1004081.
112. Pippig DA HJ, Cui S, Kirchhofer A, Lammens K, Lammens A, Schmidt A, Rothenfusser S, Hopfner KP. 2009. The regulatory domain of the RIG-I family ATPase LGP2 senses double-stranded RNA. Nucleic Acids Res 37:2014-25.
113. Murali A LX, Ranjith-Kumar CT, Bhardwaj K, Holzenburg A, Li P, Kao CC. 2008. Structure and function of LGP2, a DEX(D/H) helicase that regulates the innate immunity response. J Biol Chem 283:15825-33.
114. Komuro A HC. 2006. RNA- and virus-independent inhibition of antiviral signaling by RNA helicase LGP2. J Virol 80:12332-42.

115. Yum S LM, Fang Y, Chen ZJ. 2021. TBK1 recruitment to STING activates both IRF3 and NF-κB that mediate immune defense against tumors and viral infections. Proc Natl Acad Sci U S A 118:e2100225118.
116. Sun L WJ, Du F, Chen X, Chen ZJ. 2013. Cyclic GMP-AMP synthase is a cytosolic DNA sensor that activates the type I interferon pathway. Science 339:786-91.
117. Civril F DT, de Oliveira Mann CC, Ablasser A, Moldt M, Witte G, Hornung V, Hopfner KP. 2013. Structural mechanism of cytosolic DNA sensing by cGAS. Nature 498:332-7.
118. Hertzog J RJ. 2020. Regulation and inhibition of the DNA sensor cGAS. EMBO Rep 21.
119. de Oliveira Mann CC KR, Witte G, Hopfner KP. 2016. Structural and biochemical characterization of the cell fate determining nucleotidyltransferase fold protein MAB21L1. Sci Rep 6.
120. Zhou W WA, de Oliveira Mann CC, Morehouse BR, Nowak RP, Fischer ES, Gray NS, Mekalanos JJ, Kranzusch PJ. 2018. Structure of the Human cGAS-DNA Complex Reveals Enhanced Control of Immune Surveillance. Cell 174:300-311.e11.
121. Kranzusch PJ LA, Berger JM, Doudna JA. 2013. Structure of human cGAS reveals a conserved family of second-messenger enzymes in innate immunity. Cell Rep 3:1362-8.
122. Hall J RE, Shanker S, Wang H, Byrnes LJ, Horst R, Wong J, Brault A, Dumlao D, Smith JF, Dakin LA, Schmitt DC, Trujillo J, Vincent F, Griffor M, Aulabaugh AE. 2017. The catalytic mechanism of cyclic GMP-AMP synthase (cGAS) and implications for innate immunity and inhibition. Protein Sci 26:2367-2380.
123. Kranzusch PJ VR. 2013. cGAS dimerization entangles DNA recognition. Immunity 39:992-4.
124. Li T CZ. 2018. The cGAS-cGAMP-STING pathway connects DNA damage to inflammation, senescence, and cancer. J Exp Med 215:1287-1299.
125. Soponpong S AP, Kawai T, Tassanakajon A. 2019. A Cytosolic Sensor, PmDDX41, Binds Double Stranded-DNA and Triggers the Activation of an Innate Antiviral Response in the Shrimp Penaeus monodon via the STING-Dependent Signaling Pathway. Front Immunol 10:2069.
126. Weinreb JT BT. 2022. Clinical and mechanistic insights into the roles of DDX41 in haematological malignancies. FEBS Lett 596:2736-2745.
127. Perčulija V, Ouyang, S 2019. Diverse Roles of DEAD/DEAH-Box Helicases in Innate Immunity and Diseases. *In* Tuteja R (ed), Helicases from All Domains of Life.
128. Bosso M KF. 2020. Emerging Role of PYHIN Proteins as Antiviral Restriction Factors. Viruses 12:1464.
129. Chu LH GA, Dorfleutner A, Stehlik C. 2015. An updated view on the structure and function of PYRIN domains. Apoptosis doi:doi: 10.1007/s10495-014-1065-1:157-73.
130. Shaw N LZ. 2014. Role of the HIN domain in regulation of innate immune responses. Mol Cell Biol 34:2-15.
131. Ablasser A S-BJ, Hemmerling I, Horvath GL, Schmidt T, Latz E, Hornung V. 2013. Cell intrinsic immunity spreads to bystander cells via the intercellular transfer of cGAMP. Nature 503:530–534.
132. Franchi L ET, Muñoz-Planillo R, Nuñez G. 2009. The inflammasome: a caspase-1-activation platform that regulates immune responses and disease pathogenesis. Nat Immunol 10:241-7.

133. Wang B YQ. 2017. AIM2 inflammasome activation and regulation: A structural perspective. J Struct Biol 200:279-282.
134. Proell M GM, Mace PD, Reed JC, Riedl SJ. 2013. The CARD plays a critical role in ASC foci formation and inflammasome signalling. Biochem J 449:613-21.
135. Piper SC FJ, Kay L, Parker LC, Sabroe I, Sleeman MA, Briend E, Finch DK. 2013. The role of interleukin-1 and interleukin-18 in pro-inflammatory and anti-viral responses to rhinovirus in primary bronchial epithelial cells. PLoS One 8.
136. Vande Walle L LM. 2011. Inflammasomes: caspase-1-activating platforms with critical roles in host defense. Front Microbiol 2.
137. Maelfait J LL, Bridgeman A, Ragan KB, Upton JW, Rehwinkel J. 2017. Sensing of viral and endogenous RNA by ZBP1/DAI induces necroptosis. EMBO J 36:2529-2543.
138. Ravichandran S SV, Kim KK. 2019. Z-DNA in the genome: from structure to disease. Biophys Rev 11:383-387.
139. Li S ZY, Guan Z, Ye M, Li H, You M, Zhou Z, Zhang C, Zhang F, Lu B, Zhou P, Peng K. 2023. SARS-CoV-2 Z-RNA activates the ZBP1-RIPK3 pathway to promote virus-induced inflammatory responses. Cell Res 33:201-214.
140. Maelfait J RJ. 2023. The Z-nucleic acid sensor ZBP1 in health and disease. J Exp Med 220:e20221156.
141. Zhang D LJ, Han J. 2010. Receptor-interacting protein (RIP) kinase family. Cell Mol Immunol 7:243-9.
142. Bhat N FK. 2014. Recognition of cytosolic DNA by cGAS and other STING-dependent sensors. Eur J Immunol 44:634-40.
143. Ishii KJ KT, Koyama S, Matsui K, Kumar H, Kawai T, Uematsu S, Takeuchi O, Takeshita F, Coban C, Akira S. 2008. TANK-binding kinase-1 delineates innate and adaptive immune responses to DNA vaccines. Nature 451:725-9.
144. Zahid A IH, Li B, Jin T. 2020. Molecular and Structural Basis of DNA Sensors in Antiviral Innate Immunity. Front Immunol 11:613039.
145. Pengyan Xia SW, Pu Gao, Guangxia Gao, Zusen Fan. 2016. DNA sensor cGAS-mediated immune recognition. Protein & Cell 7:777–791.
146. Kim YG MM, Brandt T, Pearcy M, Hauns K, Lowenhaupt K, Jacobs BL, Rich A. 2003. A role for Z-DNA binding in vaccinia virus pathogenesis. Proc Natl Acad Sci U S A 100:6974-9.
147. TH M. 2009. Pathogen recognition and inflammatory signaling in innate immune defenses. Clin Microbiol Rev 22:240-73.
148. Leger MM R-RN, Najle SR, Ruiz-Trillo I. 2022. Rel/NF-κB Transcription Factors Emerged at the Onset of Opisthokonts. Genome Biol Evol 14:evab289.
149. D B. 2009. Discovering NF-kappaB. Cold Spring Harb Perspect Biol 1:a000026.
150. Sen R BD. 1986. Inducibility of kappa immunoglobulin enhancer-binding protein Nf-kappa B by a posttranslational mechanism. Cell 47:921-8.
151. Zabel U SR, Baeuerle PA. 1991. DNA binding of purified transcription factor NF-kappa B. Affinity, specificity, Zn2+ dependence, and differential half-site recognition. J Biol Chem 266:252-60.
152. Yu Y WY, Huang C. 2009. The biological functions of NF-kappaB1 (p50) and its potential as an anti-cancer target. Curr Cancer Drug Targets 9:566-71.
153. Giuliani C BI, Napolitano G. 2018. The Role of the Transcription Factor Nuclear Factor-kappa B in Thyroid Autoimmunity and Cancer. Front Endocrinol (Lausanne) 9:471.
154. Wan F LM. 2009. Specification of DNA binding activity of NF-kappaB proteins. Cold Spring Harb Perspect Biol 1:a000067.

155. Dobrzanski P RR, Bravo R. 1993. Both N- and C-terminal domains of RelB are required for full transactivation: role of the N-terminal leucine zipper-like motif. Mol Cell Biol 13:1572-82.
156. Yang MG SL, Han J, Zheng C, Liang H, Zhu J, Jin T. 2019. Biological characteristics of transcription factor RelB in different immune cell types: implications for the treatment of multiple sclerosis. Mol Brain 12:115.
157. Simeonidis S SD, Chen G, Hendrickson WA, Thanos D. 1999. Mechanisms by which IkappaB proteins control NF-kappaB activity. Proc Natl Acad Sci U S A 96:49-54.
158. Karin M B-NY. 2000. Phosphorylation meets ubiquitination: the control of NF-[kappa]B activity. Annu Rev Immunol 18:621-63.
159. Oeckinghaus A GS. 2009. The NF-kappaB family of transcription factors and its regulation. Cold Spring Harb Perspect Biol 1:a000034.
160. Li J MA, Tsai MD. 2006. Ankyrin repeat: a unique motif mediating protein-protein interactions. Biochemistry 45:15168-78.
161. Shih VF TR, Caldwell A, Hoffmann A. 2011. A single NFκB system for both canonical and non-canonical signaling. Cell Res 21:86-102.
162. A I. 2010. The IKK complex, a central regulator of NF-kappaB activation. Cold Spring Harb Perspect Biol 2:a000158.
163. Liu F XY, Parker AS, Verma IM. 2012. IKK biology. Immunol Rev 246:239-53.
164. Hinz M SC. 2014. The IκB kinase complex in NF-κB regulation and beyond. EMBO Rep 15:46-61.
165. May MJ LS, Shim JH, Madge LA, Ghosh S. 2004. A novel ubiquitin-like domain in IkappaB kinase beta is required for functional activity of the kinase. J Biol Chem 279:45528-39.
166. Rahighi S IF, Kawasaki M, Akutsu M, Suzuki N, Kato R, Kensche T, Uejima T, Bloor S, Komander D, Randow F, Wakatsuki S, Dikic I. 2009. Specific recognition of linear ubiquitin chains by NEMO is important for NF-kappaB activation. Cell 136:1098-109.
167. Laplantine E FE, Chiaravalli J, Lopez T, Lakisic G, Véron M, Agou F, Israël A. 2009. NEMO specifically recognizes K63-linked poly-ubiquitin chains through a new bipartite ubiquitin-binding domain. EMBO J 28:2885-95.
168. Wagner S CI, Rogov V, Kreike M, Ikeda F, Löhr F, Wu CJ, Ashwell JD, Dötsch V, Dikic I, Beyaert R. 2008. Ubiquitin binding mediates the NF-kappaB inhibitory potential of ABIN proteins. Oncogene 27:3739-45.
169. Cordier F GO, Traincard F, Véron M, Delepierre M, Agou F. 2009. The zinc finger of NEMO is a functional ubiquitin-binding domain. J Biol Chem 284:2902-2907.
170. Miller BS ZE. 2001. Complete reconstitution of human IkappaB kinase (IKK) complex in yeast. Assessment of its stoichiometry and the role of IKKgamma on the complex activity in the absence of stimulation. J Biol Chem 276:36320-6.
171. Zhao J HS, Minassian A, Li J, Feng P. 2015. Recent advances on viral manipulation of NF-κB signaling pathway. Curr Opin Virol 15:103-11.
172. Cai C TY, Zhai J, Zheng C. 2022. The RING finger protein family in health and disease. Signal Transduct Target Ther 7:300.
173. HH P. 2018. Structure of TRAF Family: Current Understanding of Receptor Recognition. Front Immunol 9:1999.
174. Xie P. 2013. TRAF molecules in cell signaling and in human diseases. J Mol Signal 8.
175. Park H. 1999. Structure of TRAF Family: Current Understanding of Receptor Recognition. Front Immunol 9.

176. Hayden MS GS. 2014. Regulation of NF-κB by TNF family cytokines. Semin Immunol 26:253-66.
177. Li X JS, Tapping RI. 2010. Toll-like receptor signaling in cell proliferation and survival. Cytokine 49:1-9.
178. Goel S OR, Jeganathan S, Bader V, Krause LJ, Kriegler S, Stender ID, Christine CW, Nakamura K, Hoffmann JE, Winter R, Tatzelt J, Winklhofer KF. 2023. Linear ubiquitination induces NEMO phase separation to activate NF-κB signaling. Life Sci Alliance 6:e202201607.
179. Ciechanover A SA. 1998. The ubiquitin-proteasome pathway: the complexity and myriad functions of proteins death. Proc Natl Acad Sci U S A 95:2727-30.
180. Kanarek N LN, Schueler-Furman O, Ben-Neriah Y. 2010. Ubiquitination and degradation of the inhibitors of NF-kappaB. Cold Spring Harb Perspect Biol 2:a000166.
181. Giridharan S, Srinivasan M. 2018. Mechanisms of NF-kappaB p65 and strategies for therapeutic manipulation. J Inflamm Res 11:407-419.
182. Huxford T HD, Malek S, Ghosh G. 1998. The crystal structure of the IkappaBalpha/NF-kappaB complex reveals mechanisms of NF-kappaB inactivation. Cell 95:759-70.
183. Wang VY HW, Asagiri M, Spann N, Hoffmann A, Glass C, Ghosh G. 2012. The transcriptional specificity of NF-κB dimers is coded within the κB DNA response elements. Cell Rep 2:824-39.
184. Croston GE CZ, Goeddel DV. 1995. NF-kappa B activation by interleukin-1 (IL-1) requires an IL-1 receptor-associated protein kinase activity. J Biol Chem 270:16514-7.
185. SC S. 2017. The non-canonical NF-κB pathway in immunity and inflammation. Nat Rev Immunol 17:545-558.
186. Hostager BS BG. 2013. CD40-Mediated Activation of the NF-κB2 Pathway. Front Immunol 4:376.
187. Elgueta R BM, de Vries VC, Wasiuk A, Guo Y, Noelle RJ. 2009. Molecular mechanism and function of CD40/CD40L engagement in the immune system. Immunol Rev 229:152-72.
188. Sasaki Y CS, Kutok JL, Rajewsky K, Schmidt-Supprian M. 2004. TNF family member B cell-activating factor (BAFF) receptor-dependent and -independent roles for BAFF in B cell physiology. J Immunol 173:2245-52.
189. Hoesel B, Schmid, J.A 2013. The complexity of NF-κB signaling in inflammation and cancer. Mol Cancer 12.
190. Luo JL KH, Karin M. 2005. IKK/NF-kappaB signaling: balancing life and death--a new approach to cancer therapy. J Clin Invest 115:115.
191. Zhao Y KB, Mollah ZU, Kay TW, Thomas HE. 2011. NF-κB in type 1 diabetes. . Inflamm Allergy Drug Targets 10:208-17.
192. Edwards MR BN, Clarke D, Birrell M, Belvisi M, Johnston SL. 2009. Targeting the NF-kappaB pathway in asthma and chronic obstructive pulmonary disease. Pharmacol Ther 121:1-13.
193. Miyamoto M FT, Kimura Y, Maruyama M, Harada H, Sudo Y, Miyata T, Taniguchi T. 1988. Regulated expression of a gene encoding a nuclear factor, IRF-1, that specifically binds to IFN-beta gene regulatory elements. Cell 54:903-13.
194. Negishi H, Taniguchi T, Yanai H. 2018. The Interferon (IFN) Class of Cytokines and the IFN Regulatory Factor (IRF) Transcription Factor Family. Cold Spring Harb Perspect Biol 10.

195. Mamane Y, Heylbroeck, C, Ge´nin, P, Algarte´, M, Servant, MJ, LePage, C, DeLuca, C, Kwon, H, Lin, R, Hiscott, J. 1999. Interferon regulatory factors: the next generation. GENE 237:1-14.
196. Tamura T, Yanai H, Savitsky D, Taniguchi T. 2008. The IRF family transcription factors in immunity and oncogenesis. Annu Rev Immunol 26:535-84.
197. Chiang HS, Liu HM. 2019. The Molecular Basis of Viral Inhibition of IRF- and STAT-Dependent Immune Responses. Front Immunol 9:3086.
198. Fujii Y ST, Kusumoto M, Kyogoku Y, Taniguchi T, Hakoshima T. 1999. Crystal structure of an IRF-DNA complex reveals novel DNA recognition and cooperative binding to a tandem repeat of core sequences. EMBO J 18:5028-5041.
199. Kindler E TV, Weber F. 2016. Interaction of SARS and MERS Coronaviruses with the Antiviral Interferon Response. Adv Virus Res 96:219-243.
200. S L. 2021. Interferon stimulated binding of ISRE is cell type specific and is predicted by homeostatic chromatin state. Cytokine X 17:100056.
201. Chen W RWJ. 2010. Structural insights into interferon regulatory factor activation. Cell Signal 22:883-7.
202. Antonczyk A, Krist B, Sajek M, Michalska A, Piaszyk-Borychowska A, Plens-Galaska M, Wesoly J, Bluyssen HAR. 2019. Direct Inhibition of IRF-Dependent Transcriptional Regulatory Mechanisms Associated With Disease. Front Immunol 10:1176.
203. Jefferies CA. 2019. Regulating IRFs in IFN Driven Disease. Front Immunol 10:325.
204. Couzinet A TK, Chen HM, Nishimura K, Wang Z, Morishita Y, Takeda K, Yagita H, Yanai H, Taniguchi T, Tamura T. 2008. A cell-type-specific requirement for IFN regulatory factor 5 (IRF5) in Fas-induced apoptosis. Proc Natl Acad Sci U S A 105:2556-61.
205. Shen H PR, Rajavelu P, Duan X, Gould KA, Choubey D. 2010. Gender-dependent expression of murine Irf5 gene: implications for sex bias in autoimmunity. J Mol Cell Biol 2:284-90.
206. Yanai H CH, Inuzuka T, Kondo S, Mak TW, Takaoka A, Honda K, Taniguchi T. 2007. Role of IFN regulatory factor 5 transcription factor in antiviral immunity and tumor suppression. Proc Natl Acad Sci U S A 104:3402-7.
207. Barnes BJ MP, Pitha PM. 2001. Virus-specific activation of a novel interferon regulatory factor, IRF-5, results in the induction of distinct interferon alpha genes. J Biol Chem 276:23382-90.
208. Cheng TF BS, Ando O, Van Scoy S, Kumar KP, Reich NC. 2006. Differential activation of IFN regulatory factor (IRF)-3 and IRF-5 transcription factors during viral infection. J Immunol 176:7462-70.
209. Barnes BJ KM, Field AE, Pitha PM. 2002. Multiple regulatory domains of IRF-5 control activation, cellular localization, and induction of chemokines that mediate recruitment of T lymphocytes. Mol Cell Biol 22:5721-40.
210. Li C ML, Chen X. 2011. Interferon regulatory factor 3-CL, an isoform of IRF3, antagonizes activity of IRF3. Cell Mol Immunol 8:67-74.
211. Petro T. 2020. IFN Regulatory Factor 3 in Health and Disease. J Immunol 205:1981-1989.
212. Sato M SH, Hata N, Asagiri M, Ogasawara K, Nakao K, Nakaya T, Katsuki M, Noguchi S, Tanaka N, Taniguchi T. 2000. Distinct and essential roles of transcription factors IRF-3 and IRF-7 in response to viruses for IFN-alpha/beta gene induction. Immunity 13:539-48.

213. DeFilippis VR RB, Keck TM, Hansen SG, Nelson JA, Früh KJ. 2006. Interferon regulatory factor 3 is necessary for induction of antiviral genes during human cytomegalovirus infection. J Virol 80:1032-7.
214. Grandvaux N SM, tenOever B, Sen GC, Balachandran S, Barber GN, Lin R, Hiscott J. 2002. Transcriptional profiling of interferon regulatory factor 3 target genes: direct involvement in the regulation of interferon-stimulated genes. J Virol 76:5532-9.
215. Saliba DG HA, Eames HL, Oikonomopoulos S, Teixeira A, Blazek K, Androulidaki A, Wong D, Goh FG, Weiss M, Byrne A, Pasparakis M, Ragoussis J, Udalova IA. 2014. IRF5:RelA interaction targets inflammatory genes in macrophages. Cell Rep 8:1308-17.
216. Takaoka A YH, Kondo S, Duncan G, Negishi H, Mizutani T, Kano S, Honda K, Ohba Y, Mak TW, Taniguchi T. 2005. Integral role of IRF-5 in the gene induction programme activated by Toll-like receptors. Nature 434:243-9.
217. Escalante CR BA, Pongubala JM, Shatova E, Shen L, Singh H, Aggarwal AK. 2002. Crystal structure of PU.1/IRF-4/DNA ternary complex. Mol Cell 10:1097-105.
218. Pang SH MM, Gangatirkar P, Zheng Z, Ebert A, Song G, Dickins RA, Corcoran LM, Mullighan CG, Busslinger M, Huntington ND, Nutt SL, Carotta S. 2016. PU.1 cooperates with IRF4 and IRF8 to suppress pre-B-cell leukemia. Leukemia 30:1375-87.
219. Oikawa T YT, Kihara-Negishi F, Yamamoto H, Kondoh N, Hitomi Y, Hashimoto Y. 1999. The role of Ets family transcription factor PU.1 in hematopoietic cell differentiation, proliferation and apoptosis. Cell Death 6:599-608.
220. Richardson RJ DJ, Malhotra S, Hardman MJ, Knowles L, Boot-Handford RP, Shore P, Whitmarsh A, Dixon MJ. 2006. Irf6 is a key determinant of the keratinocyte proliferation-differentiation switch. Nat Genet 38:1329-34.
221. Kwa MQ NT, Huynh J, Ramnath D, De Nardo D, Lam PY, Reynolds EC, Hamilton JA, Sweet MJ, Scholz GM. 2014. Interferon regulatory factor 6 differentially regulates Toll-like receptor 2-dependent chemokine gene expression in epithelial cells. J Biol Chem 289:19758-68.
222. Ma W HG, Wang Z, Wang L, Gao Q. 2023. IRF7: role and regulation in immunity and autoimmunity. Front Immunol 14:1236923.
223. Ning S, Pagano, J. & Barber, G. 2011. IRF7: activation, regulation, modification and function. Genes Immun 12:399–414.
224. Fink K GN. 2013. STAT2 and IRF9: Beyond ISGF3. JAKSTAT 2:e27521.
225. Platanitis E, Demiroz D, Schneller A, Fischer K, Capelle C, Hartl M, Gossenreiter T, Muller M, Novatchkova M, Decker T. 2019. A molecular switch from STAT2-IRF9 to ISGF3 underlies interferon-induced gene transcription. Nat Commun 10:2921.
226. Ren G CK, Zhang Z, Zhao K. 2015. Division of labor between IRF1 and IRF2 in regulating different stages of transcriptional activation in cellular antiviral activities. Cell Biosci 5:17.
227. Chen X GY, Li K, Luo T, Mu Y, Chen X. 2021. IRF1 and IRF2 act as positive regulators in antiviral response of large yellow croaker (Larimichthys crocea) by induction of distinct subgroups of type I IFNs. Dev Comp Immunol 118:103996.
228. Klune JR DR, Kimura S, Ueki S, Cardinal J, Nakao A, Nace G, Evankovich J, Murase N, Tsung A, Geller DA. 2012. Interferon regulatory factor-2 is protective against hepatic ischemia-reperfusion injury. Am J Physiol Gastrointest Liver Physiol 303:G666-73.

229. Paul A TT, Ng SK. 2018. Interferon Regulatory Factor 9 Structure and Regulation. Front Immunol 9:1831.
230. Chen K LJ, Cao X. 2017. Regulation of type I interferon signaling in immunity and inflammation: A comprehensive review. J Autoimmun 83:111.
231. TH M. 2019. IRF and STAT Transcription Factors - From Basic Biology to Roles in Infection, Protective Immunity, and Primary Immunodeficiencies. Front Immunol 9:3047.
232. Gómez-Herranz M TJ, Sloan RD. 2023. IFITM proteins: Understanding their diverse roles in viral infection, cancer, and immunity. J Biol Chem 299:102741.
233. Navarro L, David M. 1999. p38-dependent activation of interferon regulatory factor 3 by lipopolysaccharide. J Biol Chem 274:35535-8.
234. Devasthanam A. 2014. Mechanisms underlying the inhibition of interferon signaling by viruses. Virulence 5:270-277.
235. Lawler C, Brady, G. 2020. Poxviral Targeting of Interferon Regulatory Factor Activation. Viruses 12:1191.
236. Randall CM, Biswas S, Selen CV, Shisler JL. 2013. Inhibition of interferon gene activation by death-effector domain-containing proteins from the molluscum contagiosum virus. Proc Natl Acad Sci U S A 111:E265-72.
237. Perez de Diego R, Sancho-Shimizu V, Lorenzo L, Puel A, Plancoulaine S, Picard C, Herman M, Cardon A, Durandy A, Bustamante J, Vallabhapurapu S, Bravo J, Warnatz K, Chaix Y, Cascarrigny F, Lebon P, Rozenberg F, Karin M, Tardieu M, Al-Muhsen S, Jouanguy E, Zhang SY, Abel L, Casanova JL. 2010. Human TRAF3 adaptor molecule deficiency leads to impaired Toll-like receptor 3 response and susceptibility to herpes simplex encephalitis. Immunity 33:400-411.
238. Meyts I, Casanova JL. 2021. Viral infections in humans and mice with genetic deficiencies of the type I IFN response pathway. Eur J Immunol 51:1039-1061.
239. Bourdon M, Manet C, Montagutelli X. 2020. Host genetic susceptibility to viral infections: the role of type I interferon induction. Genes Immun 21:365-379.
240. Dropulic LK, Cohen JI. 2011. Severe viral infections and primary immunodeficiencies. Clin Infect Dis 53:897-909.
241. Crow YJ, Stetson DB. 2021. The type I interferonopathies: 10 years on. Nat Rev Immunol doi:doi: 10.1038/s41577-021-00633-9.
242. d'Angelo DM, Di Filippo P, Breda L, Chiarelli F. 2021. Type I Interferonopathies in Children: An Overview. Front Pediatr 9:631329.
243. Paun A, Pitha PM. 2007. The IRF family, revisited. Biochimie 89:744-53.
244. Yanai H, Chiba S, Hangai S, Kometani K, Inoue A, Kimura Y, Abe T, Kiyonari H, Nishio J, Taguchi-Atarashi N, Mizushima Y, Negishi H, Grosschedl R, Taniguchi T. 2018. Revisiting the role of IRF3 in inflammation and immunity by conditional and specifically targeted gene ablation in mice. Proc Natl Acad Sci U S A 115:5253-5258.
245. Au W, Moore, PA, Lowther, W, Juang, YT, Pitha, PM. 1995. Identification of a member of the interferon regulatory factor family that binds to the interferon-stimulated response element and activates expression of interferon-induced genes. PNAS 92:11657-11661.
246. Escalante CR, Nistal-Villan E, Shen L, Garcia-Sastre A, Aggarwal AK. 2007. Structure of IRF-3 bound to the PRDIII-I regulatory element of the human interferon-beta enhancer. Mol Cell 26:703-16.
247. Whittemore L, Maniatis,T. 1990. Postinduction repression of the beta-interferon gene is mediated through two positive regulatory domains. Proc Natl Acad Sci U S A 87:7799–7803.

248. Collins S, Noyce, RS, Mossman, KL. 2004. Innate Cellular Response to Virus Particle Entry Requires IRF3 but

Not Virus Replication. JOURNAL OF VIROLOGY 78:1706–1717.
249. Andrejeva J NH, Habjan M, Thiel V, Goodbourn S, Randall RE. 2013. ISG56/IFIT1 is primarily responsible for interferon-induced changes to patterns of parainfluenza virus type 5 transcription and protein synthesis. J Gen Virol 94:59-68.
250. De Ioannes P, Escalante CR, Aggarwal AK. 2011. Structures of apo IRF-3 and IRF-7 DNA binding domains: effect of loop L1 on DNA binding. Nucleic Acids Res 39:7300-7.
251. Panne D, Maniatis T, Harrison SC. 2004. Crystal structure of ATF-2/c-Jun and IRF-3 bound to the interferon-beta enhancer. EMBO J 23:4384-93.
252. Wang JT, Chang LS, Chen CJ, Doong SL, Chang CW, Chen MR. 2014. Glycogen synthase kinase 3 negatively regulates IFN regulatory factor 3 transactivation through phosphorylation at its linker region. Innate Immun 20:78-87.
253. Dragan AI, Hargreaves VV, Makeyeva EN, Privalov PL. 2007. Mechanisms of activation of interferon regulator factor 3: the role of C-terminal domain phosphorylation in IRF-3 dimerization and DNA binding. Nucleic Acids Res 35:3525-34.
254. Jing T, Zhao B, Xu P, Gao X, Chi L, Han H, Sankaran B, Li P. 2020. The Structural Basis of IRF-3 Activation upon Phosphorylation. J Immunol 205:1886-1896.
255. LIN R, HEYLBROECK, C, PITHA, PM, HISCOTT, J. 1998. Virus-Dependent Phosphorylation of the IRF-3 Transcription

Factor Regulates Nuclear Translocation, Transactivation

Potential, and Proteasome-Mediated Degradation. Molecular and Cellular Biology 18:2986-2996.
256. Takahasi K, Suzuki, NN, Horiuchi, M, Mori, M, Suhara, W, Okabe, Y, Fukuhara, Y, Terasawa, H, Akira, S, Fujita, T, Inagaki, F 2003. X-ray crystal structure of IRF-3 and its functional implications. Nature Structural & Molecular Biology volume 10:922–927.
257. Wang Z, Ji J, Peng D, Ma F, Cheng G, Qin FX. 2016. Complex Regulation Pattern of IRF3 Activation Revealed by a Novel Dimerization Reporter System. J Immunol 196:4322-30.
258. Courreges MC, Kantake N, Goetz DJ, Schwartz FL, McCall KD. 2012. Phenylmethimazole blocks dsRNA-induced IRF3 nuclear translocation and homodimerization. Molecules 17:12365-77.
259. Qin BY, Liu C, Lam SS, Srinath H, Delston R, Correia JJ, Derynck R, Lin K. 2003. Crystal structure of IRF-3 reveals mechanism of autoinhibition and virus-induced phosphoactivation. Nat Struct Biol 10:913-21.
260. Lin R MY, Hiscott J. 2000. Multiple regulatory domains control IRF-7 activity in response to virus infection. J Biol Chem 275:34320-7.
261. Chen W, Srinath H, Lam SS, Schiffer CA, Royer WE, Jr., Lin K. 2008. Contribution of Ser386 and Ser396 to activation of interferon regulatory factor 3. J Mol Biol 379:251-60.
262. Attisano L, Lee-Hoeflich, ST. 2001. The Smads. Genome Biology 2:3010.1–3010.8.
263. Seoane J, Gomis RR. 2017. TGF-beta Family Signaling in Tumor Suppression and Cancer Progression. Cold Spring Harb Perspect Biol 9.

264. Qing J, Liu C, Choy L, Wu RY, Pagano JS, Derynck R. 2004. Transforming growth factor beta/Smad3 signaling regulates IRF-7 function and transcriptional activation of the beta interferon promoter. Mol Cell Biol 24:1411-25.
265. Qing F LZ. 2023. Interferon regulatory factor 7 in inflammation, cancer and infection. Front Immunol 14:1190841.
266. Pokharel SM, Shil NK, Bose S. 2016. Autophagy, TGF-beta, and SMAD-2/3 Signaling Regulates Interferon-beta Response in Respiratory Syncytial Virus Infected Macrophages. Front Cell Infect Microbiol 6:174.
267. Xu P, Bailey-Bucktrout S, Xi Y, Xu D, Du D, Zhang Q, Xiang W, Liu J, Melton A, Sheppard D, Chapman HA, Bluestone JA, Derynck R. 2014. Innate antiviral host defense attenuates TGF-beta function through IRF3-mediated suppression of Smad signaling. Mol Cell 56:723-37.
268. Guinn Z, Lampe AT, Brown DM, Petro TM. 2016. Significant role for IRF3 in both T cell and APC effector functions during T cell responses. Cell Immunol 310:141-149.
269. Tian M, Wang X, Sun J, Lin W, Chen L, Liu S, Wu X, Shi L, Xu P, Cai X, Wang X. 2020. IRF3 prevents colorectal tumorigenesis via inhibiting the nuclear translocation of beta-catenin. Nat Commun 11:5762.
270. Doyle S, Vaidya, S, O'Connell, R, Dadgostar, H, Dempsey, P, Wu,T, Rao, G, Sun, R, Haberland, M, Modlin, R, Cheng, G. 2002. IRF3 Mediates a TLR3:TLR4-Specific Antiviral Gene Program. Immunity 17:251-263.
271. Reikine S, Nguyen JB, Modis Y. 2014. Pattern Recognition and Signaling Mechanisms of RIG-I and MDA5. Front Immunol 5:342.
272. Vercammen E, Staal J, Beyaert R. 2008. Sensing of viral infection and activation of innate immunity by toll-like receptor 3. Clin Microbiol Rev 21:13-25.
273. Wan D, Jiang W, Hao J. 2020. Research Advances in How the cGAS-STING Pathway Controls the Cellular Inflammatory Response. Front Immunol 11:615.
274. El-Zayat SR, Sibaii H, Mannaa FA. 2019. Toll-like receptors activation, signaling, and targeting: an overview. Bulletin of the National Research Centre 43.
275. Gosu V, Son S, Shin D, Song KD. 2019. Insights into the dynamic nature of the dsRNA-bound TLR3 complex. Sci Rep 9:3652.
276. Fekonja O, Bencina M, Jerala R. 2012. Toll/interleukin-1 receptor domain dimers as the platform for activation and enhanced inhibition of Toll-like receptor signaling. J Biol Chem 287:30993-1002.
277. Manavalan B, Basith S, Choi S. 2011. Similar Structures but Different Roles - An Updated Perspective on TLR Structures. Front Physiol 2:41.
278. Wang Y, Liu L, Davies DR, Segal DM. 2010. Dimerization of Toll-like receptor 3 (TLR3) is required for ligand binding. J Biol Chem 285:36836-41.
279. Nguyen VP, Chen J, Petrus MN, Goldman CK, Kruhlak MJ, Bamford RN, Waldmann TA. 2014. A new domain in the Toll/IL-1R domain-containing adaptor inducing interferon-beta factor protein amino terminus is important for tumor necrosis factor-alpha receptor-associated factor 3 association, protein stabilization and interferon signaling. J Innate Immun 6:377-93.
280. Deng T, Hu, B, Wang, X, Lin, L, Zhou, J, Xu, Y, Yan,Y, Zheng, X, Zhou, J. 2021. Inhibition of Antiviral Innate Immunity by Avibirnavirus VP3 via

Blocking TBK1-TRAF3 Complex Formation and IRF3 Activation. mSystems 6.
281. Outlioua A, Pourcelot M, Arnoult D. 2018. The Role of Optineurin in Antiviral Type I Interferon Production. Front Immunol 9:853.

282. Chau TL, Gioia R, Gatot JS, Patrascu F, Carpentier I, Chapelle JP, O'Neill L, Beyaert R, Piette J, Chariot A. 2008. Are the IKKs and IKK-related kinases TBK1 and IKK-epsilon similarly activated? Trends Biochem Sci 33:171-80.
283. van Zuylen WJ, Doyon P, Clement JF, Khan KA, D'Ambrosio LM, Do F, St-Amant-Verret M, Wissanji T, Emery G, Gingras AC, Meloche S, Servant MJ. 2012. Proteomic profiling of the TRAF3 interactome network reveals a new role for the ER-to-Golgi transport compartments in innate immunity. PLoS Pathog 8:e1002747.
284. Häcker H, Tseng, PH. & Karin, M. 2011. Expanding TRAF function: TRAF3 as a tri-faced immune regulator. Nat Rev Immunol 11:457–468
285. Lin CY, Shih MC, Chang HC, Lin KJ, Chen LF, Huang SW, Yang ML, Ma SK, Shiau AL, Wang JR, Chen KR, Ling P. 2021. Influenza a virus NS1 resembles a TRAF3-interacting motif to target the RNA sensing-TRAF3-type I IFN axis and impair antiviral innate immunity. J Biomed Sci 28:66.
286. Andersen LL, Mork N, Reinert LS, Kofod-Olsen E, Narita R, Jorgensen SE, Skipper KA, Honing K, Gad HH, Ostergaard L, Orntoft TF, Hornung V, Paludan SR, Mikkelsen JG, Fujita T, Christiansen M, Hartmann R, Mogensen TH. 2015. Functional IRF3 deficiency in a patient with herpes simplex encephalitis. J Exp Med 212:1371-9.
287. Xie X, Jin J, Zhu L, Jie Z, Li Y, Zhao B, Cheng X, Li P, Sun SC. 2019. Cell type-specific function of TRAF2 and TRAF3 in regulating type I IFN induction. Cell Biosci 9:5.
288. Zhu W, Li J, Zhang R, Cai Y, Wang C, Qi S, Chen S, Liang X, Qi N, Hou F. 2019. TRAF3IP3 mediates the recruitment of TRAF3 to MAVS for antiviral innate immunity. EMBO J 38:e102075.
289. Fang R, Jiang Q, Zhou X, Wang C, Guan Y, Tao J, Xi J, Feng JM, Jiang Z. 2017. MAVS activates TBK1 and IKKepsilon through TRAFs in NEMO dependent and independent manner. PLoS Pathog 13:e1006720.
290. Kato H, Takeuchi O, Mikamo-Satoh E, Hirai R, Kawai T, Matsushita K, Hiiragi A, Dermody TS, Fujita T, Akira S. 2008. Length-dependent recognition of double-stranded ribonucleic acids by retinoic acid-inducible gene-I and melanoma differentiation-associated gene 5. J Exp Med 205:1601-10.
291. Chiu YH, Macmillan JB, Chen ZJ. 2009. RNA polymerase III detects cytosolic DNA and induces type I interferons through the RIG-I pathway. Cell 138:576-91.
292. Ren Z DT, Zuo Z, Xu Z, Deng J, Wei Z. 2020. Regulation of MAVS Expression and Signaling Function in the Antiviral Innate Immune Response. Front Immunol 11:1030.
293. Scott I NK. 2008. The mitochondrial antiviral signaling protein, MAVS, is cleaved during apoptosis. Biochem Biophys Res Commun 375:101-6.
294. Meylan E CJ, Hofmann K, Moradpour D, Binder M, Bartenschlager R, Tschopp J. 2005. Cardif is an adaptor protein in the RIG-I antiviral pathway and is targeted by hepatitis C virus. Nature 437:1167-72.
295. Sato S SM, Yamamoto M, Watanabe Y, Kawai T, Takeda K, Akira S. 2003. Toll/IL-1 receptor domain-containing adaptor inducing IFN-beta (TRIF) associates with TNF receptor-associated factor 6 and TANK-binding kinase 1, and activates two distinct transcription factors, NF-kappa B and IFN-regulatory factor-3, in the Toll-like receptor signaling. J Immunol 171:4304-10.
296. Liu S CX, Wu J, Cong Q, Chen X, Li T, Du F, Ren J, Wu YT, Grishin NV, Chen ZJ. 2015. Phosphorylation of innate immune adaptor proteins MAVS, STING, and TRIF induces IRF3 activation. Science 13;347.

297. Hong Z, Ma T, Liu X, Wang C. 2021. cGAS-STING pathway: post-translational modifications and functions in sterile inflammatory diseases. FEBS J doi:doi: 10.1111/febs.16137.
298. Shang G, Zhang C, Chen ZJ, Bai XC, Zhang X. 2019. Cryo-EM structures of STING reveal its mechanism of activation by cyclic GMP-AMP. Nature 567:389-393.
299. Zhao B, Shu C, Gao X, Sankaran B, Du F, Shelton CL, Herr AB, Ji JY, Li P. 2016. Structural basis for concerted recruitment and activation of IRF-3 by innate immune adaptor proteins. Proc Natl Acad Sci U S A 113:E3403-12.
300. Zhao B, Du, F., Xu, P. et al. 2019. A conserved PLPLRT/SD motif of STING mediates the recruitment and activation of TBK1. NATURE 569:718-722.
301. Bo Z, Miao Y, Xi R, Zhong Q, Bao C, Chen H, Sun L, Qian Y, Jung YS, Dai J. 2020. PRV UL13 inhibits cGAS-STING-mediated IFN-beta production by phosphorylating IRF3. Vet Res 51:118.
302. Deschamps T, Kalamvoki, M. 2017. Evasion of the STING DNA-Sensing Pathway by VP11:12 of Herpes Simplex Virus 1. Journal of Virology 91.
303. Eaglesham JB PY, Kupper TS, Kranzusch PJ. 2019. Viral and metazoan poxins are cGAMP-specific nucleases that restrict cGAS-STING signalling. Nature 566:259-263.
304. Levy D, Garcı´a-Sastre, A. 2001. The virus battles: IFN induction of the antiviral state and

mechanisms of viral evasion. Cytokine & Growth Factor Reviews 12:143-156.
305. Gomez-Lucia E, Collado VM, Miro G, Domenech A. 2009. Effect of type-I interferon on retroviruses. Viruses 1:545-73.
306. Ashley CL, Abendroth A, McSharry BP, Slobedman B. 2019. Interferon-Independent Innate Responses to Cytomegalovirus. Front Immunol 10:2751.
307. Mogensen TH. 2018. IRF and STAT Transcription Factors - From Basic Biology to Roles in Infection, Protective Immunity, and Primary Immunodeficiencies. Front Immunol 9:3047.
308. Mayer A, Maelfait J, Bridgeman A, Rehwinkel J. 2017. Purification of Cyclic GMP-AMP from Viruses and Measurement of Its Activity in Cell Culture. Methods Mol Biol 1656:143-152.
309. Shimada T, Kawai, T, Takeda, K, Matsumoto, M,Inoue, JI, Tatsumi, Y, Kanamaru, A, Akira, S. 1999. IKK-i, a novel lipopolysaccharide-inducible kinase that is related to IκB kinases. International Immunology 11:1357–1362.
310. Peters R, Liao, SM, Maniatis,T. 2000. IKKε Is Part of a Novel PMA-Inducible IκB Kinase Complex. Molecular Cell 5:513-522.
311. Tojima Y, Fujimoto, A, Delhase, M, Chen, Y, Hatakeyama,S, Nakayama, KI, Kaneko, Y, Nimura, Y, Motoyama, N, Ikeda, K, Karin, M, Nakanishi , M. 2000. NAK is an IκB kinase-activating kinase. Nature 404:778–782.
312. Krappmann D, Hatada EN, Tegethoff S, Li J, Klippel A, Giese K, Baeuerle PA, Scheidereit C. 2000. The I kappa B kinase (IKK) complex is tripartite and contains IKK gamma but not IKAP as a regular component. J Biol Chem 275:29779-87.
313. Jin J, Xiao Y, Chang JH, Yu J, Hu H, Starr R, Brittain GC, Chang M, Cheng X, Sun SC. 2012. The kinase TBK1 controls IgA class switching by negatively regulating noncanonical NF-kappaB signaling. Nat Immunol 13:1101-9.
314. Wietek C, Cleaver CS, Ludbrook V, Wilde J, White J, Bell DJ, Lee M, Dickson M, Ray KP, O'Neill LA. 2006. IkappaB kinase epsilon interacts with p52 and promotes transactivation via p65. J Biol Chem 281:34973-81.

315. Mattioli I, Geng H, Sebald A, Hodel M, Bucher C, Kracht M, Schmitz ML. 2006. Inducible phosphorylation of NF-kappa B p65 at serine 468 by T cell costimulation is mediated by IKK epsilon. J Biol Chem 281:6175-83.
316. Ling L, Cao, Z, Goeddel, DV. 1998. NF-κB-inducing kinase activates IKK-α by phosphorylation of Ser-176. Proc Natl Acad Sci U S A 95:3792–3797.
317. Xiao G, Fong A, Sun SC. 2004. Induction of p100 processing by NF-kappaB-inducing kinase involves docking IkappaB kinase alpha (IKKalpha) to p100 and IKKalpha-mediated phosphorylation. J Biol Chem 279:30099-105.
318. Shin CH, Choi DS. 2019. Essential Roles for the Non-Canonical IkappaB Kinases in Linking Inflammation to Cancer, Obesity, and Diabetes. Cells 8.
319. Fitzgerald KA, McWhirter SM, Faia KL, Rowe DC, Latz E, Golenbock DT, Coyle AJ, Liao SM, Maniatis T. 2003. IKKepsilon and TBK1 are essential components of the IRF3 signaling pathway. Nat Immunol 4:491-6.
320. Panne D, McWhirter SM, Maniatis T, Harrison SC. 2007. Interferon regulatory factor 3 is regulated by a dual phosphorylation-dependent switch. J Biol Chem 282:22816-22.
321. Clement JF, Bibeau-Poirier A, Gravel SP, Grandvaux N, Bonneil E, Thibault P, Meloche S, Servant MJ. 2008. Phosphorylation of IRF-3 on Ser 339 generates a hyperactive form of IRF-3 through regulation of dimerization and CBP association. J Virol 82:3984-96.
322. Clement JF, Meloche S, Servant MJ. 2008. The IKK-related kinases: from innate immunity to oncogenesis. Cell Res 18:889-99.
323. Caillaud A, Hovanessian, AG, Levy, DE, Marié, IJ. 2005. Regulatory Serine Residues Mediate Phosphorylation-dependent and Phosphorylation-independent Activation of Interferon Regulatory Factor 7. J Biol Chem 280:17671-17677.
324. Dalskov L, Narita R, Andersen LL, Jensen N, Assil S, Kristensen KH, Mikkelsen JG, Fujita T, Mogensen TH, Paludan SR, Hartmann R. 2020. Characterization of distinct molecular interactions responsible for IRF3 and IRF7 phosphorylation and subsequent dimerization. Nucleic Acids Res 48:11421-11433.
325. Gu L, Casserly D, Brady G, Carpenter S, Bracken AP, Fitzgerald KA, Unterholzner L, Bowie AG. 2022. Myeloid cell nuclear differentiation antigen controls the pathogen-stimulated type I interferon cascade in human monocytes by transcriptional regulation of IRF7. Nat Commun 13:14.
326. McWhirter SM, Fitzgerald KA, Rosains J, Rowe DC, Golenbock DT, Maniatis T. 2004. IFN-regulatory factor 3-dependent gene expression is defective in Tbk1-deficient mouse embryonic fibroblasts. Proc Natl Acad Sci U S A 101:233-8.
327. TENOEVER B, NG,SL,CHUA, MA, MCWHIRTER, SM, GARCÍA-SASTRE, A, MANIATIS,T. 2007. Multiple Functions of the IKK-Related Kinase IKKε in Interferon-Mediated Antiviral Immunity. SCIENCE 315:1274-1278.
328. Ng SL, Friedman BA, Schmid S, Gertz J, Myers RM, Tenoever BR, Maniatis T. 2011. IkappaB kinase epsilon (IKK(epsilon)) regulates the balance between type I and type II interferon responses. Proc Natl Acad Sci U S A 108:21170-5.
329. Larabi A, Devos JM, Ng SL, Nanao MH, Round A, Maniatis T, Panne D. 2013. Crystal structure and mechanism of activation of TANK-binding kinase 1. Cell Rep 3:734-46.
330. Hagan R, Torres-Castillo, J, Doerschuk, CM. 2019. Myeloid TBK1 Signaling Contributes to the Immune Response to Influenza. Am J Respir Cell Mol Biol 60:335-345.

331. Verhelst K, Verstrepen L, Carpentier I, Beyaert R. 2013. IkappaB kinase epsilon (IKKepsilon): a therapeutic target in inflammation and cancer. Biochem Pharmacol 85:873-80.
332. Fujita F, Taniguchi Y, Kato T, Narita Y, Furuya A, Ogawa T, Sakurai H, Joh T, Itoh M, Delhase M, Karin M, Nakanishi M. 2003. Identification of NAP1, a regulatory subunit of IkappaB kinase-related kinases that potentiates NF-kappaB signaling. Mol Cell Biol 23:7780-93.
333. Ryzhakov G, Randow F. 2007. SINTBAD, a novel component of innate antiviral immunity, shares a TBK1-binding domain with NAP1 and TANK. EMBO J 26:3180-90.
334. Gatot JS, Gioia R, Chau TL, Patrascu F, Warnier M, Close P, Chapelle JP, Muraille E, Brown K, Siebenlist U, Piette J, Dejardin E, Chariot A. 2007. Lipopolysaccharide-mediated interferon regulatory factor activation involves TBK1-IKKepsilon-dependent Lys(63)-linked polyubiquitination and phosphorylation of TANK/I-TRAF. J Biol Chem 282:31131-46.
335. Goncalves A, Burckstummer T, Dixit E, Scheicher R, Gorna MW, Karayel E, Sugar C, Stukalov A, Berg T, Kralovics R, Planyavsky M, Bennett KL, Colinge J, Superti-Furga G. 2011. Functional dissection of the TBK1 molecular network. PLoS One 6:e23971.
336. Xu G, Lo YC, Li Q, Napolitano G, Wu X, Jiang X, Dreano M, Karin M, Wu H. 2011. Crystal structure of inhibitor of kappaB kinase beta. Nature 472:325-30.
337. Durand JK, Zhang Q, Baldwin AS. 2018. Roles for the IKK-Related Kinases TBK1 and IKKepsilon in Cancer. Cells 7.
338. Shu C, Sankaran B, Chaton CT, Herr AB, Mishra A, Peng J, Li P. 2013. Structural insights into the functions of TBK1 in innate antimicrobial immunity. Structure 21:1137-48.
339. Ikeda F, Hecker CM, Rozenknop A, Nordmeier RD, Rogov V, Hofmann K, Akira S, Dotsch V, Dikic I. 2007. Involvement of the ubiquitin-like domain of TBK1/IKK-i kinases in regulation of IFN-inducible genes. EMBO J 26:3451-62.
340. Barczewski AH, Ragusa MJ, Mierke DF, Pellegrini M. 2019. The IKK-binding domain of NEMO is an irregular coiled coil with a dynamic binding interface. Sci Rep 9:2950.
341. Laplantine E, Fontan E, Chiaravalli J, Lopez T, Lakisic G, Veron M, Agou F, Israel A. 2009. NEMO specifically recognizes K63-linked poly-ubiquitin chains through a new bipartite ubiquitin-binding domain. EMBO J 28:2885-95.
342. Yoshikawa A, Sato Y, Yamashita M, Mimura H, Yamagata A, Fukai S. 2009. Crystal structure of the NEMO ubiquitin-binding domain in complex with Lys 63-linked di-ubiquitin. FEBS Lett 583:3317-22.
343. Helgason E, Phung QT, Dueber EC. 2013. Recent insights into the complexity of Tank-binding kinase 1 signaling networks: the emerging role of cellular localization in the activation and substrate specificity of TBK1. FEBS Lett 587:1230-7.
344. Zhu G, Liu Y, Shaw S. 2005. Protein kinase specificity. A strategic collaboration between kinase peptide specificity and substrate recruitment. Cell Cycle 4:52-6.
345. Sasai M, Shingai M, Funami K, Yoneyama M, Fujita T, Matsumoto M, Seya T. 2006. NAK-associated protein 1 participates in both the TLR3 and the cytoplasmic pathways in type I IFN induction. J Immunol 177:8676-83.
346. Zhao W, Wang L, Zhang M, Wang P, Yuan C, Qi J, Meng H, Gao C. 2012. Tripartite motif-containing protein 38 negatively regulates TLR3/4- and RIG-I-mediated IFN-beta production and antiviral response by targeting NAP1. J Immunol 188:5311-8.

347. Fu T, Liu J, Wang Y, Xie X, Hu S, Pan L. 2018. Mechanistic insights into the interactions of NAP1 with the SKICH domains of NDP52 and TAX1BP1. Proc Natl Acad Sci U S A 115:E11651-E11660.
348. Verstrepen L, Verhelst K, Carpentier I, Beyaert R. 2011. TAX1BP1, a ubiquitin-binding adaptor protein in innate immunity and beyond. Trends Biochem Sci 36:347-54.
349. Lei X, Dong X, Ma R, Wang W, Xiao X, Tian Z, Wang C, Wang Y, Li L, Ren L, Guo F, Zhao Z, Zhou Z, Xiang Z, Wang J. 2020. Activation and evasion of type I interferon responses by SARS-CoV-2. Nat Commun 11:3810.
350. Lei J, Kusov Y, Hilgenfeld R. 2018. Nsp3 of coronaviruses: Structures and functions of a large multi-domain protein. Antiviral Res 149:58-74.
351. Bakshi S, Taylor J, Strickson S, McCartney T, Cohen P. 2017. Identification of TBK1 complexes required for the phosphorylation of IRF3 and the production of interferon beta. Biochem J 474:1163-1174.
352. Unterholzner L, Sumner RP, Baran M, Ren H, Mansur DS, Bourke NM, Randow F, Smith GL, Bowie AG. 2011. Vaccinia virus protein C6 is a virulence factor that binds TBK-1 adaptor proteins and inhibits activation of IRF3 and IRF7. PLoS Pathog 7:e1002247.
353. Pourcelot M, Zemirli N, Silva Da Costa L, Loyant R, Garcin D, Vitour D, Munitic I, Vazquez A, Arnoult D. 2016. The Golgi apparatus acts as a platform for TBK1 activation after viral RNA sensing. BMC Biol 14:69.
354. Gleason CE, Ordureau A, Gourlay R, Arthur JSC, Cohen P. 2011. Polyubiquitin binding to optineurin is required for optimal activation of TANK-binding kinase 1 and production of interferon beta. J Biol Chem 286:35663-35674.
355. Kachaner D, Genin P, Laplantine E, Weil R. 2012. Toward an integrative view of Optineurin functions. Cell Cycle 11:2808-18.
356. Pflug KM, Sitcheran R. 2020. Targeting NF-kappaB-Inducing Kinase (NIK) in Immunity, Inflammation, and Cancer. Int J Mol Sci 21.
357. Lee-Kirsch M. 2017. The Type I Interferonopathies. AnnuRev 68:297–315.
358. Kato H OS, Fujita T. 2017. RIG-I-Like Receptors and Type I Interferonopathies. J Interferon Cytokine Res 37:207-213.
359. Gorman JA HC, Errett JS, Stone AE, Allenspach EJ, Ge Y, Arkatkar T, Clough C, Dai X, Khim S, Pestal K, Liggitt D, Cerosaletti K, Stetson DB, James RG, Oukka M, Concannon P, Gale M Jr, Buckner JH, Rawlings DJ. 2017. The A946T variant of the RNA sensor IFIH1 mediates an interferon program that limits viral infection but increases the risk for autoimmunity. Nat Immunol 18:744-752.
360. Blum SI TJ, Barra JM, Burg AR, Shang Q, Qiu S, Shechter O, Hayes AR, Green TJ, Geurts AM, Chen YG, Tse HM. 2023. MDA5-dependent responses contribute to autoimmune diabetes progression and hindrance. JCI Insight 8:e157929.
361. Postal M VJ, Fernandez-Ruiz R, Paredes JL, Appenzeller S, Niewold TB. 2020. Type I interferon in the pathogenesis of systemic lupus erythematosus. Curr Opin Immunol 67:87-94.
362. Pothlichet J NT, Vitour D, Solhonne B, Crow MK, Si-Tahar M. 2011. A loss-of-function variant of the antiviral molecule MAVS is associated with a subset of systemic lupus patients. EMBO Mol Med 3:142-52.
363. Sirobhushanam S LS, Kahlenberg JM. 2021. Interferons in Systemic Lupus Erythematosus. Rheum Dis Clin North Am 47:297-315.
364. Okabe Y ST, Nagata S. 2009. Regulation of the innate immune response by threonine-phosphatase of Eyes absent. Nature 460:520-4.

365. Sun W WH, Qi CF, Wu J, Scott B, Bolland S. 2019. Antiviral Adaptor MAVS Promotes Murine Lupus With a B Cell Autonomous Role. Front Immunol 10:2452.
366. Matz AJ QL, Karlinsey K, Vella AT, Zhou B. 2023. Capturing the multifaceted function of adipose tissue macrophages. Front Immunol 14:1148188.
367. Ellulu MS PI, Khaza'ai H, Rahmat A, Abed Y. 2017. Obesity and inflammation: the linking mechanism and the complications. Arch Med Sci 13:851-863.
368. Dinh KM KK, Mikkelsen S, Pedersen OB, Petersen MS, Thørner LW, Hjalgrim H, Rostgaard K, Ullum H, Erikstrup C. 2019. Low-grade inflammation is negatively associated with physical Health-Related Quality of Life in healthy individuals: Results from The Danish Blood Donor Study (DBDS). PLoS One 14:e0214468.
369. Sanada Y KT, Suehiro H, Yamamoto T, Nishimura F, Kato N, Yanaka N. 2014. IκB kinase epsilon expression in adipocytes is upregulated by interaction with macrophages. Biosci Biotechnol Biochem doi:doi:10.1080/09168451.2014.925776:1357-62.
370. Xiao QA HQ, Li L, Song Y, Chen YR, Zeng J, Xia X. 2022. Role of IKKε in the Metabolic Diseases: Physiology, Pathophysiology, and Pharmacology. Front Pharmacol 13:888588.
371. Mowers J UM, Reilly SM, Simon J, Leto D, Chiang SH, Chang L, Saltiel AR. 2013. Inflammation produces catecholamine resistance in obesity via activation of PDE3B by the protein kinases IKKε and TBK1. Elife 2:e01119.
372. Oral EA RS, Gomez AV, Meral R, Butz L, Ajluni N, Chenevert TL, Korytnaya E, Neidert AH, Hench R, Rus D, Horowitz JF, Poirier B, Zhao P, Lehmann K, Jain M, Yu R, Liddle C, Ahmadian M, Downes M, Evans RM, Saltiel AR. 2017. Inhibition of IKKε and TBK1 Improves Glucose Control in a Subset of Patients with Type 2 Diabetes. Cell Metab 26:157-170.e7.
373. Song J LM, Song J, Li M, Li C, Liu K, Zhu Y, Zhang HLi C, Liu K, Zhu Y, Zhang H. 2022. Friend or foe: RIG- I like receptors and diseases. Autoimmun Rev 21:103161.
374. Zhuang C CR, Zheng Z, Lu J, Hong C. 2022. Toll-Like Receptor 3 in Cardiovascular Diseases. Heart Lung Circ 31:e93-e109.
375. Zhou J ZZ, Li J, Feng Z. 2023. Significance of the cGAS-STING Pathway in Health and Disease. Int J Mol Sci 24:13316.
376. Liu Y PF. 2023. Updated roles of cGAS-STING signaling in autoimmune diseases. Front Immunol 14:1254915.
377. Farré R DS, Meijers B. 2022. Of Mice and MAVS-Diabetic Kidney Disease and the Leaky Gut. J Am Soc Nephrol 33:1053-1055.
378. Wang Q SZ, Cao S, Lin X, Wu M, Li Y, Yin J, Zhou W, Huang S, Zhang A, Zhang Y, Xia W, Jia Z. 2022. Reduced Immunity Regulator MAVS Contributes to Non-Hypertrophic Cardiac Dysfunction by Disturbing Energy Metabolism and Mitochondrial Homeostasis. Front Immunol 13:919038.
379. Huang C AJ. 2023. MAVS is a double-edged sword. Mol Ther Nucleic Acids 33:869-870.
380. Komine O YH, Fujimori-Tonou N, Koike M, Jin S, Moriwaki Y, Endo F, Watanabe S, Uematsu S, Akira S, Uchiyama Y, Takahashi R, Misawa H, Yamanaka K. 2018. Innate immune adaptor TRIF deficiency accelerates disease progression of ALS mice with accumulation of aberrantly activated astrocytes. Cell Death Differ 25:2130-2146.
381. Burfeind KG ZX, Levasseur PR, Michaelis KA, Norgard MA, Marks DL. 2018. TRIF is a key inflammatory mediator of acute sickness behavior and cancer cachexia. Brain Behav Immun 73:364-374.

382. Zhou Y TT, Liu G, Gao X, Gao Y, Zhuang Z, Lu Y, Wang H, Li W, Wu L, Zhang D, Hang C. 2021. TRAF3 mediates neuronal apoptosis in early brain injury following subarachnoid hemorrhage via targeting TAK1-dependent MAPKs and NF-κB pathways. Cell Death Dis 12:10.
383. Rae W SJ, Verhoeven D, Youssef M, Kotagiri P, Savinykh N, Coomber EL, Boneparth A, Chan A, Gong C, Jansen MH, du Long R, Santilli G, Simeoni I, Stephens J, Wu K, Zinicola M, Allen HL, Baxendale H, Kumararatne D, Gkrania-Klotsas E, Scheffler Mendoza SC, Yamazaki-Nakashimada MA, Ruiz LB, Rojas-Maruri CM, Lugo Reyes SO, Lyons PA, Williams AP, Hodson DJ, Bishop GA, Thrasher AJ, Thomas DC, Murphy MP, Vyse TJ, Milner JD, Kuijpers TW, Smith KGC. 2022. Immunodeficiency, autoimmunity, and increased risk of B cell malignancy in humans with TRAF3 mutations. Sci Immunol 7:eabn3800.
384. Wu J LX, Pan Z, Xu L, Zhang H. 2021. Overexpression of IRF3 Predicts Poor Prognosis in Clear Cell Renal Cell Carcinoma. Int J Gen Med 14:5675-5692.
385. Chen YJ LS, Dong L, Liu TT, Shen XZ, Zhang NP, Liang L. 2021. Interferon regulatory factor family influences tumor immunity and prognosis of patients with colorectal cancer. J Transl Med 19:379.
386. Aoki M WL, Murakami J, Zhao Y, Yun H, de Perrot M. 2021. IRF3 Knockout Results in Partial or Complete Rejection of Murine Mesothelioma. Journal of Clinical Medicine 10:5196.
387. Aricò E CL, Capone I, Gabriele L, Belardelli F. 2019. Type I Interferons and Cancer: An Evolving Story Demanding Novel Clinical Applications. Cancers (Basel) 11:1943.
388. J L. 2016. Virus Structure and Classification. Essential Human Virology doi:doi: 10.1016/B978-0-12-800947-5.00002-8:19–29.
389. Roos WH II, Evilevitch A, Wuite GJ. 2007. Viral capsids: mechanical characteristics, genome packaging and delivery mechanisms. Cell Mol Life Sci 64:1484-97.
390. Castellanos M PR, Carrillo PJ, de Pablo PJ, Mateu MG. 2012. Mechanical disassembly of single virus particles reveals kinetic intermediates predicted by theory. Biophys J 102:2615-24.
391. STRAUSS JH SE. 2008. Overview of Viruses and Virus Infection. Viruses and Human Disease doi:doi: 10.1016/B978-0-12-373741-0.50004-0:1–33.
392. MW T. 2014. What Is a Virus? . Viruses and Man: A History of Interactions doi:doi: 10.1007/978-3-319-07758-1_2.
393. Lucas M KU, Lucas A, Klenerman P. 2001. Viral escape mechanisms--escapology taught by viruses. Int J Exp Pathol 82:269-86.
394. K M. 2012. Are viruses our oldest ancestors? EMBO Rep 13:1033.
395. Moelling K BF. 2019. Viruses and Evolution - Viruses First? A Personal Perspective. Front Microbiol 10.
396. Marchi J LM, Walczak AM, Mora T. 2021. Antigenic waves of virus-immune coevolution. Proc Natl Acad Sci U S A 118.
397. Kaminskyy V ZB. 2010. To kill or be killed: how viruses interact with the cell death machinery. J Intern Med 267:473-82.
398. Alempic JM LA, Goncharov AE, Grosse G, Strauss J, Tikhonov AN, Fedorov AN, Poirot O, Legendre M, Santini S, Abergel C, Claverie JM. 2023. An Update on Eukaryotic Viruses Revived from Ancient Permafrost. Viruses 15.
399. Pereira Andrade ACDS VdMBP, Rodrigues RAL, Bastos TM, Azevedo BL, Dornas FP, Oliveira DB, Drumond BP, Kroon EG, Abrahão JS. 2019. New Isolates of Pandoraviruses: Contribution to the Study of Replication Cycle Steps. J Virol 93.

400. Durmuş S ÜK. 2017. Comparative interactomics for virus-human protein-protein interactions: DNA viruses versus RNA viruses. FEBS Open Bio 7:96-107.
401. Rampersad S TP. 2018. Replication and Expression Strategies of Viruses. Viruses doi: doi: 10.1016/B978-0-12-811257-1.00003-6:55–82.
402. J L. 2016. Virus Replication. Essential Human Virology doi:doi: 10.1016/B978-0-12-800947-5.00004-1:49–70.
403. FS C. 2016. How Viruses Invade Cells. Biophys J 110:1028-32.
404. Yang Z, Gray, M. & Winter, L. 2021. Why do poxviruses still matter? Cell Biosci 11.
405. Laliberte JP MB. 2010. Lipid membranes in poxvirus replication. Viruses 2:972-986.
406. Blacklaws BA GA, Tippelt S, Jepson PD, Deaville R, Van Bressem MF, Pearce GP. 2013. Molecular characterization of poxviruses associated with tattoo skin lesions in UK cetaceans. PLoS One 8:e71734.
407. Plotkin S, Plotkin, S. 2011. The development of vaccines: how the past led to the future. Nat Rev Microbiol 9:889–893.
408. Belongia EA NA. 2003. Smallpox vaccine: the good, the bad, and the ugly. Clin Med Res 1:87-92.
409. DALES S SL. 1961. The development of vaccinia virus in Earle's L strain cells as examined by electron microscopy. J Biophys Biochem Cytol 10:475-503.
410. (CDC) CfDCaP. 1980. Public Health Image Library (PHIL). Accessed
411. Bidgood SR SJ, Novy K, Collopy A, Albrecht D, Krause M, Burden JJ, Wollscheid B, Mercer J. 2022. Poxviruses package viral redox proteins in lateral bodies and modulate the host oxidative response. PLoS Pathog 18:e1010614.
412. Ember SWJ RH, Ferguson BJ, Smith GL. 2012. Vaccinia virus protein C4 inhibits NF-κB activation and promotes virus virulence. J Gen Virol 93:2098-2108.
413. Neidel S RH, Torres AA, Smith GL. 2019. NF-κB activation is a turn on for vaccinia virus phosphoprotein A49 to turn off NF-κB activation. Proc Natl Acad Sci U S A 116:5699-5704.
414. Zhang RY PM, French J, Ren H, Smith GL. 2022. Vaccinia virus BTB-Kelch proteins C2 and F3 inhibit NF-κB activation. J Gen Virol 103.
415. Spyrou V VG. 2015. Orf virus infection in sheep or goats. Vet Microbiol 181:178-82.
416. AlDaif BA MA, Fleming SB. 2022. The parapoxvirus Orf virus inhibits IFN-β expression induced by dsRNA. Virus Res 307:198619.
417. Khatiwada S DG, Nagendraprabhu P, Chaulagain S, Luo S, Diel DG, Flores EF, Rock DL. 2017. A parapoxviral virion protein inhibits NF-κB signaling early in infection. PLoS Pathog 13:e1006561.
418. Goebel SJ JG, Perkus ME, Davis SW, Winslow JP, Paoletti E. 1990. The complete DNA sequence of vaccinia virus. Virology 179:247-66, 517-63.
419. Greseth MD TP. 2022. The Life Cycle of the Vaccinia Virus Genome. Annu Rev Virol 9:239-259.
420. SN I. 2019. Working Safely with Vaccinia Virus: Laboratory Technique and Review of Published Cases of Accidental Laboratory Infections with Poxviruses. Methods Mol Biol 2023:1-27.
421. Walsh SR DR. 2011. Vaccinia viruses: vaccines against smallpox and vectors against infectious diseases and tumors. Expert Rev Vaccines 10:1221-40.
422. Molteni C, Forni, D, Cagliani, R, Clerici, M, Sironi, M. 2022. Genetic ancestry and population structure of vaccinia virus. npj Vaccines 7:92.

423. Tolonen N DL, Schleich S, Krijnse Locker J. 2001. Vaccinia virus DNA replication occurs in endoplasmic reticulum-enclosed cytoplasmic mini-nuclei. Mol Biol Cell 12:2031-46.
424. Smith GL, Vanderplasschen, A. 1998. Extracellular Enveloped Vaccinia Virus. *In* Enjuanes L, Siddell, SG, Spaan, W (ed), Advances in Experimental Medicine and Biology. Springer, Boston. doi:doi: https://doi.org/10.1007/978-1-4615-5331-1_51.
425. Smith GL LM. 2004. The exit of vaccinia virus from infected cells. Virus Res 106:189-97.
426. Schin AM DU, Moss B. 2021. Insights into the Organization of the Poxvirus Multicomponent Entry-Fusion Complex from Proximity Analyses in Living Infected Cells. J Virol 95:e0085221.
427. Laliberte JP WA, Moss B. 2011. The membrane fusion step of vaccinia virus entry is cooperatively mediated by multiple viral proteins and host cell components. PLoS Pathog 7:e1002446.
428. B M. 2015. Membrane fusion during poxvirus entry. Semin Cell Dev Biol 60:89-96.
429. Roberts K, Smith, GL. 2008. Vaccinia virus morphogenesis and dissemination. Trends Microbiol 16:472-479.
430. B M. 2013. Poxvirus DNA replication. Cold Spring Harb Perspect Biol 5:a010199.
431. Yang Z RS, Martens CA, Bruno DP, Porcella SF, Moss B. 2011. Expression profiling of the intermediate and late stages of poxvirus replication. J Virol 85:9899-908.
432. Meade N TH, Chakrabarty RP, Hesser CR, Park C, Chandel NS, Walsh D. 2023. The poxvirus F17 protein counteracts mitochondrially orchestrated antiviral responses. Nat Commun 14:7889.
433. Rubins KH HL, Bell GW, Wang C, Lefkowitz EJ, Brown PO, Relman DA. 2008. Comparative analysis of viral gene expression programs during poxvirus infection: a transcriptional map of the vaccinia and monkeypox genomes. PLoS One 3:e2628.
434. B M. 2015. Poxvirus membrane biogenesis. Virology 479-480:619-26.
435. (ed). 1824. A practical synopsis of cutaneous diseases, according to the arrangement of Dr. Willan, exhibiting a concise view of the diagnostic symptoms and the method of treatment. Collins & Croft, Philadelphia. Accessed
436. Henderson W. 1841. Notice of the Molluscum Contagiosum. Edinb Med Surg J 56:213–218.
437. Paterson R. 1841. Cases and Observations on the Molluscum Contagiosum of Bateman, with an Account of the Minute Structure of the Tumours. Edinb Med Surg J 56:279-288.
438. Meirowsky E, Keys S, Behr G. 1946. The cytology of molluscum contagiosum, with special regard to the significance of the so-called vacuoles. J Invest Dermatol 7:165-9.
439. Brown S, Nalley, JF, Kraus, SJ. 1981. Molluscum_Contagiosum. Sexually Transmitted Diseases 8:227-234.
440. Juliusberg M. 1905. Zur Kenntnis des Virus des Molluscum contagiosum des Menschen. Dtsch Med Wochenschr 31:1598–1599.
441. Goodpasture E, Woodruff, CE. 1931. A COMPARISON OF THE INCLUSION BODIES OF FOWL- POX AND MOLLUSCUM CONTAGIOSUM. Am J Pathol 7:7-8.1.

442. Bugert JJ MN, Kehm R. 2001. Molluscum contagiosum virus expresses late genes in primary human fibroblasts but does not produce infectious progeny. Virus Genes 22:27-33.
443. Melnick JL B, H, Banfield, WG, Strauss, MJ, Gaylord, WH. 1952. ELECTRON MICROSCOPY OF VIRUSES OF HUMAN PAPILLOMA, MOLLUSCUM CONTAGIOSUM, AND VACCINIA, INCLUDING OBSERVATIONS ON THE FORMATION OF VIRUS WITHIN THE CELL. ANNALS 54:1214-1225.
444. Bugert J. 2008. Molluscum Contagiosum Virus. *In* Mahy B, Regenmortel, MHV (ed), Encyclopedia of Virology (Third Edition). Academic Press,
445. Mihara M. 1991. Three-dimensional ultrastructural study of molluscum contagiosum in the skin using scanning-electron microscopy

. British Journal of Dermatology 125: 557-560

.
446. De Almeida Jr H, Abuchaim, MO, Schneider, MA, Marques, L, De Castro, LAS. 2013. Scanning electron microscopy of molluscum contagiosum. An Bras Dermatol 88:90-93.
447. Darai G, Reisner, H, Scholz, J, Schnitzler, P, De Ruiz H. 1986. Analysis of the genome of molluscum contagiosum virus by restriction endonuclease analysis and molecular cloning. J Med Virol doi:doi: 10.1002/jmv.1890180105:29-39.
448. Porter CD, Muhlemann MF, Cream JJ, Archard LC. 1987. Molluscum contagiosum: characterization of viral DNA and clinical features. Epidemiol Infect 99:563-6.
449. Porter C, Archard, LC. 1992. Characterisation by restriction mapping of three subtypes of molluscum contagiosum virus. J Med Virol 38:1-6.
450. Senkevich T, Koonin, EV, Bugert, JJ, Darai, G, Moss, B. 1997. The Genome of Molluscum Contagiosum Virus: Analysis and Comparison with Other Poxviruses. VIROLOGY 233:19-42.
451. Du MZ ZC, Wang H, Liu S, Wei W, Guo FB. 2018. The GC Content as a Main Factor Shaping the Amino Acid Usage During Bacterial Evolution Process. Front Microbiol 9:2948.
452. Schlub TE HE. 2020. Properties and abundance of overlapping genes in viruses. Virus Evol 6:veaa009.
453. Šmarda P BP, Horová L, Leitch IJ, Mucina L, Pacini E, Tichý L, Grulich V, Rotreklová O. 2014. Ecological and evolutionary significance of genomic GC content diversity in monocots. Proc Natl Acad Sci U S A 111:E4096-102.
454. Ehmann R, Brandes K, Antwerpen M, Walter M, K VS, Stegmaier E, Essbauer S, Bugert J, Teifke JP, Meyer H. 2021. Molecular and genomic characterization of a novel equine molluscum contagiosum-like virus. J Gen Virol 102.
455. Callegaro C, Sotto, MN. 2009. Molluscum contagiosum: immunomorphological aspects of keratinocytes markers of differentiation and adhesion. J Cutan Pathol 36:1279-1285.
456. Shisler J. 2015. Immune Evasion Strategies of Molluscum Contagiosum Virus. *In* Maramorosch K, Mettenleiter, TC (ed), Advances in Virus Research. Academic Press,
457. Meza-Romero R, Navarrete-Dechent C, Downey C. 2019. Molluscum contagiosum: an update and review of new perspectives in etiology, diagnosis, and treatment. Clin Cosmet Investig Dermatol 12:373-381.
458. Cohen JI DW, Ali MA, Turk SP, Cowen EW, Freeman AF, Wang K. 2012. Detection of molluscum contagiosum virus (MCV) DNA in the plasma of an

immunocompromised patient and possible reduction of MCV DNA with CMX-001. J Infect Dis 205:794-7.
459. Vora RV PA, Kota RK. 2015. Extensive Giant Molluscum Contagiosum in a HIV Positive Patient. J Clin Diagn Res 9:WD01-2.
460. Pérez-Díaz CE B-GC, Rodríguez MC, Faccini-Martínez ÁA, Calixto OJ, Benítez F, Mantilla-Florez YF, Bravo-Ojeda JS, Espinal A, Morales-Pertuz C. 2015. Giant Molluscum Contagiosum in an HIV positive patient. Int J Infect Dis 38:153-5.
461. SK T. 2003. Molluscum contagiosum: the importance of early diagnosis and treatment. Am J Obstet Gynecol 189:S12-6.
462. Hughes CM DI, Reynolds MG. Understanding U.S. 2013. healthcare providers' practices and experiences with molluscum contagiosum. PLoS One 8:e76948.
463. Bhatia N HA, Del Rosso JQ. 2023. Comprehensive Management of Molluscum Contagiosum: Assessment of Clinical Associations, Comorbidities, and Management Principles. J Clin Aesthet Dermatol 16:S12-S17.
464. Gerlero P H-MÁ. 2018. Update on the Treatment of molluscum Contagiosum in children. Actas Dermosifiliogr 109:408-415.
465. Frey SE CR, Tacket CO, Treanor JJ, Wolff M, Newman FK, Atmar RL, Edelman R, Nolan CM, Belshe RB. 2002. National Institute of Allergy and Infectious Diseases Smallpox Vaccine Study Group. Clinical responses to undiluted and diluted smallpox vaccine. N Engl J Med 346:1265-74.
466. Nestle FO, Di Meglio P, Qin JZ, Nickoloff BJ. 2009. Skin immune sentinels in health and disease. Nat Rev Immunol 9:679-91.
467. Watanabe T, Nakamura, K, Wakugawa, M, et al. 2000. Antibodies to Molluscum Contagiosum Virus in the General Population and Susceptible Patients. Arch Dermatol 136:1518-1522.
468. Silva DC M-SE, Gomes Jde A, Fonseca FG, Correa-Oliveira R. 2010. Clinical signs, diagnosis, and case reports of Vaccinia virus infections. Braz J Infect Dis 14:129-34.
469. Brady G, Haas DA, Farrell PJ, Pichlmair A, Bowie AG. 2017. Molluscum Contagiosum Virus Protein MC005 Inhibits NF-kappaB Activation by Targeting NEMO-Regulated IkappaB Kinase Activation. J Virol 91.
470. Phelan T, Lawler, C, Pichlmair, A, Little, M.A, Bowie, A.G, Brady, G. 2023. Molluscum Contagiosum Virus Protein MC008 Targets NF-kB

Activation by Inhibiting Ubiquitination of NEMO. J Virol 97.
471. Biswas S, Shisler JL. 2017. Molluscum Contagiosum Virus MC159 Abrogates cIAP1-NEMO Interactions and Inhibits NEMO Polyubiquitination. J Virol 91.
472. Brady G, Haas DA, Farrell PJ, Pichlmair A, Bowie AG. 2015. Poxvirus Protein MC132 from Molluscum Contagiosum Virus Inhibits NF-B Activation by Targeting p65 for Degradation. J Virol 89:8406-15.
473. Nichols DB, Shisler JL. 2009. Poxvirus MC160 protein utilizes multiple mechanisms to inhibit NF-kappaB activation mediated via components of the tumor necrosis factor receptor 1 signal transduction pathway. J Virol 83:3162-74.
474. De Martini W, Coutu, J, Bugert, J, Iversen, T, Cottrell, J, Nichols, DB 2019. The molluscum contagiosum virus protein MC163 inhibits TNF-α-induced NF-κB activation. FUTURE VIROLOGY 14.
475. Xiang Y MB. 1999. IL-18 binding and inhibition of interferon gamma induction by human poxvirus-encoded proteins. Proc Natl Acad Sci U S A 96:11537-42.

476. Jin Q AJ, Hossain MM, Alkhatib G. 2011. Role for the conserved N-terminal cysteines in the anti-chemokine activities by the chemokine-like protein MC148R1 encoded by Molluscum contagiosum virus. Virology 417:449-56.
477. Elasifer H WE, Prod'homme V, Davies J, Forbes S, Stanton RJ, Patel M, Fielding CA, Roberts D, Traherne JA, Gruber N, Bugert JJ, Aicheler RJ, Wilkinson GWG. 2020. Downregulation of HLA-I by the molluscum contagiosum virus mc080 impacts NK-cell recognition and promotes CD8+ T-cell evasion. J Gen Virol 101:863-872.
478. MJ A. 1999. The role of tapasin in MHC class I antigen assembly. Immunol Res 20:79-88.
479. Kim SJ AD, Syed GH, Siddiqui A. 2018. The essential role of mitochondrial dynamics in antiviral immunity. Mitochondrion 41:21-27.
480. Coutu J RM, Bugert J, Brian Nichols D. 2017. The Molluscum Contagiosum Virus protein MC163 localizes to the mitochondria and dampens mitochondrial mediated apoptotic responses. Virology 505:91-101.
481. Mohr S GS, Massimi P, Darai G, Banks L, Martinou JC, Zeier M, Muranyi W. 2008. Targeting the retinoblastoma protein by MC007L, gene product of the molluscum contagiosum virus: detection of a novel virus-cell interaction by a member of the poxviruses. J Virol 82:10625-33.
482. Shifera AS HJ. 2010. Factors modulating expression of Renilla luciferase from control plasmids used in luciferase reporter gene assays. Anal Biochem 396:167-72.
483. Jiwaji M DR, Pansare K, McLean P, Yang J, Kolch W, Pitt AR. 2010. The Renilla luciferase gene as a reference gene for normalization of gene expression in transiently transfected cells. BMC Mol Biol 11:103.
484. Hannah R, Jennens-Clough, ML, Wood, KV. 1998. MipTec Proceedings: Transcriptional Assay Screens Using Renilla Luciferase as an Internal Control. SLAS Technology 3:41-43.
485. Kim HR, Jang I, Song HS, Kim SH, Kim HS, Kwon YK. 2022. Genetic Diversity of Fowlpox Virus and Putative Genes Involved in Its Pathogenicity. Microbiol Spectr 10:e0141522.
486. Yang H, Ma G, Lin CH, Orr M, Wathelet MG. 2004. Mechanism for transcriptional synergy between interferon regulatory factor (IRF)-3 and IRF-7 in activation of the interferon-beta gene promoter. Eur J Biochem 271:3693-703.
487. Juang YT, Lowther W, Kellum M, Au WC, Lin R, Hiscott J, Pitha PM. 1998. Primary activation of interferon A and interferon B gene transcription by interferon regulatory factor 3. Proc Natl Acad Sci U S A 95:9837-42.
488. Cheng WY HX, Jia HJ, Chen GH, Jin QW, Long ZL, Jing ZZ. 2018. The cGas-Sting Signaling Pathway Is Required for the Innate Immune Response Against Ectromelia Virus. Front Immunol 9:1297.
489. Oshiumi H, Matsumoto M, Funami K, Akazawa T, Seya T. 2003. TICAM-1, an adaptor molecule that participates in Toll-like receptor 3-mediated interferon-beta induction. Nat Immunol 4:161-7.
490. Valentine R, Smith GL. 2010. Inhibition of the RNA polymerase III-mediated dsDNA-sensing pathway of innate immunity by vaccinia virus protein E3. The Journal of general virology 91:2221-2229.
491. Gil J, Rullas, Alcamı, J, Esteban, M. 2001. MC159L protein from the poxvirus molluscum contagiosum virus inhibits NF-κB activation and apoptosis induced by PKR. Journal of General Virology 182.

492. Ahuja D, Sáenz-Robles, M. & Pipas, J. 2005. SV40 large T antigen targets multiple cellular pathways to elicit cellular transformation. Oncogene 24:7729–7745.
493. Ferreira CB SR, Rodriguez-Plata MT, Rasaiyaah J, Milne RS, Thrasher AJ, Qasim W, Towers GJ. 2019. Lentiviral Vector Production Titer Is Not Limited in HEK293T by Induced Intracellular Innate Immunity. Mol Ther Methods Clin Dev 17:209-219.
494. Wu D, Wang, Z, Zhang, J, Robinson, AG, Lyu, B, Chen, Z, Wang, C, Wei, B, Xia, X, Zhang, Q, Zhou, X. 2022. Apoptotic caspase inhibits innate immune signaling by cleaving NF-κBs in both Mammals and Flies. Cell Death Dis 13:731.
495. Jonckheere AI, Smeitink JA, Rodenburg RJ. 2012. Mitochondrial ATP synthase: architecture, function and pathology. J Inherit Metab Dis 35:211-25.
496. Neupane P, Bhuju S, Thapa N, Bhattarai HK. 2019. ATP Synthase: Structure, Function and Inhibition. Biomol Concepts 10:1-10.
497. Naghdi S VP, Hajnóczky G. . 2015. Motifs of VDAC2 required for mitochondrial Bak import and tBid-induced apoptosis. Proc Natl Acad Sci U S A 112.
498. Vazquez C, Beachboard DC, Horner SM. 2017. Methods to Visualize MAVS Subcellular Localization. Methods Mol Biol 1656:131-142.
499. Seth RB, Sun L, Ea CK, Chen ZJ. 2005. Identification and characterization of MAVS, a mitochondrial antiviral signaling protein that activates NF-kappaB and IRF 3. Cell 122:669-82.
500. Kawai T, Takahashi K, Sato S, Coban C, Kumar H, Kato H, Ishii KJ, Takeuchi O, Akira S. 2005. IPS-1, an adaptor triggering RIG-I- and Mda5-mediated type I interferon induction. Nat Immunol 6:981-8.
501. Horner SM, Liu HM, Park HS, Briley J, Gale M, Jr. 2011. Mitochondrial-associated endoplasmic reticulum membranes (MAM) form innate immune synapses and are targeted by hepatitis C virus. Proc Natl Acad Sci U S A 108:14590-5.
502. Nazmi A MR, Dutta K, Basu A. 2012. STING mediates neuronal innate immune response following Japanese encephalitis virus infection. Sci Rep 2:347.
503. Zhong B, Yang Y, Li S, Wang YY, Li Y, Diao F, Lei C, He X, Zhang L, Tien P, Shu HB. 2008. The adaptor protein MITA links virus-sensing receptors to IRF3 transcription factor activation. Immunity 29:538-50.
504. Ishikawa H, Barber GN. 2008. STING is an endoplasmic reticulum adaptor that facilitates innate immune signalling. Nature 455:674-8.
505. Nitta S, Sakamoto N, Nakagawa M, Kakinuma S, Mishima K, Kusano-Kitazume A, Kiyohashi K, Murakawa M, Nishimura-Sakurai Y, Azuma S, Tasaka-Fujita M, Asahina Y, Yoneyama M, Fujita T, Watanabe M. 2013. Hepatitis C virus NS4B protein targets STING and abrogates RIG-I-mediated type I interferon-dependent innate immunity. Hepatology 57:46-58.
506. Holm CK, Rahbek SH, Gad HH, Bak RO, Jakobsen MR, Jiang Z, Hansen AL, Jensen SK, Sun C, Thomsen MK, Laustsen A, Nielsen CG, Severinsen K, Xiong Y, Burdette DL, Hornung V, Lebbink RJ, Duch M, Fitzgerald KA, Bahrami S, Mikkelsen JG, Hartmann R, Paludan SR. 2016. Influenza A virus targets a cGAS-independent STING pathway that controls enveloped RNA viruses. Nat Commun 7:10680.
507. Yu CY, Chang TH, Liang JJ, Chiang RL, Lee YL, Liao CL, Lin YL. 2012. Dengue virus targets the adaptor protein MITA to subvert host innate immunity. PLoS Pathog 8:e1002780.
508. Aguirre S, Maestre AM, Pagni S, Patel JR, Savage T, Gutman D, Maringer K, Bernal-Rubio D, Shabman RS, Simon V, Rodriguez-Madoz JR, Mulder LC, Barber

GN, Fernandez-Sesma A. 2012. DENV inhibits type I IFN production in infected cells by cleaving human STING. PLoS Pathog 8:e1002934.
509. Suzuki T, Oshiumi H, Miyashita M, Aly HH, Matsumoto M, Seya T. 2013. Cell type-specific subcellular localization of phospho-TBK1 in response to cytoplasmic viral DNA. PLoS One 8:e83639.
510. Al Hamrashdi M BG. 2022. Regulation of IRF3 activation in human antiviral signaling pathways. Biochem Pharmacol 200:115026.
511. Lin R LJ, Nakhaei P, Sun Q, Yang L, Paz S, Wilkinson P, Julkunen I, Vitour D, Meurs E, Hiscott J. 2006. Dissociation of a MAVS/IPS-1/VISA/Cardif-IKKepsilon molecular complex from the mitochondrial outer membrane by hepatitis C virus NS3-4A proteolytic cleavage. J Virol 80.
512. Paz S VM, Arguello M, Sun Q, Lacoste J, Nguyen TL, Zhao T, Shestakova EA, Zaari S, Bibeau-Poirier A, Servant MJ, Lin R, Meurs EF, Hiscott J. 2009. Ubiquitin-regulated recruitment of IkappaB kinase epsilon to the MAVS interferon signaling adapter. Mol Cell Biol 29.
513. Choi H, Park, A, Kang, S, Lee, E, Lee, TA, Ra, EA, Lee, J, Lee, S, Park, B. 2018. Human cytomegalovirus-encoded US9 targets MAVS and STING signaling to evade type I interferon immune responses. Nat Commun 9.
514. Ohta A NY. 2011. Mitochondria and viruses. . Mitochondrion 11:1-12.
515. Shibazaki M KA, Takeshima K, Ito J, Suganami M, Koyanagi N, Maruzuru Y, Sato K, Kawaguchi Y. 2020. Phosphoregulation of a Conserved Herpesvirus Tegument Protein by a Virally Encoded Protein Kinase in Viral Pathogenicity and Potential Linkage between Its Evolution and Viral Phylogeny. J Virol 94:e01055-20.
516. Nazar AS, Cheng G, Shin HS, Brothers PN, Dhib-Jalbut S, Shin ML, Vanguri P. 1997. Induction of IP-10 chemokine promoter by measles virus: comparison with interferon-gamma shows the use of the same response element but with differential DNA-protein binding profiles. J Neuroimmunol 77:116-27.
517. Ohmori Y, Hamilton TA. 1993. Cooperative interaction between interferon (IFN) stimulus response element and kappa B sequence motifs controls IFN gamma- and lipopolysaccharide-stimulated transcription from the murine IP-10 promoter. J Biol Chem 268:6677-88.
518. Servant MJ GN, tenOever BR, Duguay D, Lin R, and Hiscott J. 2003. Identification of the minimal phosphoacceptor site required for in vivo activation of interferon regulatory factor 3 in response to virus and double-stranded RNA. The Journal of biological chemistry 278.
519. Tanaka Y aCZ. 2012. STING specifies IRF3 phosphorylation by TBK1 in the cytosolic DNA signaling pathway. Sci Signal 6;5.
520. Wang P, Deng Y, Guo Y, Xu Z, Li Y, Ou X, Xie L, Lu M, Zhong J, Li B, Hu L, Deng S, Peng T, Cai M, Li M. 2020. Epstein-Barr Virus Early Protein BFRF1 Suppresses IFN-beta Activity by Inhibiting the Activation of IRF3. Front Immunol 11:513383.
521. Wong LR, Ye ZW, Lui PY, Zheng X, Yuan S, Zhu L, Fung SY, Yuen KS, Siu KL, Yeung ML, Cai Z, Woo PC, Yuen KY, Chan CP, Jin DY. 2020. Middle East Respiratory Syndrome Coronavirus ORF8b Accessory Protein Suppresses Type I IFN Expression by Impeding HSP70-Dependent Activation of IRF3 Kinase IKKepsilon. J Immunol 205:1564-1579.
522. Nandi S, Chanda S, Bagchi P, Nayak MK, Bhowmick R, Chawla-Sarkar M. 2014. MAVS protein is attenuated by rotavirus nonstructural protein 1. PLoS One 9:e92126.

523. Dai T WL, Wang S, Wang J, Xie F, Zhang Z, Fang X, Li J, Fang P, Li F, Jin K, Dai J, Yang B, Zhou F, van Dam H, Cai D, Huang H, Zhang L. 2018. FAF1 Regulates Antiviral Immunity by Inhibiting MAVS but Is Antagonized by Phosphorylation upon Viral Infection. Cell Host Microbe 24.
524. Yaron JR ZL, Guo Q, Burgin M, Schutz LN, Awo E, Wise L, Krause KL, Ildefonso CJ, Kwiecien JM, Juby M, Rahman MM, Chen H, Moyer RW, Alcami A, McFadden G, Lucas AR. 2020. Deriving Immune Modulating Drugs from Viruses-A New Class of Biologics. J Clin Med 9:972.
525. Bursill CA ME, Wang L, Hibbitt OC, Wade-Martins R, Paterson DJ, Greaves DR, Channon KM. 2009. Lentiviral gene transfer to reduce atherosclerosis progression by long-term CC-chemokine inhibition. Gene Ther 16:93-102.
526. Gileva IP NT, Antonets DV, Lebedev LR, Kochneva GV, Grazhdantseva AV, Shchelkunov SN. 2006. Properties of the recombinant TNF-binding proteins from variola, monkeypox, and cowpox viruses are different. Biochim Biophys Acta 1764:1710-8.
527. DeBruyne LA LK, Bishop DK, Bromberg JS. 2000. Gene transfer of virally encoded chemokine antagonists vMIP-II and MC148 prolongs cardiac allograft survival and inhibits donor-specific immunity. Gene Ther 7:575-82.
528. Dias-Pinto P, G.Oliveira, JG. 2021. Innate Immune Response in Human Kidney Transplantation: IRF3 and IRF7 Together with Interferon-Alpha Are Significantly Up-Regulated in Acute Rejection. Journal of Nephrology 11.
529. Vargason AM, Anselmo, A.C. & Mitragotri, S. 2021. The evolution of commercial drug delivery technologies. Nat Biomed Eng 5:951–967.
530. Sun Z HJ, Fishelson Z, Wang C, Zhang S. 2023. Cell-Penetrating Peptide-Based Delivery of Macromolecular Drugs: Development, Strategies, and Progress. Biomedicines 11:1971.
531. Malam Y, Loizidou, M,Seifalian, AM. 2009. Liposomes and nanoparticles: nanosized vehicles for drug delivery in cancer. 30:592-599.